PB87-134342

Vortex Shedding Flow Meter Performance at High Flow Velocities

(U.S.) National Bureau of Standards (NEL)
Boulder, CO

Prepared for

National Aeronautics and Space Administration
Huntsville, AL

Oct 86

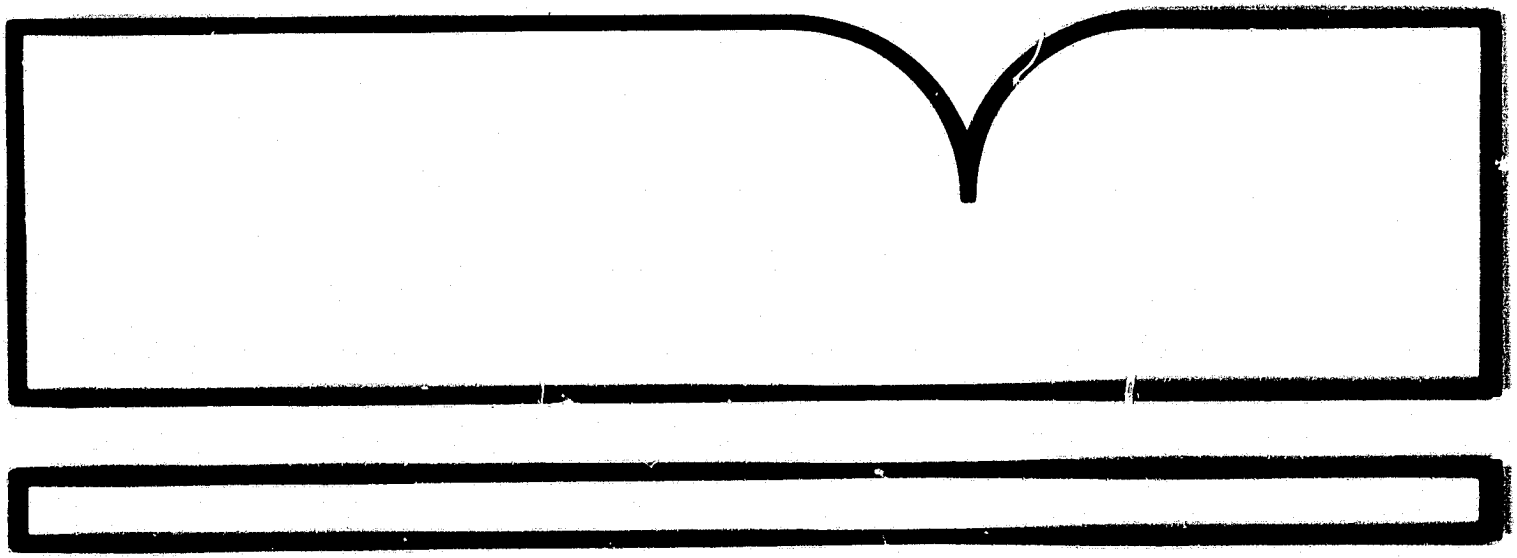

U.S. Department of Commerce
National Technical Information Service
NTIS

NBS-114A (REV. 2-80)

U.S. DEPT. OF COMM. BIBLIOGRAPHIC DATA SHEET (See instructions)	1. PUBLICATION OR REPORT NO. NBS/TN-1302	2. Performing Organ. Report No. PB87 134342/AS	3. Publication Date October 1986

4. TITLE AND SUBTITLE

VORTEX SHEDDING FLOW METER PERFORMANCE AT HIGH FLOW VELOCITIES

5. AUTHOR(S)

J. D. Siegwarth

6. PERFORMING ORGANIZATION (If joint or other than NBS, see instructions)

NATIONAL BUREAU OF STANDARDS
DEPARTMENT OF COMMERCE
WASHINGTON, D.C. 20234

7. Contract/Grant No. H-63458B

8. Type of Report & Period Covered

9. SPONSORING ORGANIZATION NAME AND COMPLETE ADDRESS (Street, City, State, ZIP)

NASA Marshall Space Flight Center
Huntsville
Alabama 35812

NBS Category No.
NBS-250

10. SUPPLEMENTARY NOTES

Also Available from
GPO as SN003-003-02777-4

☐ Document describes a computer program; SF-185, FIPS Software Summary, is attached.

11. ABSTRACT (A 200-word or less factual summary of most significant information. If document includes a significant bibliography or literature survey, mention it here)

In some of the ducts of the space shuttle main engines (SSME), the maximum liquid oxygen flow velocities approach 10 times those at which liquid flow measurements are normally made. The hydrogen gas flow velocities in other ducts exceed the maximum for gas flow measurement by more than a factor of 3. The results presented here show from water flow tests that vortex shedding flow meters of the appropriate design can measure water flow to velocities in excess of 55 m/s, which is a Reynolds number of about 2×10^6. Air flow tests have shown that the same meter can measure flow to a Reynolds number of at least 22×10^6. Vortex shedding meters were installed in two of the SSME ducts and tested with water flow. Narrow spectrum lines were obtained and the meter output frequencies were proportional to flow to ±0.5% or better over the test range with no flow conditioning, even though the ducts had multiple bends preceding the meter location. Meters with the shedding elements only partially spanning the pipe and some meters with ring shaped shedding elements were also tested.

12. KEY WORDS (Six to twelve entries; alphabetical order; capitalize only proper names; and separate key words by semicolons)

air flow; cryogenic; flowmeter; hydrogen; liquid oxygen; vortex shedding; water flow.

13. AVAILABILITY

☒ Unlimited
☐ For Official Distribution. Do Not Release to NTIS
☒ Order From Superintendent of Documents, U.S. Government Printing Office, Washington, D.C. 20402.
☒ Order From National Technical Information Service (NTIS), Springfield, VA. 22161

14. NO. OF PRINTED PAGES 97

15. Price

☆U.S. GOVERNMENT PRINTING OFFICE:1986—773-490/65003

USCOMM-DC 6043-P80

PB87-134342

NBS TECHNICAL NOTE 1302

U.S. DEPARTMENT OF COMMERCE / National Bureau of Standards

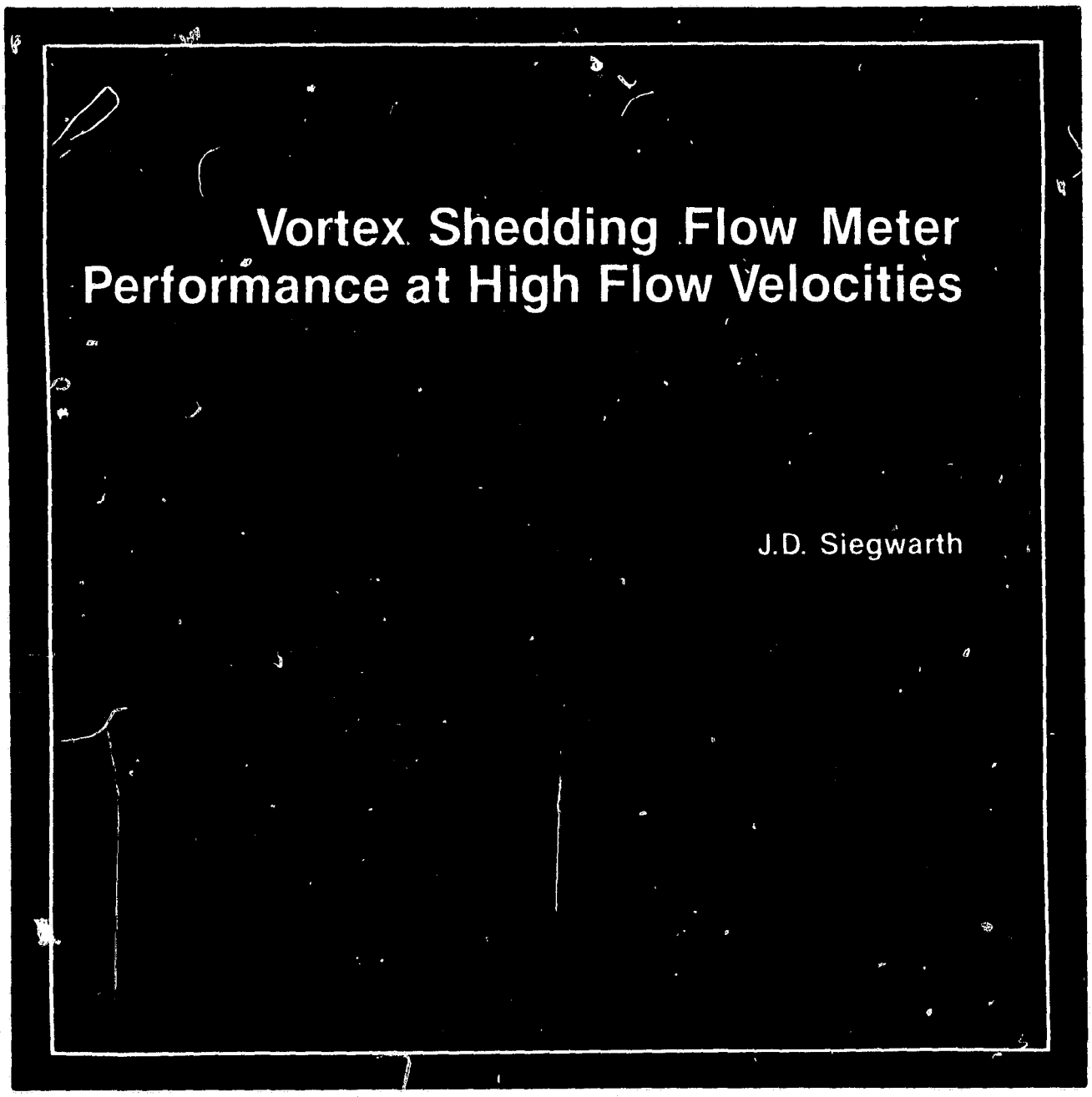

Vortex Shedding Flow Meter Performance at High Flow Velocities

J.D. Siegwarth

The National Bureau of Standards[1] was established by an act of Congress on March 3, 1901. The Bureau's overall goal is to strengthen and advance the nation's science and technology and facilitate their effective application for public benefit. To this end, the Bureau conducts research and provides: (1) a basis for the nation's physical measurement system, (2) scientific and technological services for industry and government, (3) a technical basis for equity in trade, and (4) technical services to promote public safety. The Bureau's technical work is performed by the National Measurement Laboratory, the National Engineering Laboratory, the Institute for Computer Sciences and Technology, and the Institute for Materials Science and Engineering.

The National Measurement Laboratory

Provides the national system of physical and chemical measurement; coordinates the system with measurement systems of other nations and furnishes essential services leading to accurate and uniform physical and chemical measurement throughout the Nation's scientific community, industry, and commerce; provides advisory and research services to other Government agencies; conducts physical and chemical research; develops, produces, and distributes Standard Reference Materials; and provides calibration services. The Laboratory consists of the following centers:

- Basic Standards[2]
- Radiation Research
- Chemical Physics
- Analytical Chemistry

The National Engineering Laboratory

Provides technology and technical services to the public and private sectors to address national needs and to solve national problems; conducts research in engineering and applied science in support of these efforts; builds and maintains competence in the necessary disciplines required to carry out this research and technical service; develops engineering data and measurement capabilities; provides engineering measurement traceability services; develops test methods and proposes engineering standards and code changes; develops and proposes new engineering practices; and develops and improves mechanisms to transfer results of its research to the ultimate user. The Laboratory consists of the following centers:

- Applied Mathematics
- Electronics and Electrical Engineering[2]
- Manufacturing Engineering
- Building Technology
- Fire Research
- Chemical Engineering[2]

The Institute for Computer Sciences and Technology

Conducts research and provides scientific and technical services to aid Federal agencies in the selection, acquisition, application, and use of computer technology to improve effectiveness and economy in Government operations in accordance with Public Law 89-306 (40 U.S.C. 759), relevant Executive Orders, and other directives; carries out this mission by managing the Federal Information Processing Standards Program, developing Federal ADP standards guidelines, and managing Federal participation in ADP voluntary standardization activities; provides scientific and technological advisory services and assistance to Federal agencies; and provides the technical foundation for computer-related policies of the Federal Government. The Institute consists of the following centers:

- Programming Science and Technology
- Computer Systems Engineering

The Institute for Materials Science and Engineering

Conducts research and provides measurements, data, standards, reference materials, quantitative understanding and other technical information fundamental to the processing, structure, properties and performance of materials; addresses the scientific basis for new advanced materials technologies; plans research around cross-country scientific themes such as nondestructive evaluation and phase diagram development; oversees Bureau-wide technical programs in nuclear reactor radiation research and nondestructive evaluation; and broadly disseminates generic technical information resulting from its programs. The Institute consists of the following Divisions:

- Ceramics
- Fracture and Deformation [3]
- Polymers
- Metallurgy
- Reactor Radiation

[1] Headquarters and Laboratories at Gaithersburg, MD, unless otherwise noted; mailing address Gaithersburg, MD 20899.
[2] Some divisions within the center are located at Boulder, CO 80303.
[3] Located at Boulder, CO, with some elements at Gaithersburg, MD.

Vortex Shedding Flow Meter Performance at High Flow Velocities

J.D Siegwarth

Chemical Engineering Science Division
Center for Chemical Engineering
National Engineering Laboratory
National Bureau of Standards
Boulder, Colorado 80303

Sponsored by
NASA Marshall Space Flight Center
Huntsville, Alabama 35812

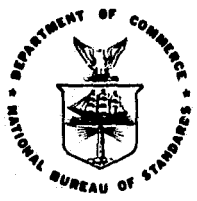

U.S. DEPARTMENT OF COMMERCE, Malcolm Baldrige, Secretary

NATIONAL BUREAU OF STANDARDS, Ernest Ambler, Director

Issued October 1986

National Bureau of Standards Technical Note 1302
Natl. Bur. Stand. (U.S.), Tech Note 1302, 94 pages (Oct. 1986)
CODEN:NBTNAE

U.S. GOVERNMENT PRINTING OFFICE
WASHINGTON: 1986

For sale by the Superintendent of Documents, U.S. Government Printing Office, Washington, DC 20402

CONTENTS

		Page
1.	INTRODUCTION	1
2.	THE VORTEX SHEDDING FLOWMETER	3
3.	TEST FACILITIES	5
4.	EXPERIMENTAL METHODS	8
5.	FULL VANE METER DESIGNS	12
	5.1 Meter Tests in a 1½-Inch Straight Duct	20
	5.2 Meter Tests in a SSME LOX Duct	33
	5.3 Vane Shape	43
	5.4 Double Cantilevered Vanes	55
6.	CANTILEVERED VANE	63
7.	RING VANES	70
8.	AIR TEST RESULTS	74
9.	CONCLUSIONS	82
10.	ACKNOWLEDGMENTS	84
11.	REFERENCES	85

Vortex Shedding Flow Meter
Performance at High Flow Velocities

J.D. Siegwarth

In some of the ducts of the space shuttle main engines (SSME), the maximum liquid oxygen flow velocities approach 10 times those at which liquid flow measurements are normally made. The hydrogen gas flow velocities in other ducts exceed the maximum for gas flow measurement by more than a factor of 3. The results presented here show from water flow tests that vortex shedding flow meters of the appropriate design can measure water flow to velocities in excess of 55 m/s, which is a Reynolds number of about 2×10^6. Air flow tests have shown that the same meter can measure flow to a Reynolds number of at least 22×10^6. Vortex shedding meters were installed in two of the SSME ducts and tested with water flow. Narrow spectrum lines were obtained and the meter output frequencies were proportional to flow to ±0.5% or better over the test range with no flow conditioning, even though the ducts had multiple bends preceding the meter location. Meters with the shedding elements only partially spanning the pipe and some meters with ring shaped shedding elements were also tested.

Key words: air flow; cryogenic; flowmeter; hydrogen; liquid oxygen; vortex shedding; water flow

1. INTRODUCTION

Fuel and liquid oxygen (LOX) flows in rocket engine ducts have been measured in the past using venturi flowmeters and more recently on the space shuttle main engine (SSME) by turbine meters. The ducts are kept as short as possible with the result that few straight sections of any length are available to install meters. Both turbine meter and venturi meter installations require extensive modification of the duct if added later. The turbine meter also has the disadvantage of introducing moving parts into the duct. The vortex shedding flowmeter was examined in this work as an alternative to these meters for SSME duct measurements.

Conventional flowmeter installations call for 10 to 20 diameters of straight pipe preceding a flowmeter of any kind and 2 to 4 diameters of straight pipe after it [1]. If flow conditioning is introduced upstream of the meter, 6 to 10 diameters of straight pipe between the conditioner and the flow meter are still recommended. On the SSME, a straight duct section exceeding 10 diameters is a luxury. Few if any of the ducts will permit a flowmeter installation following recommended practice.

Other conditions exist in the SSME ducts that are not normally encountered in conventional vortex shedding flowmeter applications. The flow velocity of LOX can exceed 50 m/s, nearly 10 times the maximum flow for which most commercially available flowmeters are designed. The fuel flow, hydrogen gas in the case of the SSME, reaches velocities of 250 m/s, more than 3 times the 76 m/s upper limit specified for commercially available flowmeters. Flowmeters on the SSME are subjected to pressures as high as 55 MPa (8000 psi) and to cryogenic temperatures. Though cryogenic vortex flowmeters are available, the high operating pressure would probably require design modifications.

The National Aeronautics and Space Administration (NASA) requirements call for a pressure loss at the highest LOX flow rate meter location not to exceed 0.69 MPa (100 psi). This immediately makes a commercially designed meter unacceptable since their pressure loss is 2.8 to 3.5 MPa (400 to 500 psi) at the highest liquid flow rate. Also, to avoid extensive duct modifications, NASA prefers that the flowmeter installs through their standard 11.2 mm diameter instrument ports on the ducts. This also means that the meter must be able to measure flow without an upstream flow conditioner. If the last two requirements can be met, the only modification of the duct required to install a flowmeter would be the addition of one or two standard SSME duct instrument ports in the appropriate place on the existing ducts.

To ascertain that vortex shedding flowmeters could be used under these conditions, tests of flowmeters under simulated SSME duct conditions were necessary. Since commercially available flowmeters cannot meet the ΔP requirements, a suitable meter had to be designed. In addition, since conventional flow is limited to much lower flow velocities, no known existing liquid flow test and calibration facilities were suitable for testing meters.

An inexpensive water test facility was built near the National Bureau of Standards (NBS) Boulder Laboratory to simulate LOX flow. Velocities equal to or greater than those in the SSME ducts can be obtained in this test facility. An existing air test facility was employed to simulate hydrogen flow. Air densities corresponding to SSME duct hydrogen densities have been used for these tests. The maximum hydrogen gas velocities could not be achieved probably because air has a velocity of sound less than one fourth that of hydrogen gas. The meter induces local supersonic velocities in the flow well before the maximum hydrogen gas velocity is achieved.

2. THE VORTEX SHEDDING FLOWMETER

Qualitative descriptions of the vortex shedding flowmeter have been published [2-5]. Only a brief description will be given here.

A cylinder with its axis perpendicular to a uniform flow field whose flow velocity exceeds a minimum value will alternately shed vortices off the sides at nearly constant intervals forming the von Kármán vortex street [6]. The shedding frequency, f, of these vortices is given by

$$f = S \frac{V}{d} , \qquad (1)$$

where V is the flow velocity and d is a characteristic dimension such as the width, W, of the shedding cylinder in a direction perpendicular to both the cylinder axis and the flow direction. The Strouhal number S can be nearly constant over a wide range of flowrates depending on the cross sectional shape of the shedding cylinder. The cylinder, often called a bluff body or shedder bar, will be called a vane in this report. Equation (1) holds even when the vane is placed across the diameter of a pipe when the pipe Reynolds number exceeds 10^4. The vane partially blocks the pipe so the average flow velocity by the vane increases as d increases. The quantities d and V in eq (1) interact so that there exists a value d for which the Strouhal constant is a minimum. Commercial meters are designed to operate around this value of d.

The remaining requirement to create a flowmeter from a vortex shedding element in a pipe is to provide a means to count the vortices shed per unit time. Various techniques are used to convert the transverse flows or transverse pressure pulses into a pulsed electrical signal. Thermal and ultrasonic techniques have been employed to sense the time varying transverse flows. Pressure sensors or strain detecting devices on the vane convert the time varying transverse pressures generated by the transverse flow to an electric signal pulse.

Though papers and brochures describing a particular meter abound, papers detailing the experimental results that led to the choice of a particular design are almost nonexistent. The bulk of the flowmeter development has been done by meter manufacturers who keep this information proprietary. A few papers do present some details of the factors considered in the selection of the vane cross sectional shape or the vortex detection method [7-10].

Early studies of vortex shedding dealt mostly with shedding from circular cylinders. Circular cylinders show a variable Strouhal constant in the 0.2 x 10 to 3.5 x 10^6 Reynolds number range [11]. Later, it was noted that the variable Strouhal constant in this range was a property of the circular cylinder [12]. The few publications that show meter factor for commercial meters as a function of Reynolds number show it to increase or decrease rapidly [4,13] above a Reynolds number of about 2 x 10^5. The decrease has been attributed to cavitation of the test liquid. If the line pressure were raised, cavitation should be suppressed so that some higher maximum Reynolds number is achieved.

To determine whether a vortex shedding meter can measure flow at high flow velocities it is necessary to demonstrate that vortices are shed from a vane with a regular period that varies in a repeatable way over the flow range of interest. If this is confirmed, additional factors must be considered in the process of turning the vortex shedding phenomenon into a useful meter. These are discussed below.

Since the meters used in the shuttle ducts will require calibration, the Strouhal constant need not be constant provided it is single valued over the range of interest and shows no rapid changes. Commercial meters, to reduce the need for calibration, are usually designed to minimize any flow dependence of the meter factor and sensitivity to fluid properties. A calibrated meter

need not have a Strouhal constant independent of whether gas or liquid is the measured fluid.

Vortex shedding is not necessarily a stable process. Even when the shedding frequency is relatively constant, the amplitude can vary to the extent that some of the shedding events either do not occur or do not generate a measurable signal if they do occur. The number of pulses lost at a given flow rate is sufficiently constant that the meter performance is not degraded because of it. Some commercial meter designs have successfully eliminated the complete fade of the signal.

The mechanism that converts the vortex generated forces into an electrical signal must be insensitive enough to other noise and vibrations in the duct that the vortex generated signal magnitude is well above them. One commercial meter examined had a power signal to noise ratio (S/N) of 30 to 40 dB with a noise peak well removed from the signal and 20 dB lower. The requirements on S/N are quite dependent on the measuring electronics. A 20 to 40 dB S/N was considered sufficient in this work. A signal with a line width at half amplitude less than 5% of the line frequency was considered adequate.

The flowmeter still must meet the requirement on pressure loss. The pressure loss at maximum flow, as noted earlier, should be well under 0.7 MPa (100 psid). Even though a commercially available meter greatly exceeds this limit, a commercial meter was tested as a starting point for the work.

3. TEST FACILITIES

Existing water test facilities do not provide adequate pressure to achieve the flowrates required to test to 50 m/s flow velocity. The static head required to provide the flow velocity is about 1.4 MPa (200 psi). High pressure water for the NBS Boulder test facility is obtained from the penstock

of a Pelton wheel driven hydroelectric plant. During the early testing at the plant site, water at pressures up to 5.4 MPa (790 psi) was available. The test facility has since been moved from the hydroplant to the City of Boulder Betasso Water Treatment Plant. This location is at a higher altitude on the same penstock. There only 3.9 MPa (570 psi) maximum pressure is available.

A drawing of the test facility is shown in figure 1. A 1½ in nominal test section was selected for the initial tests to limit the pressure loss in the 3 in nominal piping connecting the test facility to the penstock. The remainder of the test facility piping is 4 in nominal. A 4 in vortex shedding flowmeter provides a measure of the average flow velocity in the test section. This reference meter was calibrated up to about 5 m/s flow velocity. The meter factor, for the present, has been assumed constant to about 10 m/s. A 1½ in meter by the same manufacturer compared to the 4 in meter showed linear behavior to 30 m/s which was 5 m/s in the 4 in meter. This result suggests the 4 in meter is linear to much higher flow velocities.

The 4 in flowmeter is placed ahead of the test section. The test section is a straight section more than 25 diameters in length. Downstream of the test section the pipe diverges to 4 in again. A 4 in globe flow control valve is located just downstream of the diverging section. The test water exited at ambient pressure back to the creek at the hydroplant but exits to the head tank at the water treatment plant. The test piping configuration is sufficiently flexible so that various SSME duct sections and other size ducts can be substituted for the 1½ in straight test section. Flowmeters with bores of 27.9 mm, 41 mm (1½ in nominal) 50.8 mm and 58.4 mm have been tested in this facility.

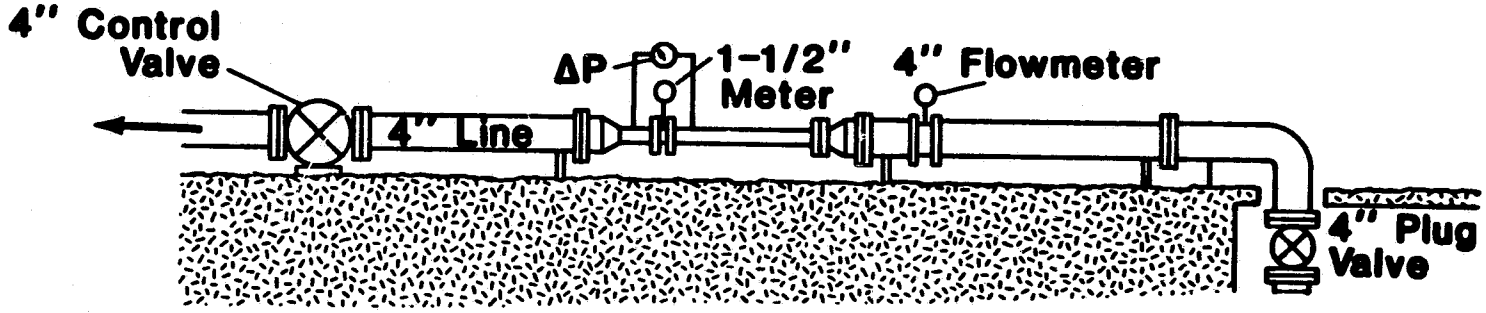

Figure 1. The water flow test facility.

The pressure at the test meter decreases as the flow rate increases not only because of pressure loss in the upstream piping but because of the head lost achieving the velocity. Most of the flowmeters tested were to the limit of the test facility.

The air test facility used for testing flowmeters at simulated H_2 gas densities is portrayed in figure 2. These tests were carried out at a local gas flow test facility [14]. Their choked nozzle flow calibration meter combined with pressure and temperature measurements at the test meter provided the velocity calibration of the test meter.

As shown in figure 2, the test air passes through the test meter first then through the choked nozzle serving as the flow calibration meter. The upstream and downstream control valves are hand adjusted to keep a constant pressure at the flowmeter while the flow is varied stepwise over the test range. The choked nozzle exhausts to ambient and is sized to provide the desired test flow range without exceeding about 2.7 MPa (400 psi) at its inlet side. Even though the control valves were manually operated, the change from one flow rate to the next requires less than a minute.

Because pressures in excess of 7 MPa (1000 psi) are required in the test section to simulate hydrogen fuel densities and because of the high flow velocity requirements, mass flows up to 16 kg/s were required to do the tests.

4. EXPERIMENTAL METHODS

The measurements and measuring instruments evolved as the work progressed so that information obtained in later tests was not always available in earlier tests.

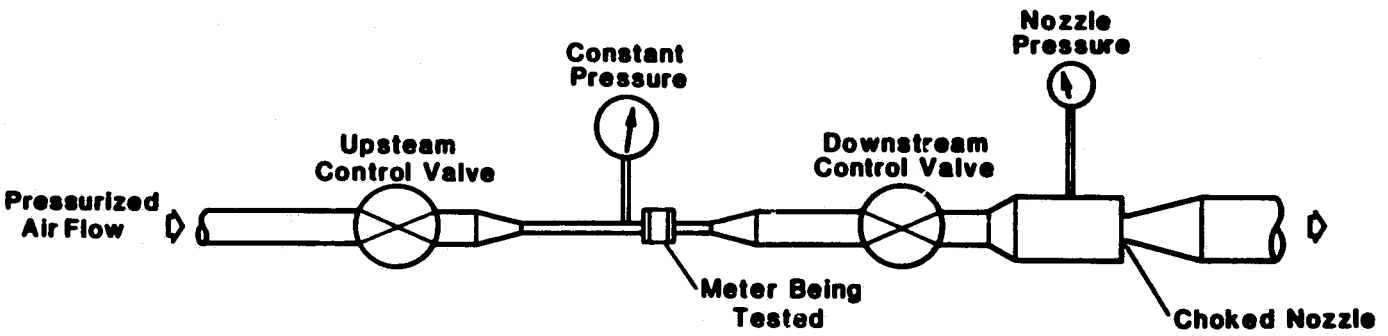

Figure 2. The air flow test facility.

The original thermal detector in the reference flowmeter above velocities of about 5 m/s became noisy and unusable. The thermal detector was removed and a pair of pressure taps inserted in such a way that an external differential pressure transducer could be connected between the two ends of the cross port in the meter vane in place of the thermal sensor. The pulsed pressure signal out of a variable-reluctance differential pressure transducer was sufficiently noise free that it could be amplified and counted directly with no other signal conditioning over the range of 10 to 75 Hz. The frequency is counted to a precision of 0.1 Hz for most tests and estimated to about 0.03 Hz. At low flows, the frequency was stable to better than 0.1 Hz in a 10 s counting interval. At higher flowrates, the frequency is stable to about ±0.1 Hz. Improvements were made to this detecting system that permitted reference flow measurements eventually from about 5 to more than 80 Hz. This range could be expanded from less than 1 Hz to more than 100 Hz by reading the frequency with a Fast Fourier Transform (FFT) spectrum analyzer.

The output frequency signal from the test meter was fed to an amplifier, then through an adjustable narrow band pass filter and to a counter for the earliest tests. Later, a second amplifier and pulse shaper were added between the filter and the counter. In recent testing, the FFT analyzer has been used to measure the frequency, sometimes after the first amplifier and sometimes directly.

An older model analyzer was used first to view the signal spectrum qualitatively and measure the signal-to-noise power ratio (S/N). The FFT analyzer made it possible to measure line width also.

The pressure loss introduced by the flowmeter was measured by a differential pressure transducer connected between two pressure taps, located

about 3 diameters upstream and downstream of the meter. At first, this pressure transducer had a 6.9 MPa (1000 psi) capacity and the line pressure was used to calibrate it by switching the downstream tap to ambient pressure. Later measurements were made with a 0.7 MPa (100 psi) range transducer calibrated against a dial test gage. This transducer was more sensitive and the installation permitted zeroing it at the operating pressure, which eliminated a line pressure induced zero shift.

Swirl was introduced into the test section to test meter sensitivity to it. Swirl was generated by four blades placed at 90° intervals around the pipe on shafts whose axes lay along pipe diameters. The planes of the blades could be angled with respect to the pipe center line. The design was after Padmanabhan and Janik,[15] but strengthened considerably to withstand the higher flowrates. External arms could be positioned from outside the duct to set and provide a measure of the blade angle with respect to the pipe center line. This generator withstood water velocities in excess of 50 m/s without failing.

Straight bladed turbine meters were used to measure the average axial swirl. These were modified commercial turbine meters. The turbine blades bent, then collapsed, at flows above 20 m/s. The collapse started by the blades bending about halfway between the wall and the hub, suggesting that the swirl measured was not well represented by an average swirl angle. Measurement of average swirl in the 1½ in test section with the swirl meter adjacent to the generator gave an average swirl angle that agreed with the generator angles to about 1 or 2°. The difference increased slightly with increasing flow. Eighteen diameters downstream, the measured swirl angle was about 0.56 of the 6.4° generator setting and 0.72 of the 25.6° generator setting at flow velocities of about 6 m/s.

The flowmeters tested in swirl introduced by this generator showed sensitivity to swirl in both the spectrum line shapes and magnitude of the meter factor, as will be discussed later. Meters subjected to swirl generated by elbows still showed sharp spectra. No measurements were made that determined whether any alteration of the meter factor resulted from elbow generated swirl. The swirl generator used by Padmanabhan and Janik[15] seemed to perform satisfactorily. Their larger pipe diameter (4 in) and the lower velocity (one tenth of that in this work), may account for the difference. Apparently, the generator did not satisfactorily produce an elbow generated swirl pattern for the tests reported here. The swirl sensitivities observed in the test meters then were peculiar to swirl generator rather than swirl generated by elbows.

5. FULL VANE METER DESIGNS

Commercial meters all use a cylinder for the vane, but the cross sections vary considerably. Most of the designs have a flat face toward the oncoming flow with sharp 90° corners to the sides. The width of this face is the greatest width of the vane. The advantages of one design over another is information not found in the literature. Whether any of these vane shapes are satisfactory at higher flow rates could be determined only by flow tests. Most of the shapes tested in this work are represented in figure 3. The preponderance of those tested were rectangular in cross section. The dimensions of the various vanes and the reasons for choosing them will be discussed in Section 5. In parallel with the testing of the various vanes, the vane suspension and vortex detection mechanism was developed.

The first flowmeters tested had pressure transducers sensing the oscillating transverse pressure generated as the vortices shed. Because the

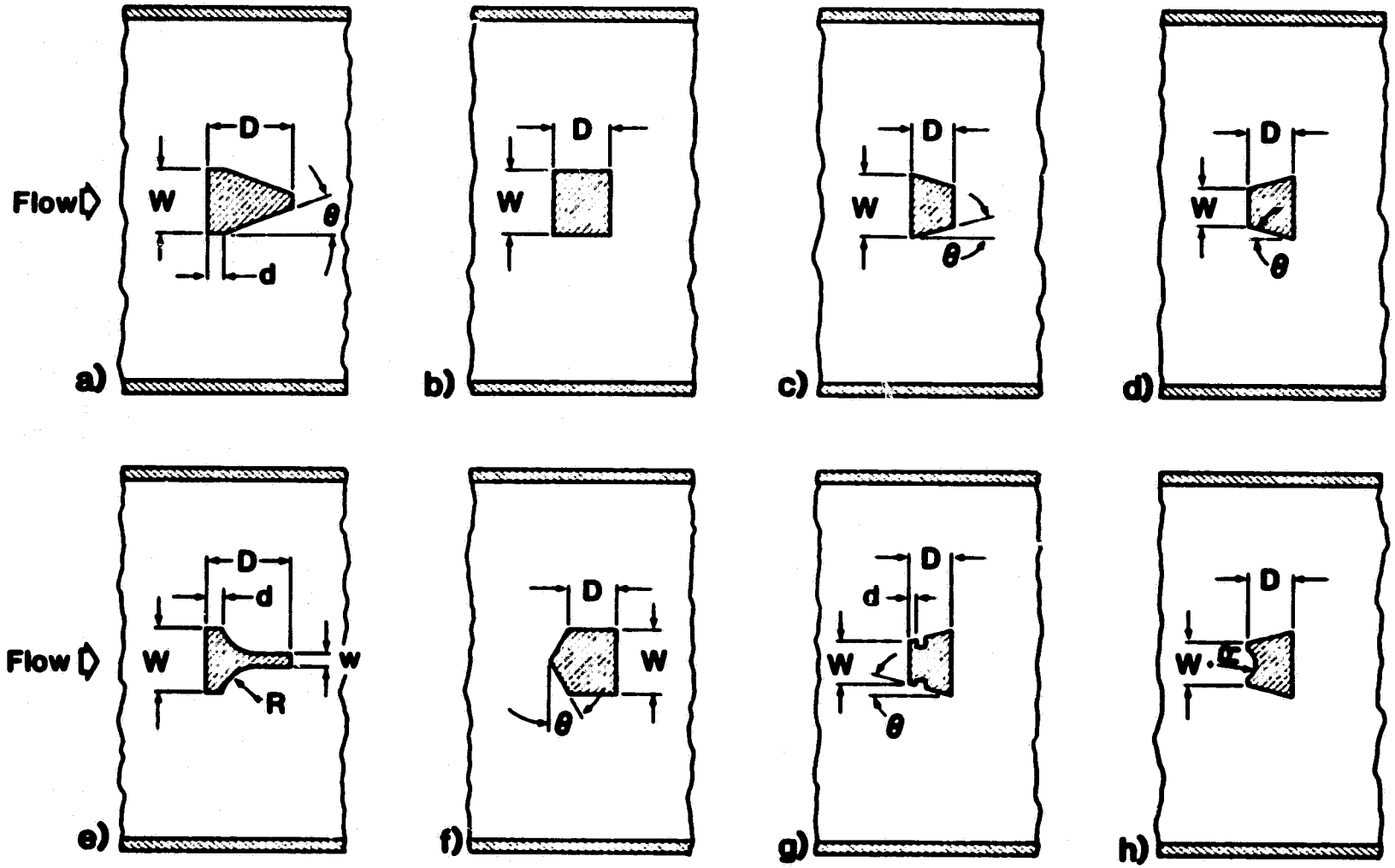

Figure 3. Most of the cross sectional shapes tested.

vane width had to be small to reduce pressure loss and because of the severe environment, installation of an adequate pressure sensing detector on the vane was not feasible. Attention turned to lift sensing methods of vortex detection early in the testing. The time varying transverse pressures result in a time varying transverse force on the vane. The resulting strain on the vane is sensed at some point on the vane support exterior to the flow region.

The first "lift" design, shown in figure 4, was quite successful. The mounting of the vane on one end was a flat spring with the thin dimension perpendicular to the pipe axis. A strain gage was attached to this spring. On the spring end, the transverse motion of the vane was restricted to 0.1 to 0.2 mm by the clearance between the vane and the body at the pipe wall.

This design has some undesirable features for a LOX environment. The vane striking the wall could provide an ignition source. Also, the sharp transitions along the one piece vane cause stress concentrations that result in metal fatigue and failure of the vane.

Figure 5 shows the next successful meter design. The strain gage has been replaced by a lead titanate zirconate (PZT) ferroelectric disc acting as a strain sensor. The sensor was mounted outside the pipe and the strain in the post was transmitted out through a dynamic "O" ring seal. Mounting the sensor outside obviates the need for waterproofing it. The PZT disc produces a strong signal with a much lower strain than that required by a conventional metallic conductor strain gage so the post holding the vane was stiff enough that no stop was required.

The figure 5 design includes another feature. This was the first link vane. The end mountings of the vane are clevises with the clevis pins

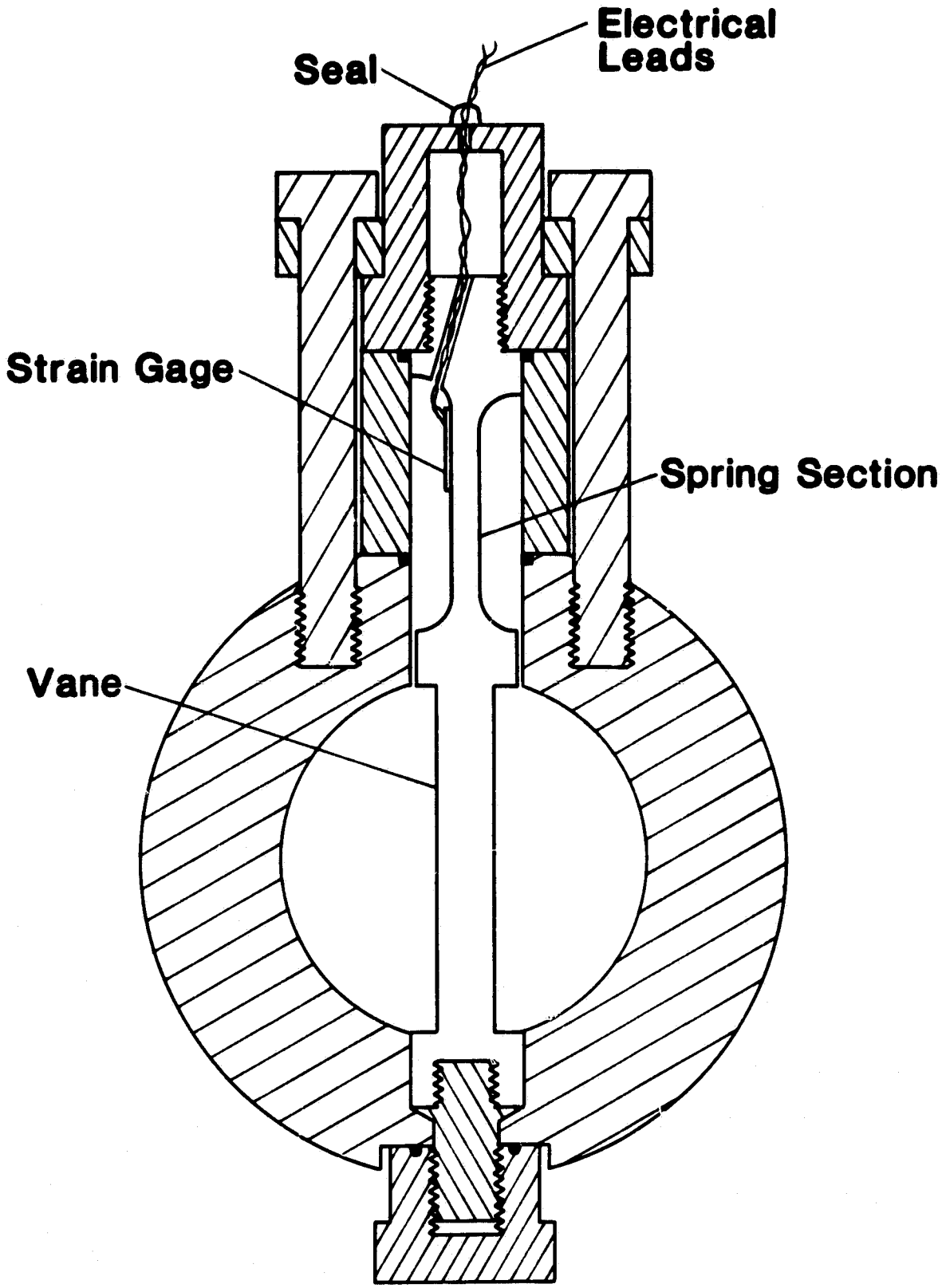

Figure 4. A scale drawing of the spring vane design, the first that produced a strong vortex signal.

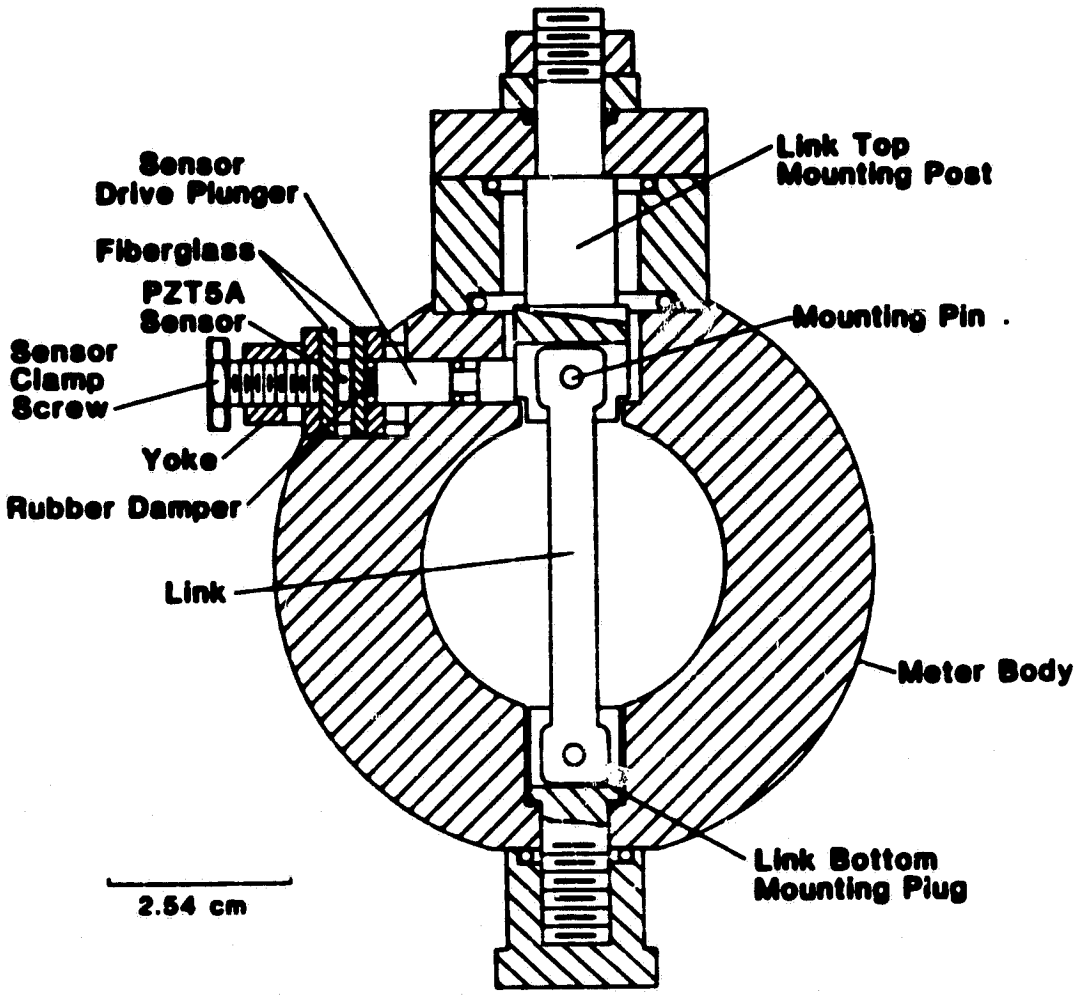

Figure 5. A scale drawing of the link vane design with a PZT strain sensor.

parallel to the flow axis. This design removed the stress concentration at the pipe wall and eliminated vane breakage provided that the vane was made of materials with reasonably good strength.

Figure 6 shows an alternative design for the sensing head and fixed end still using the PZT sensor and the link suspension. A vane and sensor assembly of this design will fit through the 11.2 mm instrument ports of the SSME ducts. The PZT sensor now detects the strain across a notch in the mounting post. The signal from this design was comparable to that from the figure 5 design.

The "O" ring seal on the drive pin must be eliminated for cryogenic service. Figure 7 shows a cryogenic version of the figure 5 design and figure 8 is a cryogenic version of the figure 6 design. The sensor in both of these designs is placed between two metal diaphragms at ambient pressure. The duct pressure acts on the sides of the diaphragms opposite the sensor. The space surrounding the PZT is filled with solid material, mostly metal, equal to the PZT thickness to support the diaphragms against the duct pressure. One conducting surface of the PZT is in contact with the diaphragm while the other surface is insulated by three 0.1 mm thick layers of insulation. The center sheet of insulation is slotted to accept a 3 mm wide by 0.1 mm thick conducting strip which transmits the electrical signal to the outside of the sensor body. The spacer material surrounding the sensor is a series of 0.4 mm thick nested rings permitting some position adjustment of the sensor location along the direction of the drive pin axis. A tube connects the two sides of the sensor assembly to equalize the pressure across the assembly.

The clevis mounting of the vane has been retained on the sensor end. The opposite end has been modified to a bayonet mount. This reduces the chances

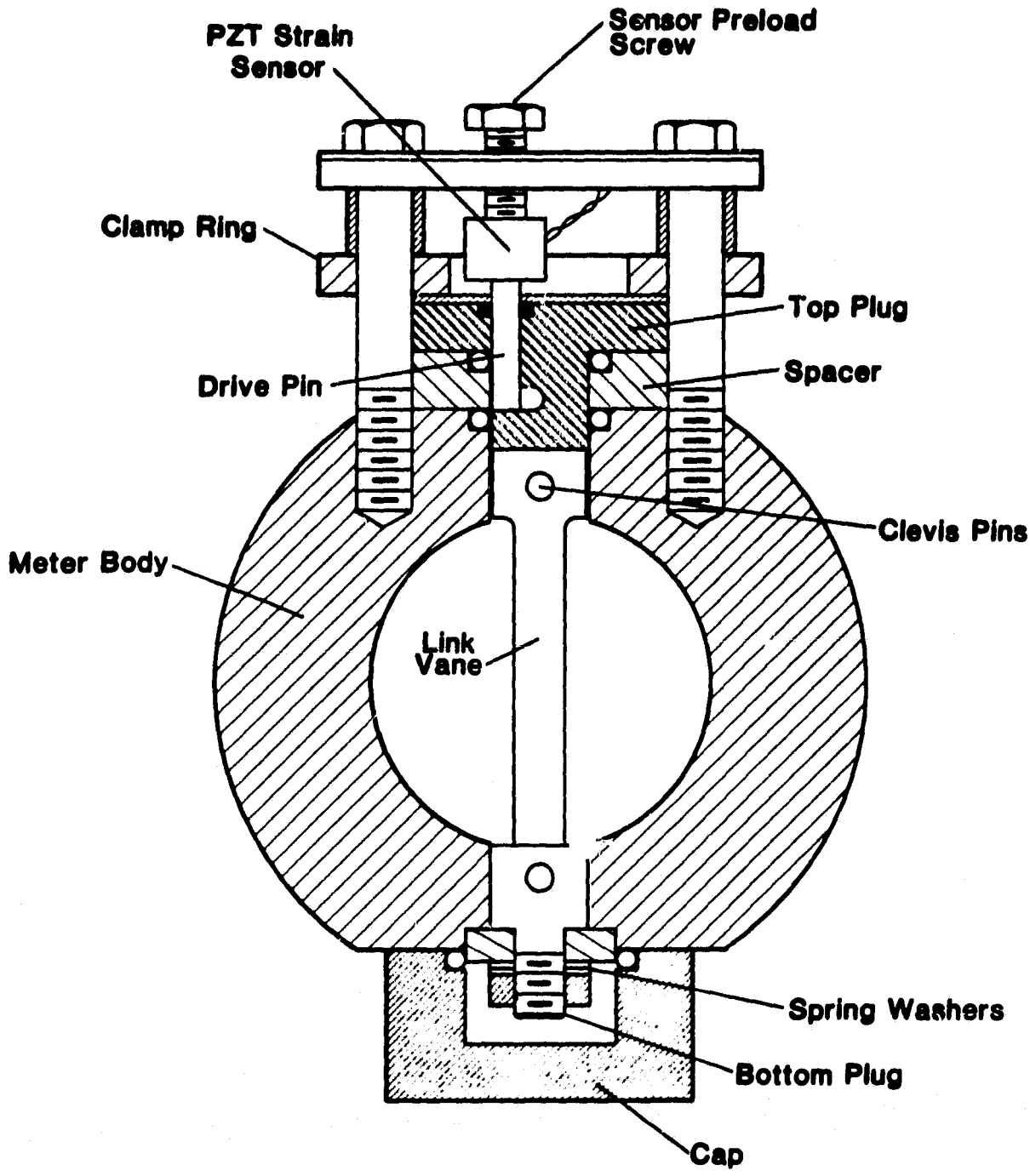

Figure 6. A scale drawing of the link vane design with an axial strain sensor.

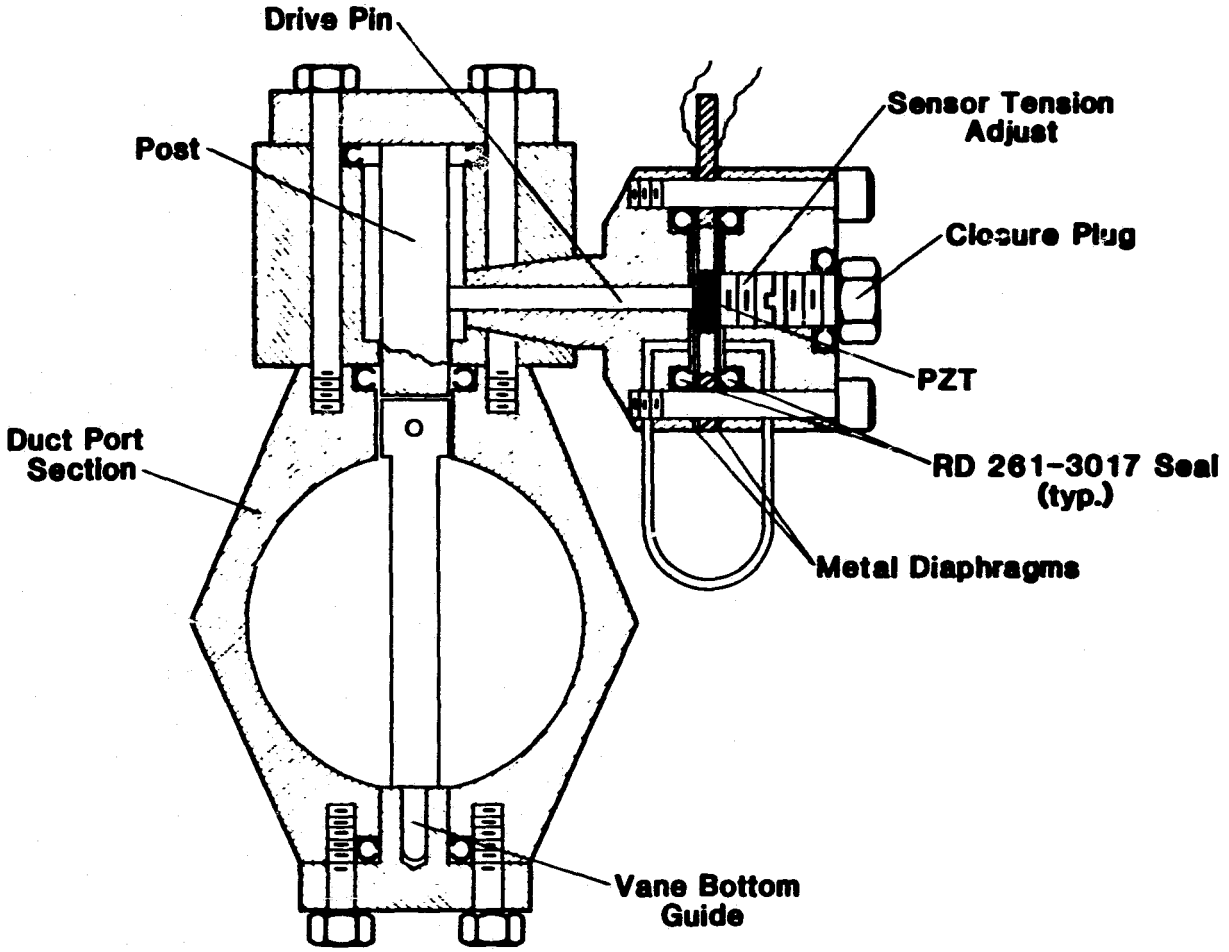

Figure 7. A scale drawing of the meter design for cryogenic service with a side drive sensor.

of transmitting any pipe vibrational mode to the sensor. The axial drive is probably the more sensitive to such a transmittal.

The axial drive sensing assembly shown in figure 8 has the sensor offset from the axis of the duct ports. A more compact sensing head has been realized by placing the PZT concentric to the axis of the ports and introducing an offset into the drive pin. An even more compact arrangement results when the sensor is offset and the pressure seal obtained by soldering, brazing, or welding the diaphragm to the meter body. This seal need have little strength. The strength of the seal is supplied by the bolts that hold the two halves of the body together.

Tests have shown that no significant noise was introduced by pressure fluctuations even though the sensor was subjected to the water test pressure over its full surface. If pressure noise does become significant at the higher SSME duct pressure, the figure 7 or side drive design offers a method for the elimination of that noise. Another sensing head can be placed on the opposite side and connected so in-phase signals cancel while the 180° out of phase vortex generated signals add. This side drive design also should offer the best isolation from pipe vibration.

5.1 Meter Tests in a 1½-Inch Straight Duct

As a starting point, a 1½ in nominal commercially available vortex shedding flowmeter with a 12.7 mm wide vane, vane 1, which has a figure 3a shape, was tested to high flow velocities in the water test facility of figure 1. Table 1 gives design details of those vanes discussed in this report. The meter factor as a function of velocity is shown in figure 9. The Strouhal

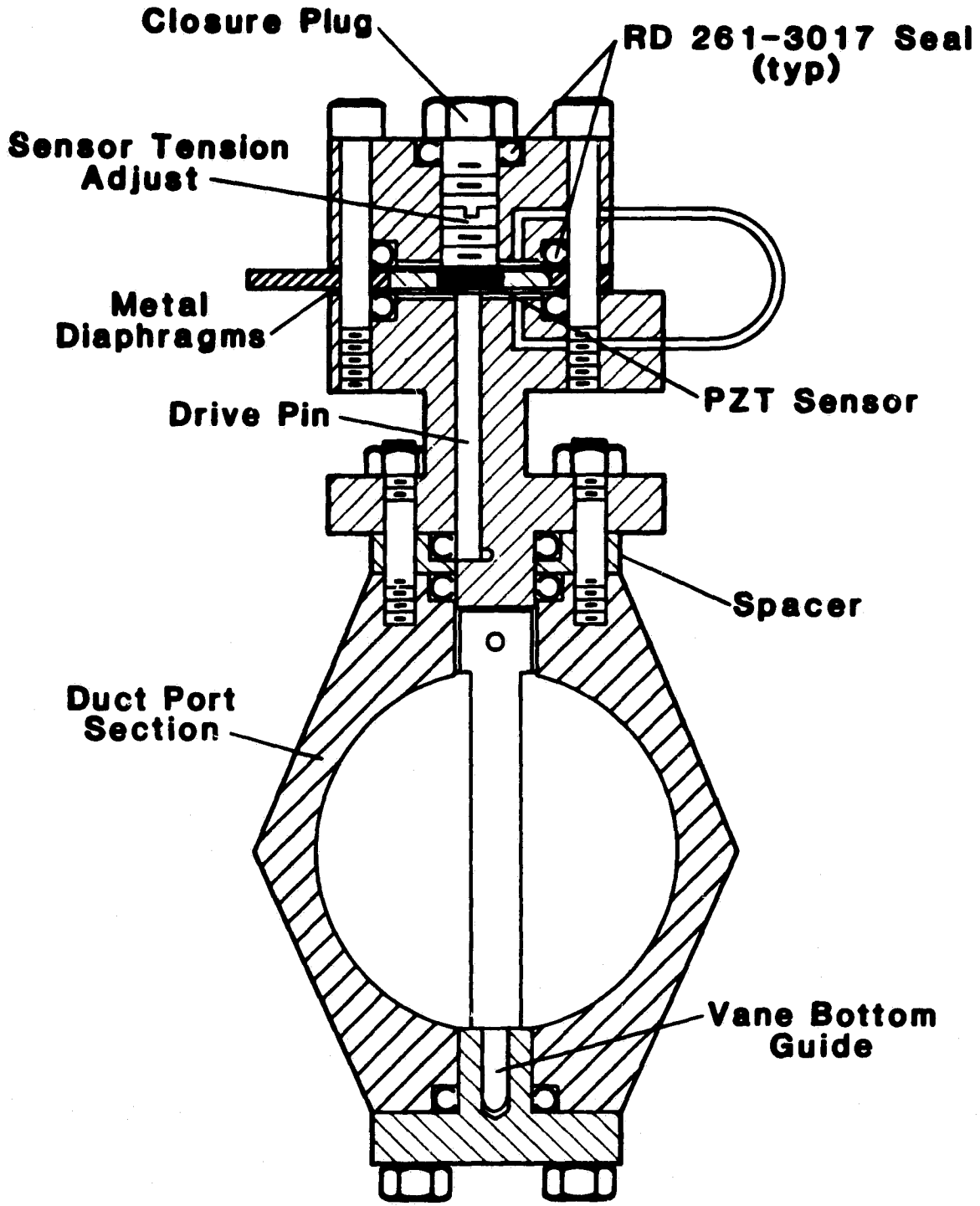

Figure 8. A scale drawing of a design for cryogenic service with an axial drive sensor.

Table 1. Meter descriptions

Vane No.	Pipe Size (mm) Type*	Shape Figure 3	W(mm)	D(mm)	θ (degrees)	Remarks
1	41P	a	12.7	19.1	17	Commercial design meter
2	41P	a	6.35	9.5	17	
3	41S	b	6.35	9.5	17	
4	41S	a	6.12	6.12	0	
5	41L	b	5.1	4.2	0	
6	41L	c	3.8	3.9	10	
7	41L	d	5.1	4.3	2	
8	59L	b	7.6	4.2	0	
9	59L	b	7.6	5.1	0	
10	59L	b	7.6	6.5	0	
11	59L	b	6.4	4.25	0	
12	59L	b	9.5	6.4	0	
13	51B	b	6.4	4.9	0	
14	59L	b	7.6	4.2	30	d=3.8 mm(corners beveled)
15	59B	b	7.6	5.1	45	d=4.6 mm
16	41L	a	5.1	7.6	17	
17[1]	41L	e	5.1	7.6	--	d=17 mm R=0 mm w=2 mm
18	41L	b	5.1	3.4	0	
19	59B	g	7.6	5.9	0	d=0.5 mm Front face curved. Radius = 3.8mm
20	59B	a	7.6	6.2	15	d=1.3 mm
21	59B	a	7.6	6.2	19	d=0.5 mm
22	59B	e	7.6	6.4	--	" R=0 mm
23	59B	g	7.6	6.4	0	"
24	59B	a	7.6	5.3	19	"
25	59B	c,d	6.5	6.4	3	"

Table 1. (cont'd) Meter descriptions

Vane No.	Pipe Size (mm) Type*	Shape Figure 3	W(mm)	D(mm)	θ (degrees)		Remarks
26	59B	e	7.6	5.1	--	d=0.5 mm	R=0 w=6.5 mm
27	59B	c,d	7.6	6.4	3		
28	59B	c,d	7.6	5.1	5		
29	59B	c,d	7.6	5.1	3		
30	41DC	d	5.1	4.3	3		
31	41DC	d	5.1	4.3	3		
32	41DC	b	5.1	4.3	--		
33	59DC	d	7.6	2.4	3		
34	59DC	b	7.5	7.5	--		
35	59B	b	7.6	7.6	--		
36	59DC	b	7.5	6.5	--		
37	59B	b	7.6	6.5	--		
38	59B	b	7.5	6.5	--		
39	59DC	b	7.5	6.5	--		
40	59DC	b	7.5	6.5	--		
41	59DC	b	7.6	6.5	--		
42	59DC	b	7.6	6.5	--		
43	59DC	d	7.6	6.5	2		
44	59DC	b	7.6	6.5	--		
50	41C	b	7.6	7.6	--	20.3 mm	Vane length
51	41C	d	5.1	4.3	2°	17.8 mm	"
52	41C	d	5.1	4.3	2°	17.8 mm	"
53	41C	g	5.1	4.3	2°	17.8 mm	"
54	59C	d	7.6	6.4	2°	25.4 mm	"
55	59C	d	7.6	6.4	2°	28.5 mm	Vane length A-286
56	59C	d	5.1	4.3	2°	22.9 mm	Vane length

Table 1. (cont'd) Meter descriptions

Vane No.	Pipe Size (mm) Type*	Shape Figure 3	W(mm)	D(mm)	θ (degrees)	Remarks
57	59C	d	5.1	4.3	2° 33.5	mm vane length A-286
58	41R	9.8 mm ID	16.4 mm OD	2.5 mm depth		
59	41R	11.7 mm ID	16.3 mm OD	1.9 mm depth		
60	41R	11.7 mm ID	16.3 mm OD	1.9 mm depth		
61	41L	b	5.1	3.4		
62	41L	a	5.1	7.6	20°	d=0.3 mm

*P, Pressure sensor; S, Spring mount; L, link mount; B, bayonet on fixed end; DC, double cantilevered; C, single cantilevered; R, ring vane

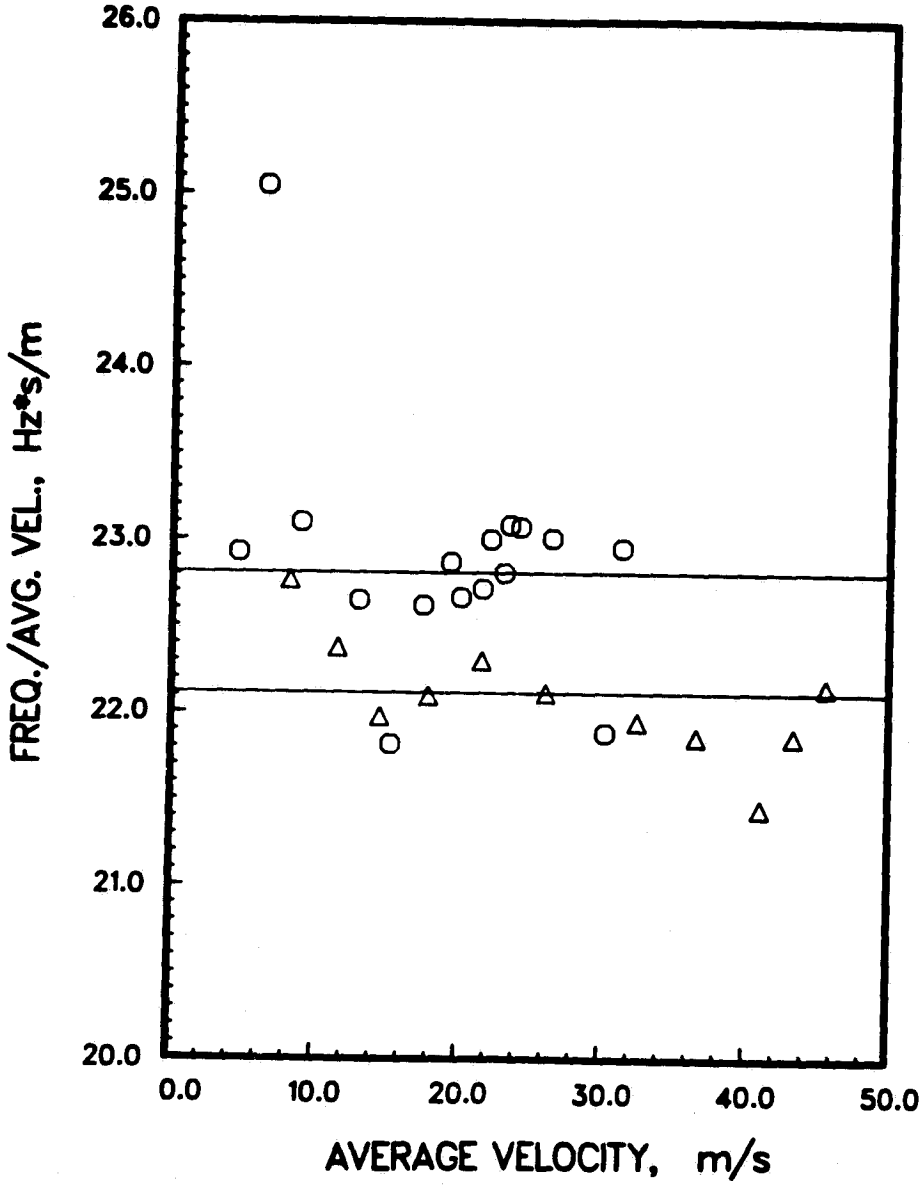

Figure 9. The meter factor as a function of velocity. Circles, a 1½ in commercial design meter, vane 1. Triangles, same meter body with a vane half as wide, vane 2.

number can be obtained by multiplying the meter factor by the vane width in meters from Table 1 for this and all subsequent plots. At the time of these first tests the reference meter was not yet performing well and the counting rate from it was read to only 0.5 Hz. At velocities above 25 m/s in the test meter, the reference meter became too noisy to read correctly. Because the pressure loss across the vane remained proportional to the flow velocity squared to about 35 m/s, the meter factor probably remained constant to nearly that flow velocity.

The vortex detector for this meter was a magnetic shuttle disc driven back and forth by the pressure transmitted through ports from opposite sides of the vane to opposite sides of the disc. This detector, made to detect vortices in flows up to 7 m/s, was destroyed by the much higher flowrates. Figure 10 shows why. The pressure loss, ΔP, across a meter should be proportional to the square of the flow rate or velocity, V. The pressure across vane 1 is 25 times larger at 35 m/s than 7 m/s and, since the transverse pressure across the vane is proportional to the axial pressure loss, the destruction of the detector is not surprising.

The pressure loss across vane 1 follows the ΔP versus V^2 curve up to about 38 m/s, where the pressure loss jumps well above the curve. This jump probably signals the onset of cavitation at the vane. If the pressure in the duct were high enough to suppress cavitation, the pressure loss would pass close to the value estimated by the manufacturer of the meter shown by the plus point in figure 10.

The pressure loss in the shuttle duct flow meters should not exceed 0.7 MPa (100 psi) which means the vane width must be reduced. The meter factor for vane 2 is shown in figure 9. This vane also has the cross sectional shape

of figure 3a but is scaled down so that the width is 6.4 mm or half that of vane 1. The pressure loss was only about one fourth that of vane 1, as shown in figure 10. The meter factor, by the Strouhal relation, would be twice as large as for vane 1. Instead, it is actually smaller than that of vane 1. This means that the velocity past vane 1 is actually more than twice the velocity past vane 2 because of the extent that vane 1 blocks the pipe.

The first method of obtaining a vortex generated signal from a 6.4 mm wide vane was attempted with a pair of transverse oppositely directed ports with a ΔP transducer connected between them. Though a vortex generated signal was obtained, the S/N was poor. Next, a single port was provided in one side of the vane and a high pressure transducer referenced to ambient pressure served as a detector. Though this detection method worked somewhat better, possibly because of the larger port, the S/N was still poor. In addition, the pressure pulsations and the vibrations rather rapidly destroyed the piezoresistive transducers used as detectors.

The transition from the vane cross section to the pipe walls is sharp in commercial meters. The test vanes were made of brass for ease of machining and were built with sharp transitions to the wall also. The forces on the vane at the highest flow velocities was sufficient to fatigue and break the vanes out. Though it has not been difficult to find designs that resist fatigue, failure at the high flow velocities was not uncommon if special care was not taken in the design to eliminate high stress concentrations.

Sensing vorticies via pressure ports did not provide a good S/N, probably because of the rather long porting between the sensing location and the pressure transducer and the small inlet area of the port. Furthermore, strength requirements ruled against introducing even a miniature pressure

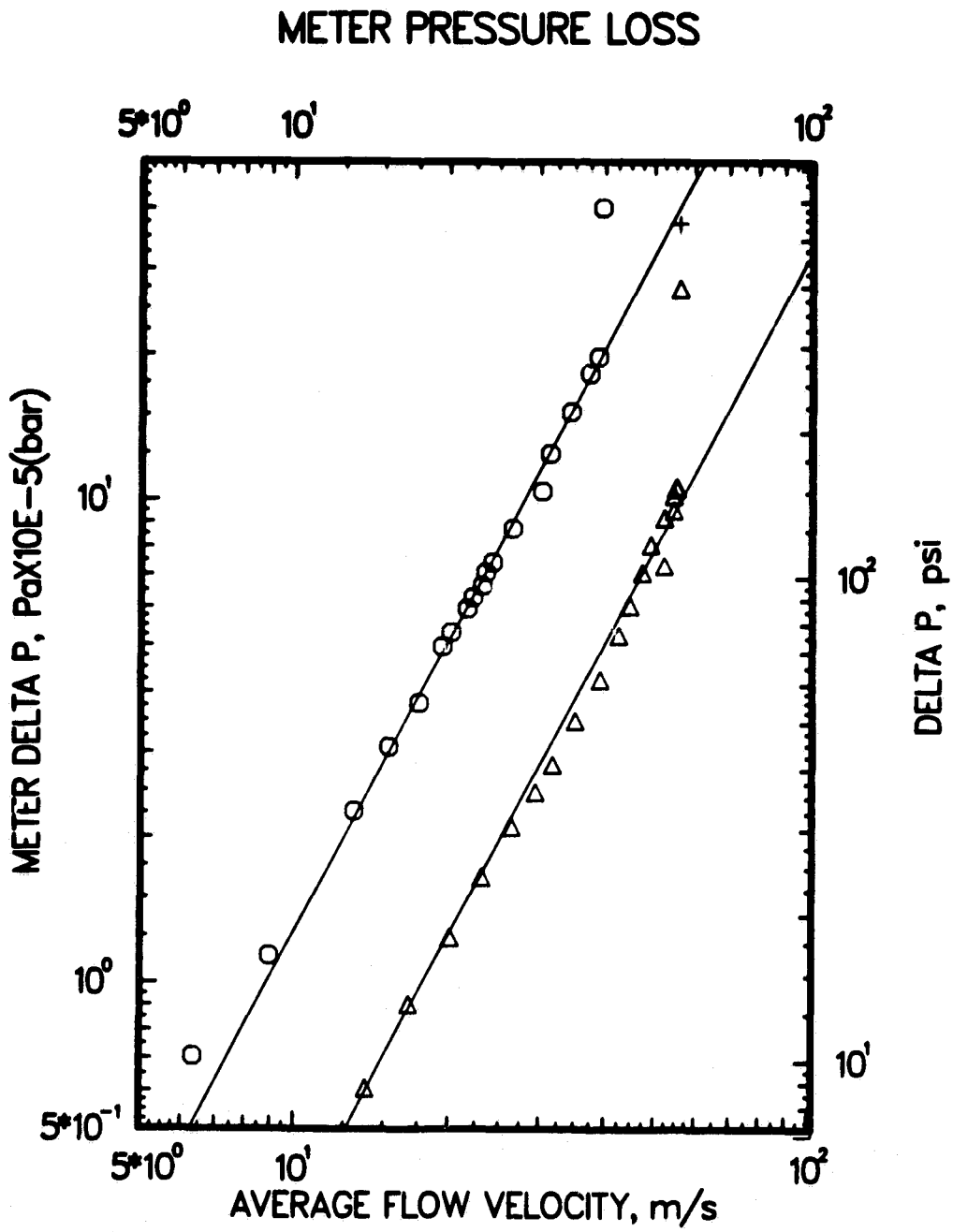

Figure 10. Pressure drop as a function of flow velocity for vane 1, circles, and vane 2, triangles.

sensor on the vane because the vane size is so small that the strength of the vane could not be safely reduced by machining a recess for a sensor. Because of this limitation, pressure sensing of the vortices was discarded in favor of strain sensing.

Some meters of the design shown in figure 4 were constructed. Vane 3 was a 6.4 mm wide vane with the figure 3a cross section and vane 4 had the figure 3b cross section with W=D=6.1 mm. These vanes were tested before a spectrum analyzer was used to examine the signal. However, the signal to noise ratio was qualitatively quite high. The filter that had been narrow banded and adjusted to follow the vortex generated signal could be wide banded to cover the full flow range and not increase the counting rate by more than a few counts over that obtained through a narrow band pass. The meter factor as a function of velocity is shown in figure 11 for vane 4, which is the more nearly linear meter of the two. The total scatter of these data is less than 1% in the nearly linear segment of the curve. Vane 3 was less linear than vane 4, with the meter factor decreasing as the flow increased prior to the sharp increase at 45 m/s.

This sharp increase in meter factor at the highest flow rates was encountered in most tests. Though it has not been demonstrated unequivocally that this is a cavitation phenomenon at the vane, the flow velocity at which this sudden increase in meter factor occurs is dependent on line pressure. The meter factor remained constant to a higher velocity at the hydroplant test site than at the Betasso Treatment Plant test site where the pressure is 15 MPa (220 psi) lower.

Hanging weights on the middle vanes 3 and 4 provided a calibration of the output voltage as a function of transverse force. Assuming this transverse

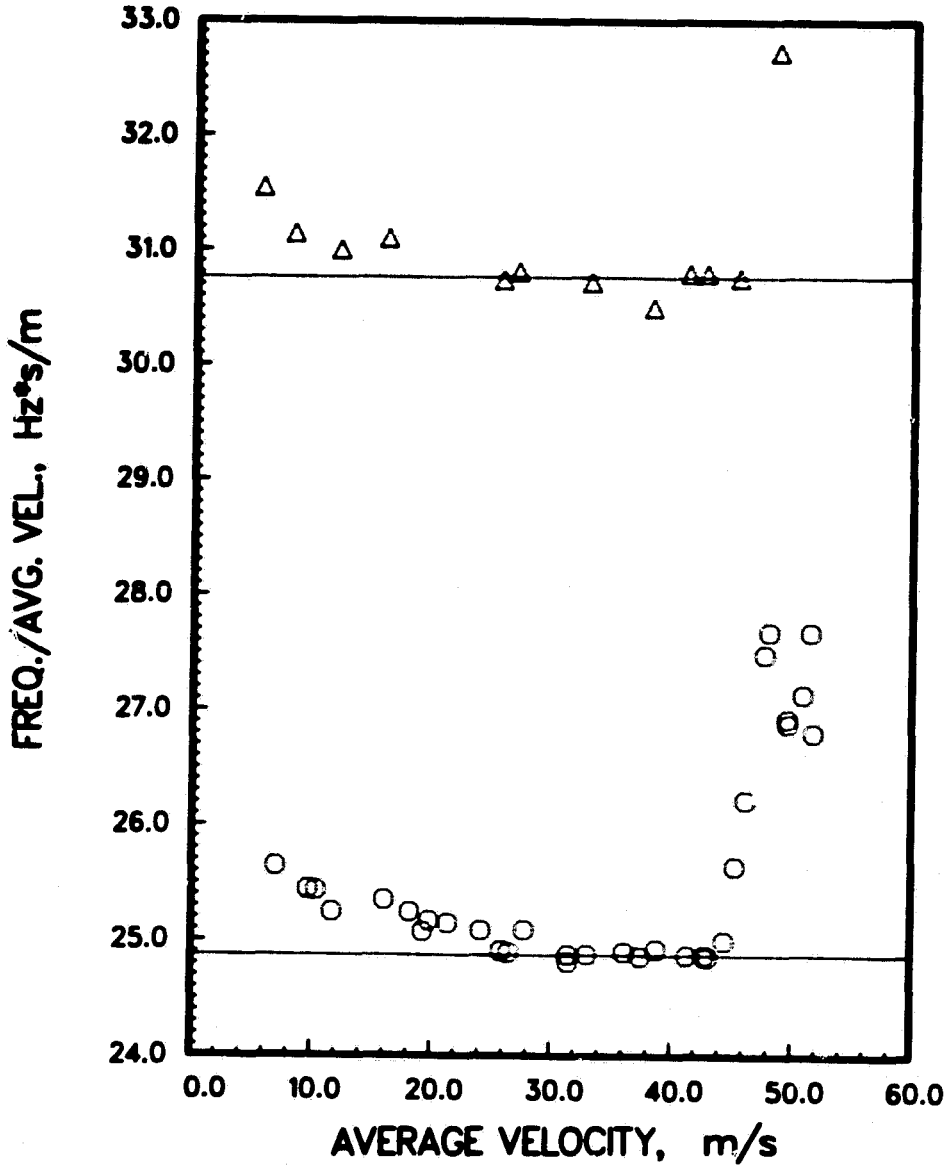

Figure 11. The circles show the meter factor of vane 4 as a function of velocity. The triangles show the meter factor of vane 5.

force results from a uniform transverse pressure and dividing this force by the transverse area of the vane gives a value for the transverse pressure. The magnitude of this transverse pressure was between 3 and 4 times the axial pressure drop to an estimated accuracy of 30%.

The first successful flow meter using a PZT sensor was vane 5. This vane, made of beryllium copper, has since undergone several hours of testing without failure, attesting to the superiority of the link vane over a single piece vane and mount where fatigue resistance is concerned. Vane 5 was only 5.1 mm in width to further reduce ΔP. The meter factor of this vane increased over that of vane 4 as shown in figure 11.

The width was further reduced to 3.8 mm for vane 6. This vane vibrated so violently that it was audible some distance from the pipe. This vane was made of beryllium copper and did not break during the short test but considerable wear occurred on the vane ends, clevis and clevis pins. The meter factor was not constant. No further testing of full vanes less than 5.1 mm in width was done in the 41 mm ID meter size. For a 5.1 mm vane width, the ratio of vane width to pipe diameter, W/D_p, is about 1/8. Most of the testing has been carried out with vanes with W/D_p around this value.

A meter of a figure 5 design, with vane 5, was subjected to swirling flow from the swirl generator. The meter was 18 diameters downstream and the generator vane angles were 11.5, 15.3, and 19.2°. The meter factor decreased with increased generator angle as shown in figure 12. The spectrum line generated by the vortex shedding broadened and S/N decreased with increasing generator angle. The swirl introduced by the generator did degrade the flowmeter performance above generator angles of about 11°.

The figure 6 design meter was first tested with vane 7. This sensing head and the slightly trapezoidal vane cross section was carried over from

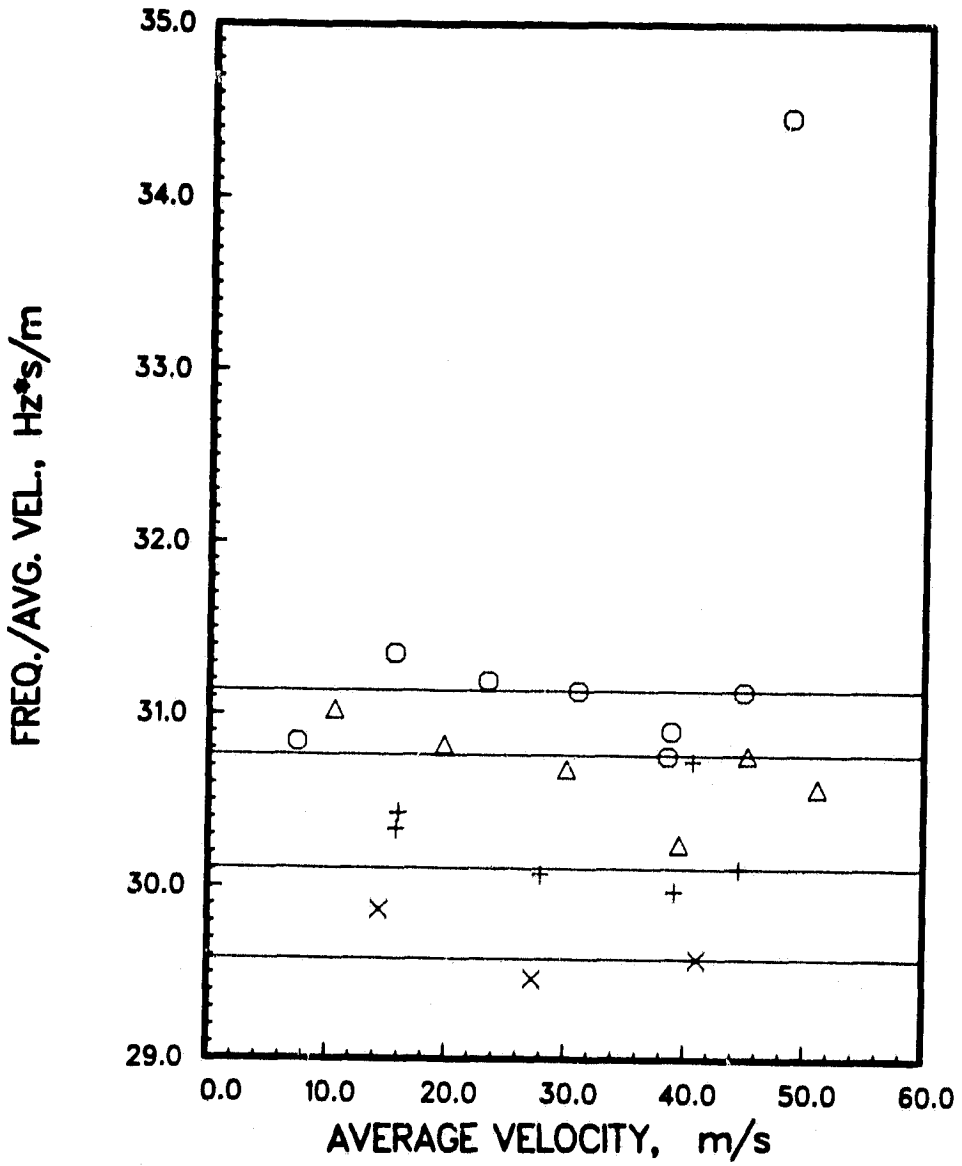

Figure 12. The effect of swirl on the meter factor of vane 5 as a function of the generator angle. Circles, 0°; triangles, 11.5°; pluses, 15.3° and X's, 19.2°.

cantilevered vane tests which are discussed in a later section. The meter factor was essentially the same as obtained for vane 5, figure 11. The spectrum lines, the first analyzed by a Fast Fourier Transform analyzer (FFT),were comparable in width and S/N with those obtained from vane 5 in the figure 5 design meter.

5.2 Meter Tests in a SSME LOX Duct

The highest flow velocity LOX duct on the SSME requiring a flowmeter is the 58.4 mm (2.3 in) ID Low Pressure Oxygen Turbo Pump drive duct or RS007035 (7035) duct. Prior to testing flowmeters in this duct, a straight test section of this approximate ID (actually 59 mm) was built to establish that the 41mm ID test results could be scaled up to this larger duct size. This test section was a single piece of pipe approximately 25 diameters in length with a pair of diametrically opposed ports brazed to it 20 diameters from the inlet end.

Tests with a vane assembly of a figure 6 design showed that 41mm vane results did scale up to the 59 mm size. Several rectangular shapes of different dimensions were tested to better define an optimum vane width and depth. Figure 13 shows the variation of the meter factor as a function of the depth for vanes 8, 9, and 10, all rectangular vanes. These vanes were all 7.6 mm wide (W/D_p =0.129). As figure 13 shows, vane 9 with a depth to width ratio (D/W) of 2/3 has the most constant meter factor over the flow range. The vane with the most constant meter factor often produces the narrowest spectrum lines and best S/N and shows the least signal fade. Figure 14 shows test results from vanes 9, 11, and 12 which all had D/W = 2/3 but different widths. The meter factor of vane 9 was the most constant over the test range.

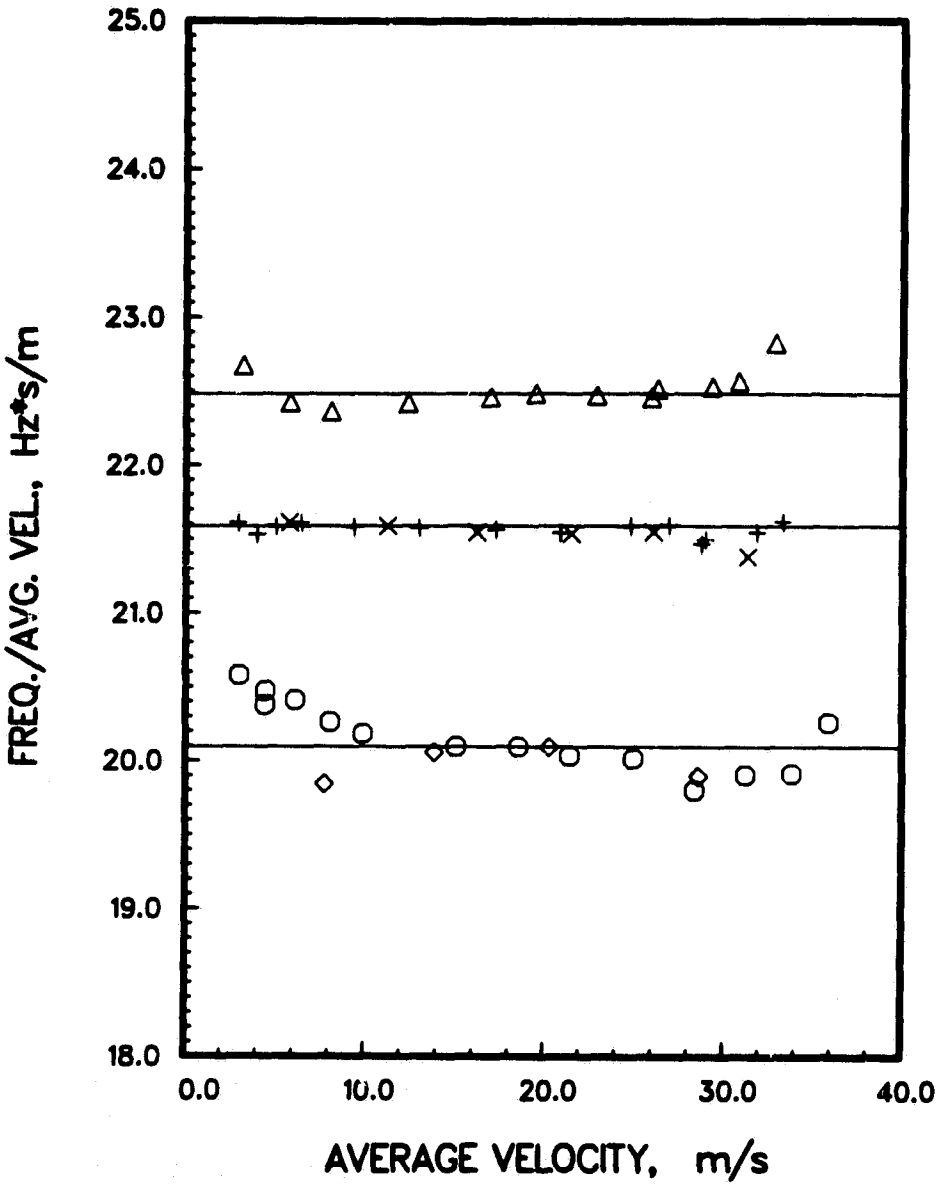

Figure 13. The meter factor of a 59 mm bore meter for vanes of the same W but different D. Triangles, vane 8; plus and X, two tests of vane 9; and circles and diamonds two tests of vane 10.

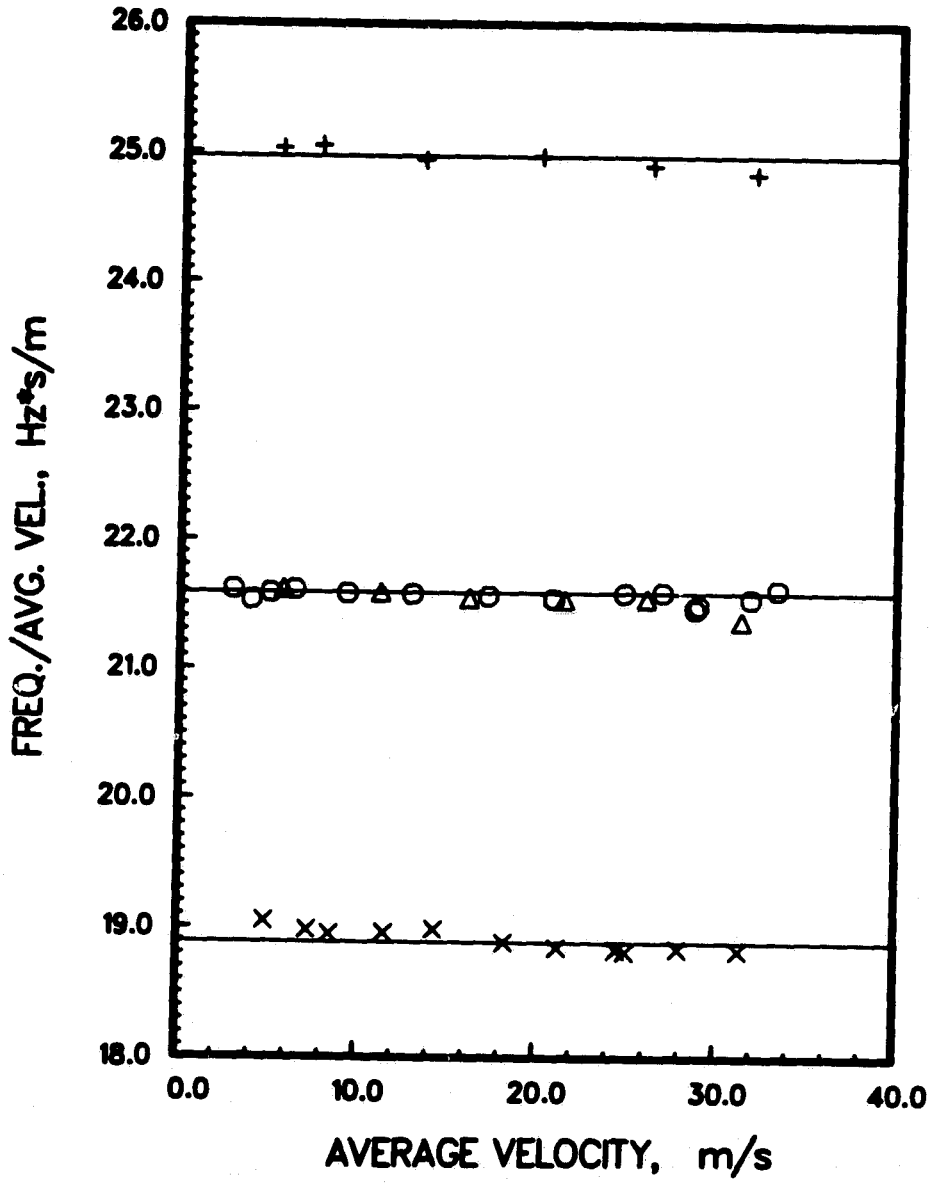

Figure 14. The meter factors of three vanes of different widths with D/W=0.67. Pluses, vane 11; circles and triangles vane 9 (shown also in figure 13); and X, vane 12.

Figure 14 shows that the frequency, f, varies inversely with W as the Strouhal equation suggests. It is not proportional, however, because the wider vanes approach the minimum of S as a function of W. Figure 13 shows that the shedding frequency is also inversely proportional to the vane depth D.

Figure 15 shows ΔP as a function of water flow velocity for a number of vanes tested in 59 mm bore test section along with the pressure loss with no vane installed. The pressure loss is around 0.25 MPa (37 psi) maximum at 30.5 m/s (100 ft/s). The maximum liquid velocity in the RS007035 duct to be measured is presently 28 m/s (92 ft/s).

Figure 16 is a drawing showing the layout of the last half of the 7035 duct. The last three bends from the exit end forward are 35°, 30° and 60° bends and in almost the same plane. The duct enters the plane of the figure perpendicularly. Three 45° bends, then a 90° entrance bend, precede this perpendicular bend. No more than two adjacent bends in the front end of the duct are in the same plane. Out-of-plane bends can generate swirl which, if sufficiently large, degrades the meter performance according to the results obtained in the 41 mm ID tests, figure 12. The distortion of the flow by a single elbow would also be expected to degrade the meter performance.

The first measurements of flow in the 7035 duct were done with a figure 6 design meter placed at the exit of the duct as illustrated in figure 16. This meter consisted of an approximately 4 diameter long 58.6 mm ID meter body. The vane in this meter was located about 3.7 diameters from the exit of the final 35° bend. Spectrum lines from this flowmeter are shown in figure 17. When the vane was perpendicular to the plane of figure 16, the top spectrum of figure 17 was obtained. When the axis of the vane was parallel to the plane of the bends, the much poorer spectrum line shown in the bottom of figure 17 was obtained. The variation of performance with orientation must result

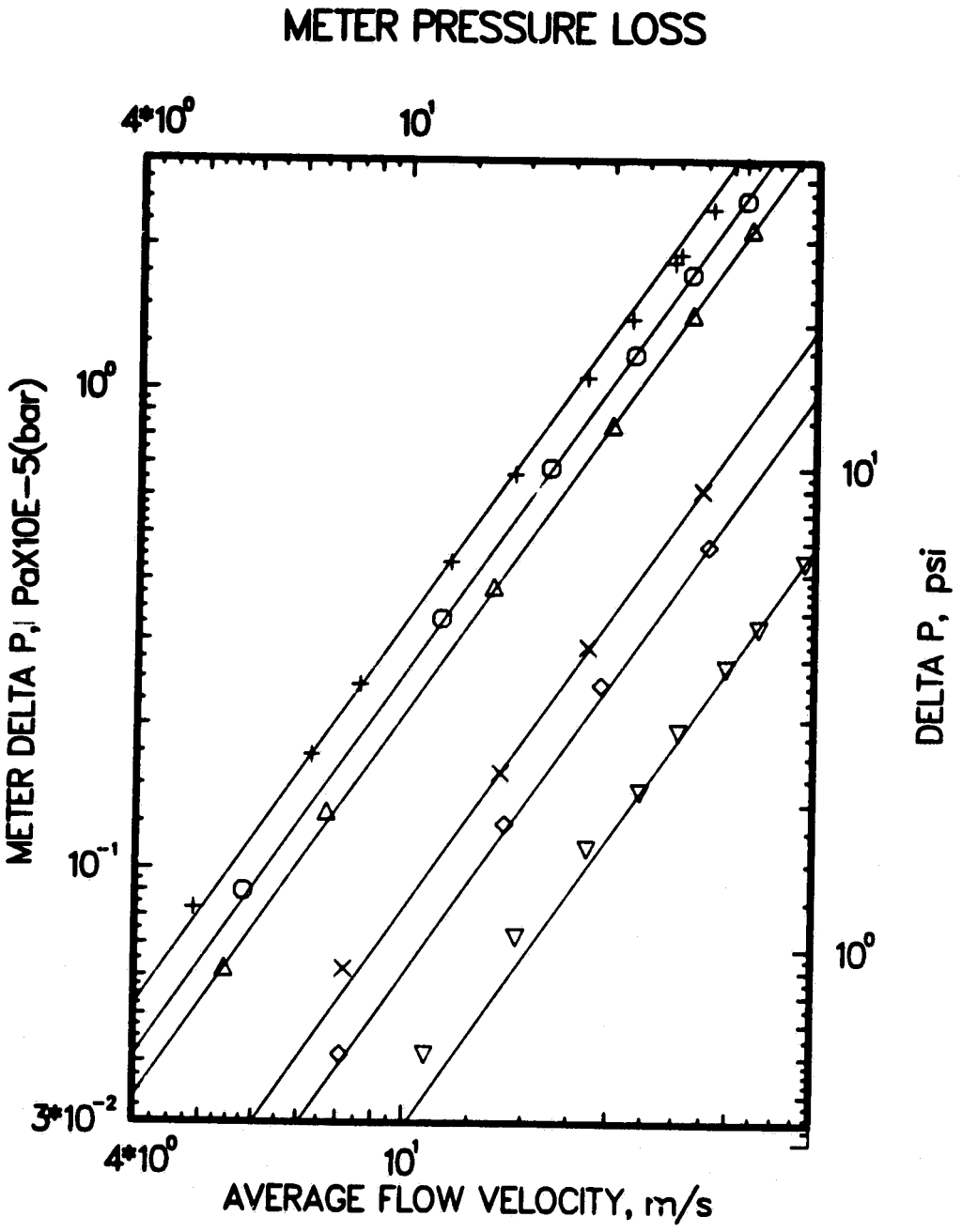

Figure 15. Pressure drop as a function of flow velocity for various vanes in the 59 mm bore test section; pluses, vane 12; point up triangles, vane 9; circles, vane 11; X's, vane 54; diamonds, vane 56; and point down triangles, pressure drop between taps with no vane present.

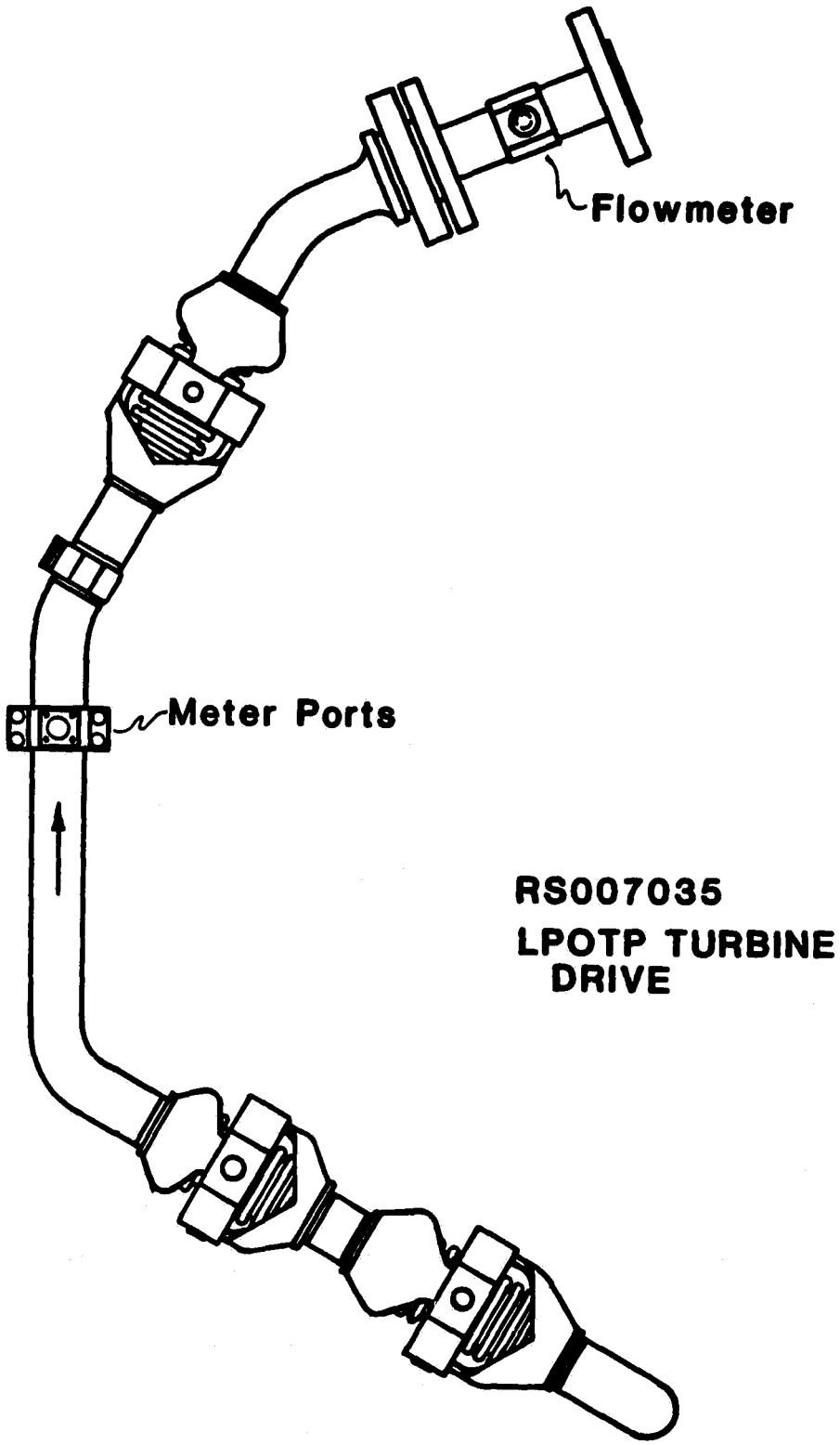

Figure 16. Diagram of the last approximately 1/3 of the RS007035 duct to the space shuttle main engine. The location of an exit end test meter and the pair of ports added for a meter installation is shown.

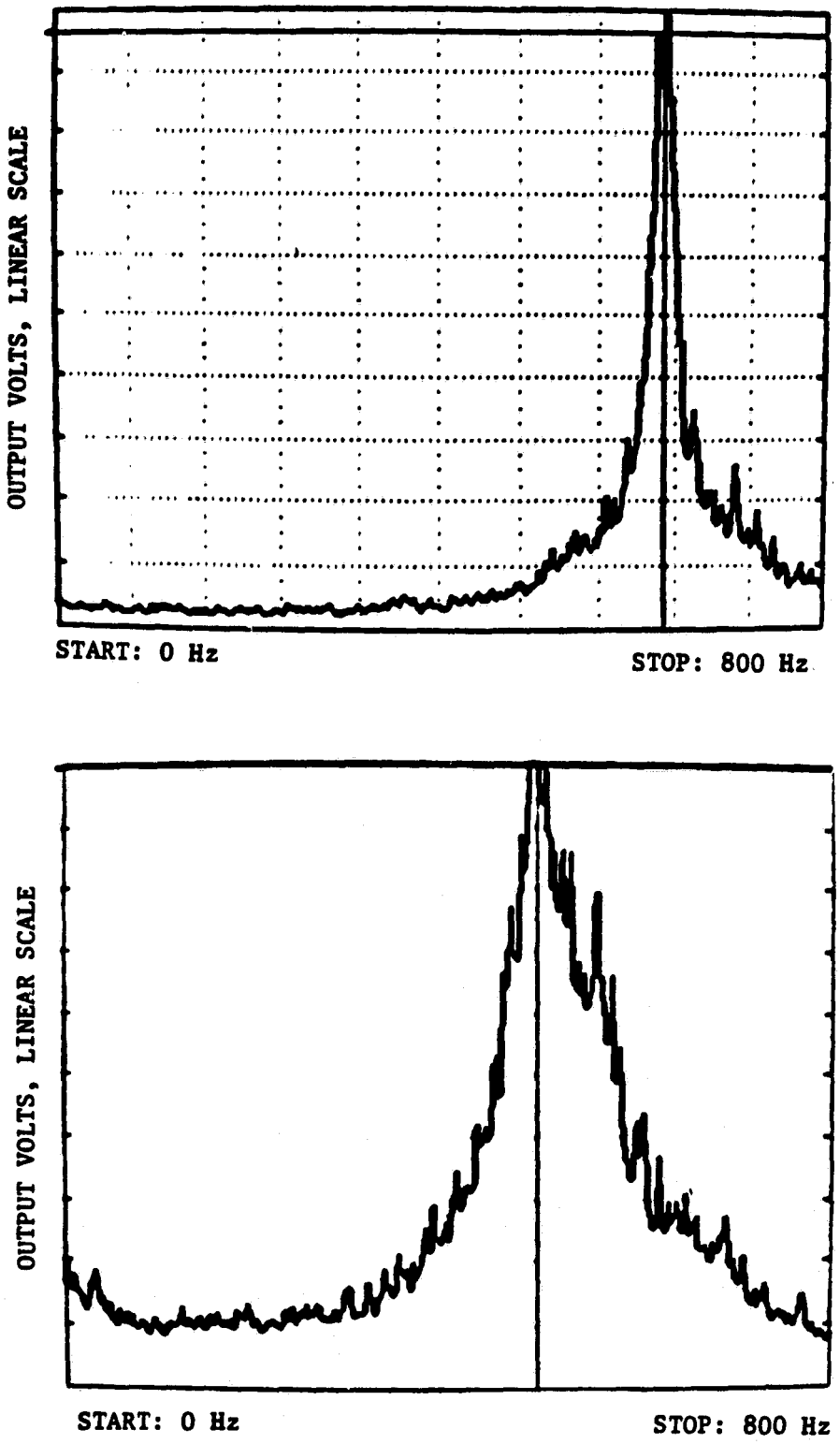

Figure 17. Spectrum lines with vane 9 in the meter at the exit end of the 7035 duct. Top, vane perpendicular to the plane of bends. Bottom, vane parallel to the plane of bends.

from the flow distortion at bends. A similar result was reported by Cousins et al. [7]. Distortion is much higher in the plane parallel to the bend than it is in the plane perpendicular [16]. This result suggests that though the average velocity on the two sides of the vane perpendicular to the plane may differ, the velocity profile along the edge of the vane must be relatively constant. The test results differed from the straight duct tests in that the meter factor of vane 9 decreased with increasing flow while the meter factor of vane 8 was constant.

Two opposite instrument ports were silver brazed to the duct at the location shown in figure 16. This location was chosen as a result of the tests of the meter at the duct exit. The axis of these ports is approximately perpendicular to the planes of the preceding 60° bend and the succeeding 30° bend. The ports were placed about two diameters ahead of the 30° bend. Not only were sharp spectrum lines produced by a meter of the figure 6 design, figure 18, but the power S/N exceeded 30 dB. The meter factor of vane 8 is shown in figure 19. The total scatter from a constant value is less than ±0.5% up to 32 m/s above which it increases sharply, probably because of cavitation.

A swirl measurement at the exit of the 7035 duct with a straight bladed turbine gave an average swirl angle of 2½°. The 2½ degree average swirl at the duct exit could be two to three times higher at the meter location since the swirl must decay from the meter ports to the end since no out-of-plane bends are present between the meter and the exit to generate more swirl. The spectrum lines, figure 18, were as narrow as any measured which suggests that the swirl from the duct bends did not affect the meter. The swirl generator producing this estimated 5 to 7° of swirl would certainly have broadened the spectrum lines to a visible degree.

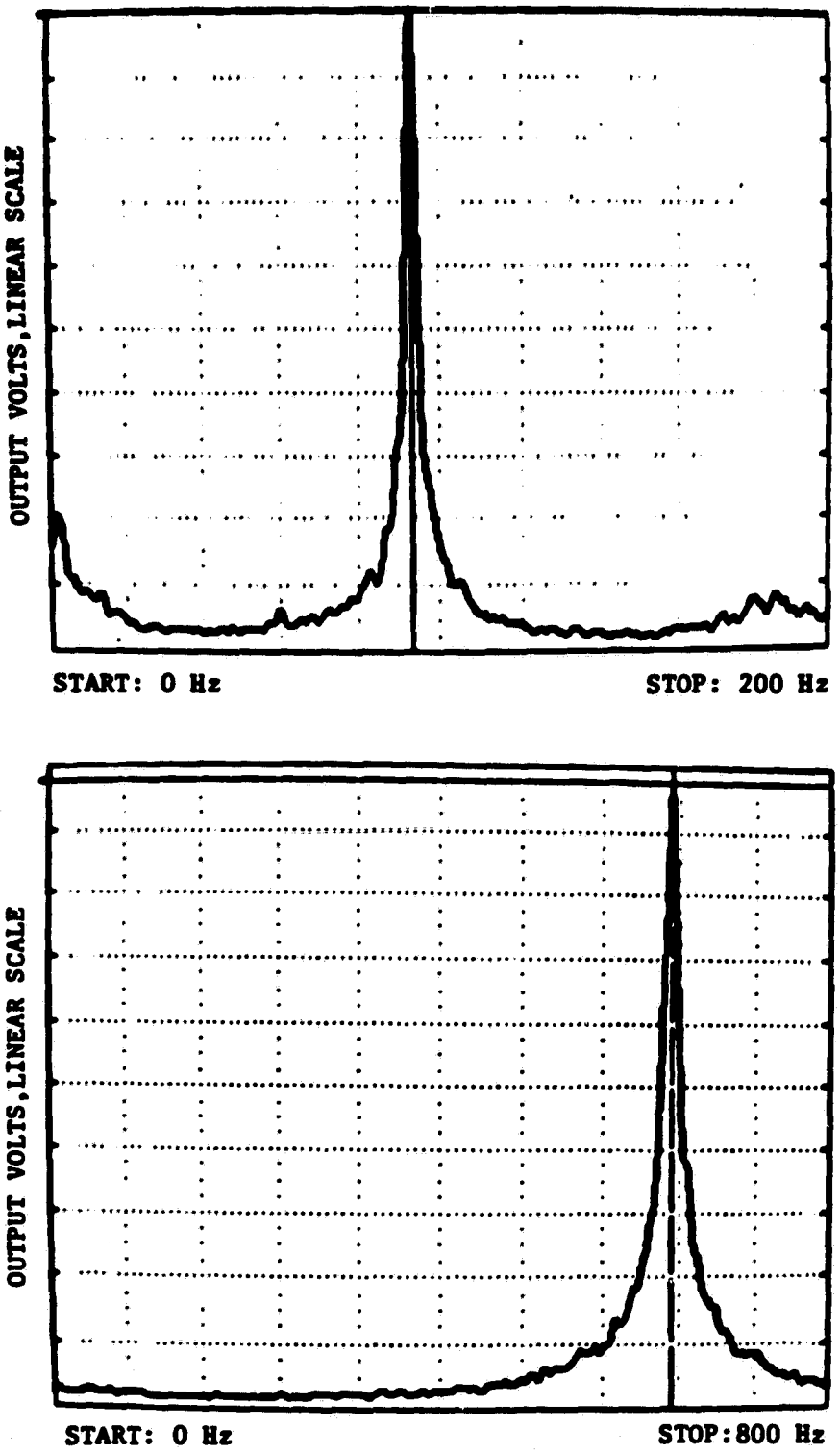

Figure 18. Spectrum lines of vane 8 in the meter ports on the 7035 duct. Top, 4.2 m/s flow velocity; bottom, 28.2 m/s flow velocity.

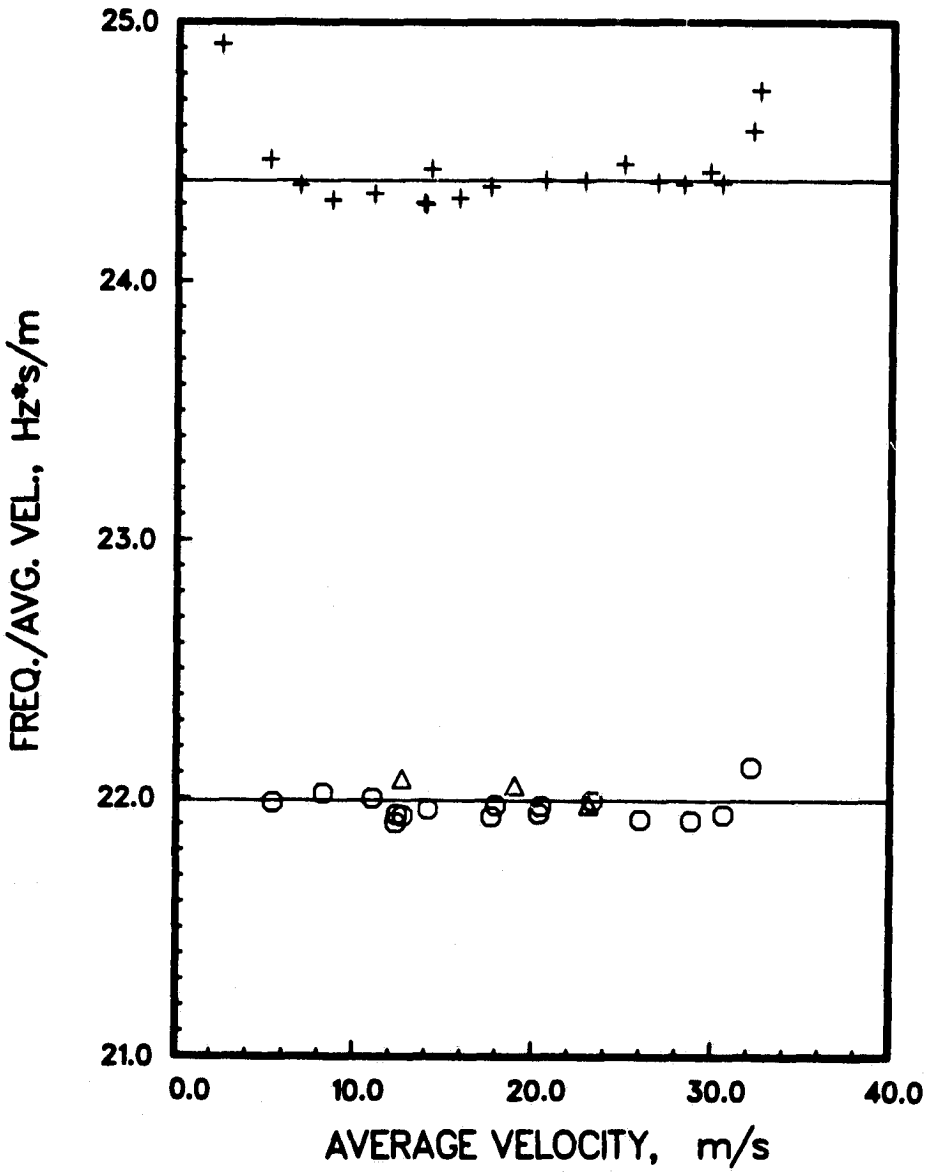

Figure 19. The circles and triangles show the meter factor of vane 8 in the 7035 duct. The pluses show the meter factor of vane 13 in the 7034 duct. Both results are for water flow.

The bend configuration of the 7035 duct might have caused a cancellation of most of the swirl at the meter location. A set of ports was brazed to RS007034 or Low Pressure Fuel Turbopump Drive duct in the location shown in figure 20. The entrance bend of the duct is 30° followed by a 90° bend. These bends are in the same plane except for a small offset at a couple of welded joints. The plane of the 36¼° bend is canted at about 120° with the plane of the first two elbows. The following 63 3/4° bend is in a plane making a 25° angle with respect to the plane of the previous bend.

The meter factor of vane 13 in a meter of the figure 7 design installed in this duct and water tested is shown in figure 19. Clean narrow spectrum lines were again obtained, figure 21.

As figure 19 and the spectra of figures 18 and 21 show, the vortex shedding flowmeter can measure flow in the shuttle ducts with no flow straightening required. The meter performance for water flow in the 7034 and 7035 ducts was as good and probably better than the performance in long straight ducts. The spectra of vane 13 were relatively clean up to 10 kHz as shown in figure 22. Other than the small second harmonic (3 x f) at 825 Hz, the other significant line was a broad line at about 3.3 kHz. This line is 30 dB down. It is probably a mechanical resonance since it is nearly independent of flow rate. It is always seen and usually occurs somewhere between 1 kHz and 5 kHz. The amplitude is generally 20 dB less than the vortex signal.

5.3 Vane Shape

Because of the wide variety of vane cross sectional shapes found in commercial meters, it is not obvious that an optimum vane shape exists for the

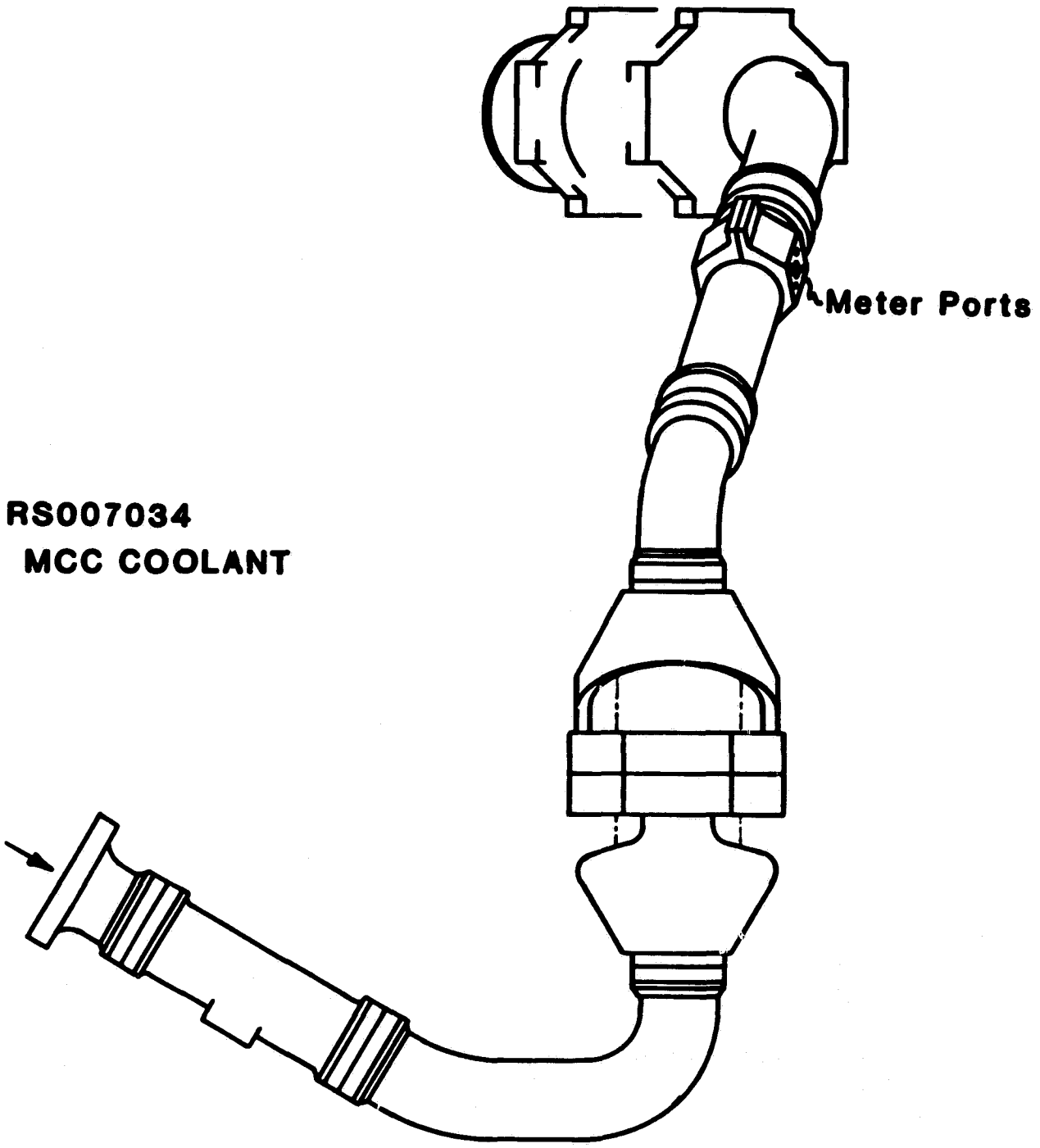

Figure 20. The RS007034 duct showing the location of the added flowmeter ports.

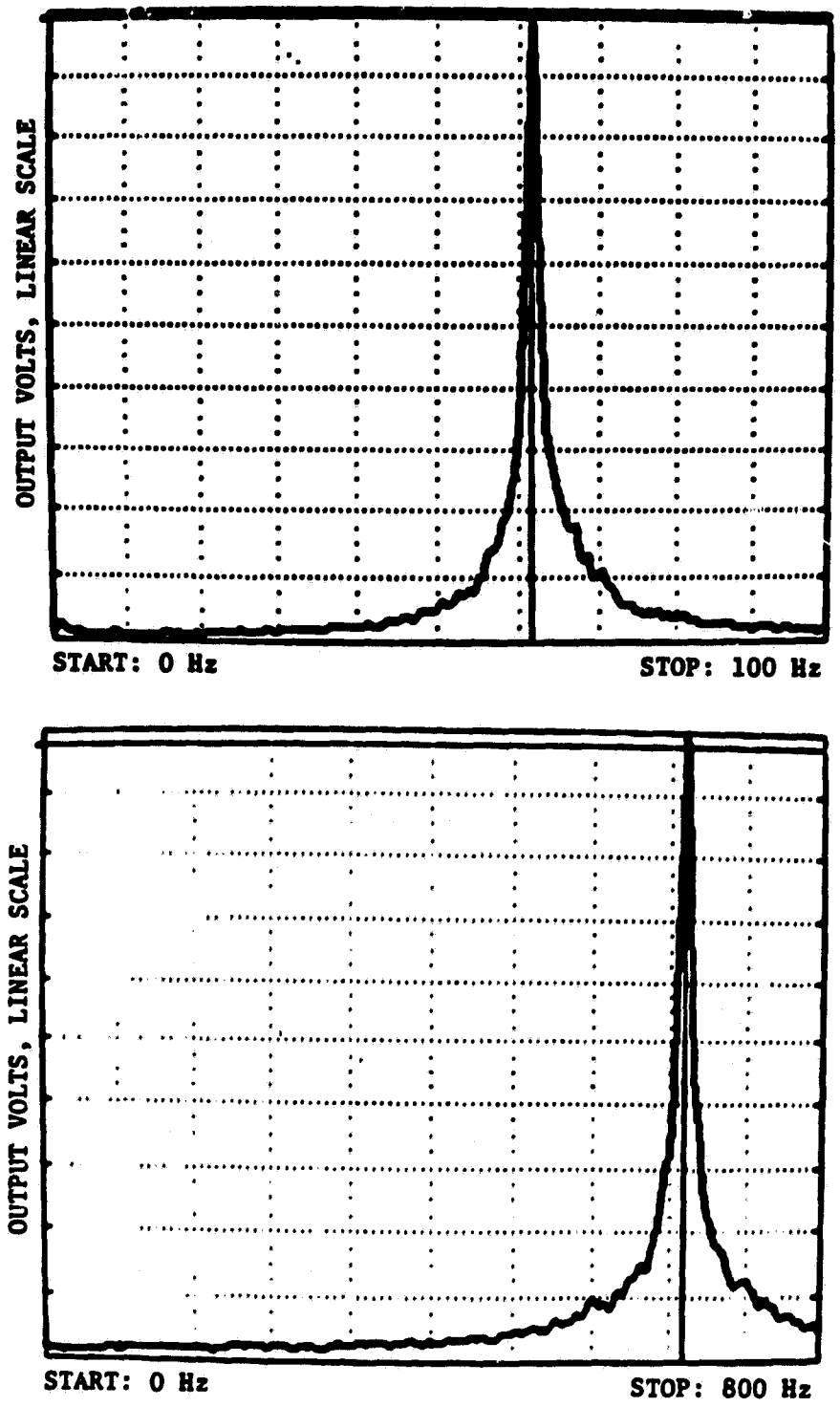

Figure 21. Spectra from vane 13 in the 7034 duct at water flow velocities of 2.5 m/s (top) and 26.8 m/s (bottom).

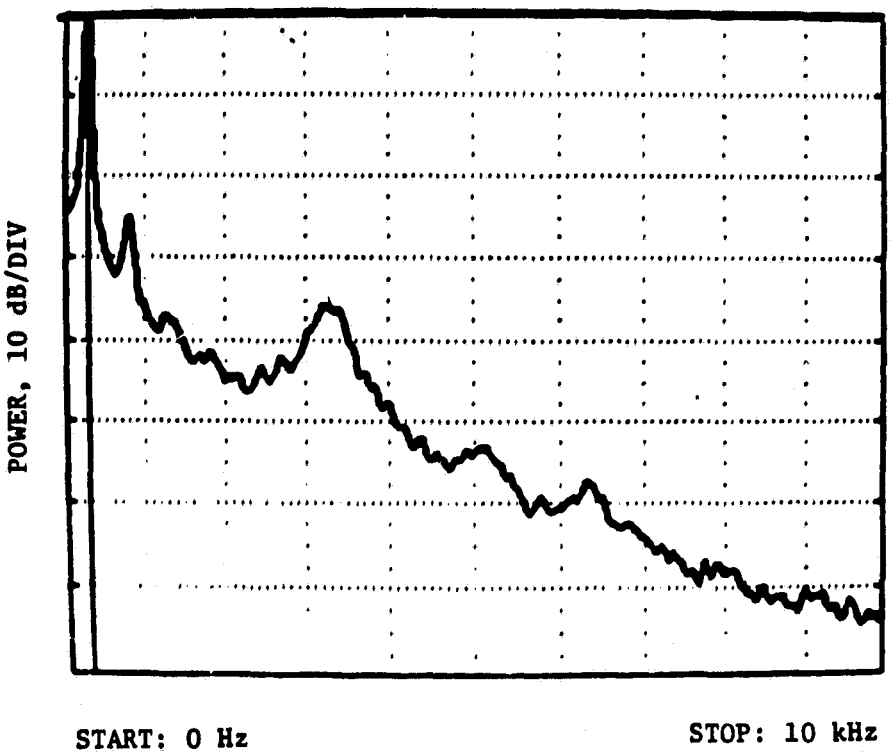

Figure 22. Log spectrum of vane 13 in the 7034 duct from 0 to 10 kHz.

commercial flow range. An optimum vane shape may exist for the narrower vane at higher flows. Vane 4 was found to be inferior to vane 3 in terms of the constancy of the meter factor. Rectangular shapes appeared to give somewhat more constant meter factors so rectangular shapes were used in most of the testing of ducts and sensing devices. Since some signal fade still occurred and some variation of the meter factor with flow was found, some tests were carried out looking for a more optimum shape.

Various manufacturers have commented that the corners between the front face and sides of their vanes must be sharp. To test for corner effects, vane 14, with the same D/W ratio as vane 8, had the corners on one face of the vane broken with a file such that the edge was beveled, though unevenly, at about 30° from the plane of the face to a depth of about 0.4 mm. The radii of the other two corners were measured as 0.1 ± 0.05 mm. The difference in performance between beveled and unbeveled front corners was evident after testing the vane with the beveled face, then the unbeveled face, forward. The meter factors for such a measurement are shown in figure 23. The average meter factor was 6% higher when the flow was toward the beveled side.

Vane 15 was a vane similar in width to vane 14 but had a greater depth. One face had sharp corners while the other face had the corners machine beveled at 45° to a side depth of about 0.5 mm. The meter factors as a function of velocity for this vane for the beveled edges forward and the sharp edges forward are also shown in figure 23. The meter factor for vane 15 with sharp corners forward was less than vane 14 because of the greater depth. The meter factor with the beveled edges forward shows a sharp minimum around 9 m/s. The average value of meter factor in the flat region is even higher, 12%, relative to the flat face meter factor, than vane 14. The radii of the

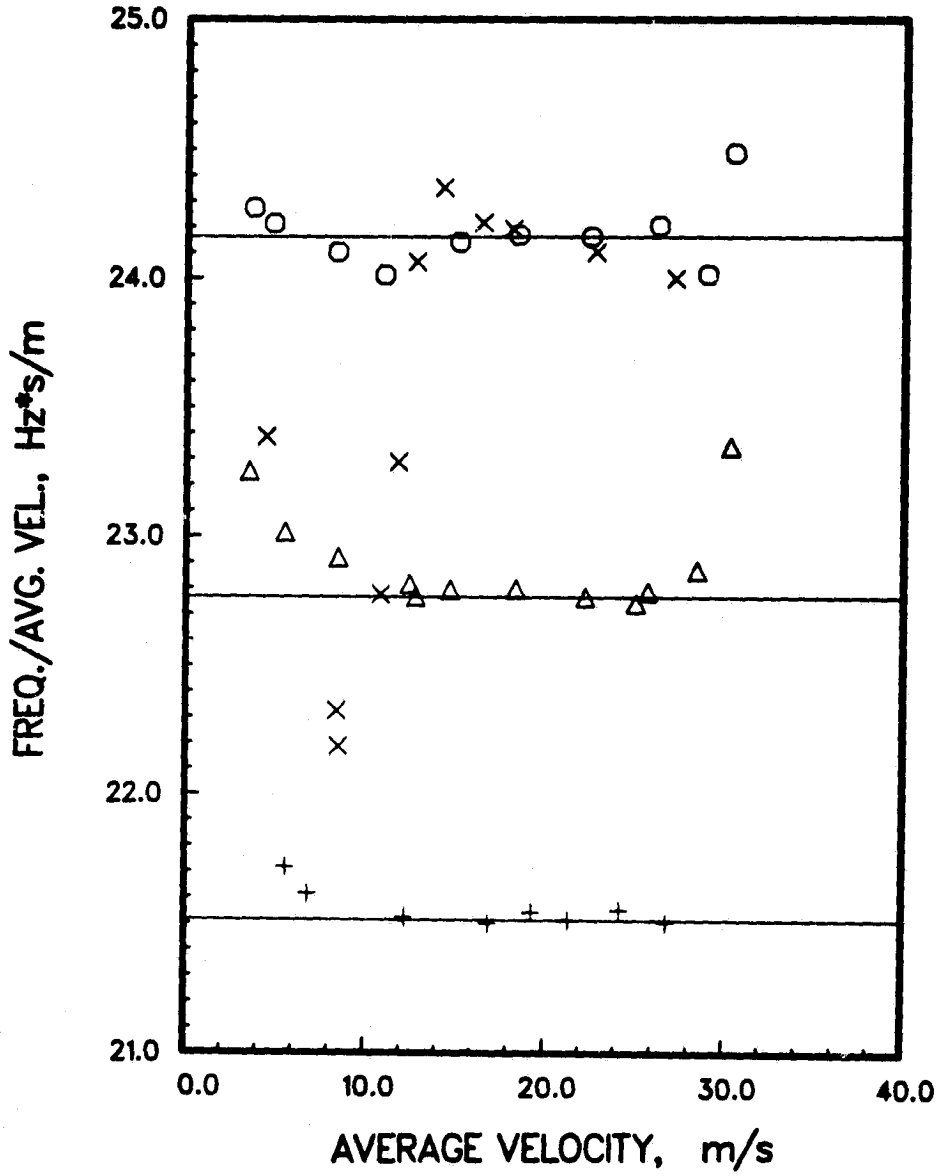

Figure 23. The effect of beveled corners on the meter factor. Triangles, vane 14 with sharp corners forward; circles, vane 14 with rounded corners forward. Pluses, vane 15 with sharp corners forward; X points, vane 15 with beveled corners forward.

"sharp" corners were not measured for this vane but were probably as sharp as vane 14. No further measurements of corner effects have been carried out. A minimum radius must exist below which the radius has no more effect on the meter performance. This radius may be larger than 0.1 mm. Corner design could prove to be a useful way to fine tune meter performance.

Some of the commercial meter vanes have values of D substantially larger than W. Vanes with cross sections similar to two of these commercial designs, vanes 16 and 17, were built and tested in the 41 mm size. Vane 16 with the figure 3a cross section showed a meter factor decreasing by about 5% at 30 m/s from the meter factor at 5 m/s. Vane 17, which had a cross section like figure 3e gave a 40 dB or better S/N but the meter factor decreased by more than 5% in the 5 m/s to 30 m/s range. The vane was made of brass for ease of machining and broke in half before the measurements were completed. Vane 18, with its rectangular shape and D/W = 0.67, gave a fairly constant meter factor for the 5 readings taken (see figure 34).

The remaining cross section shape studies were done in the 4 diameter long by 58.6 mm bore meter. They are vanes 19 through 29 in Table 1. The sensing head of figure 7 was used for most of these tests. The link ends were shimmed tight in the sensing head clevis.

Some of the reasons for choosing these particular designs were as follows: the vanes of figure 3g and 3e cross section were designed to eliminate possible effects of variation of the vortex detachment point should that be causing fading. The cross section shown in figure 3d was designed to reduce flow separation along the sides of the vane should flow separation cause fading. Vanes 20, 21, 24, were similar to a commercial vane design. The vanes shaped like figure 3c were similar to another commercial design.

None of the the vanes 19 through 29 were an improvement over the rectangular vane cross section. The rectangular vanes of 7.6 mm width, a D/W of about 0.85 and with sharp corners, gave the narrowest spectrum lines, the best S/N and the least fade.

The test results suggesting the best signal properties from a vane with D/W = 0.85 agree qualitatively with the results of Kalkhof [10] who shows curves suggesting that the variation of the signal period would be minimum around W/D = 0.85 for W/D_p = 0.125 at lower Reynolds numbers.

All of the 58.6 mm bore meter vanes tested showed varying increases in meter factor at low flows. Some of the increase may be introduced by using the head designs of figures 7 and 8. Some of this effect might also be the result of the improved resolution obtained from changes in the method of measuring meter frequency. The FFT spectrum analyzer was used to measure the meter frequency for these tests rather than the counter. After the switch to the bayonet for the end of the vane opposite of the sensor, shimming the link end to remove all lost motion reduced the amount of increase of the meter factor at low flow velocities.

One test was done to determine whether the clevis arrangement on the sensor end might be causing some disturbance since the end of the clevis penetrated slightly into the duct. A vane was made with a 3 mm thick disc at the pipe wall and the sensing head was shimmed back 3 mm to place the inner face of the disc slightly inside the pipe wall. This vane gave a meter factor indistinguishable from a vane of the same W and D with no disc.

Though determining repeatability from measurement to measurement or vane to vane of the same design was not the object of this work, some tests were repeated. Vane 5 was tested both at the hydroplant test site and later at the

water treatment plant test site to determine whether the move affected the meter factor. The magnitude of the meter factor at the two locations agreed to about 1% in the flat part of the meter factor versus velocity curve. The velocity at which the meter factor increased on the high flow rate end was lowered because of the lower pressure at the treatment plant. In general, vanes with the same W and D gave the same meter factor with minor variations when the mountings were altered. Some of the variation in meter factor with both vane and suspension design in the early 1.5 in bore tests were probably caused by the gaskets used between the flanges and the wafer design meters. A 1 to 2 mm thick rubber gasket was used whose ID was around 1 cm larger than the pipe bore. Later, it was found that these gaskets could still extrude into the flow when the meter flange bolts were tightened. The extruded gaskets can slightly constrict the flow in the vicinity of the vane. This increases the flow velocity hence the measured frequency at that flow.

Three vanes with the same W and D, including vane 37 and 38, and one identical to 38 but not included in the table, were tested in the 4 diameter long 58.6 mm bore test section with the iron test section forming the inlet duct. The meter factors were the same within the data scatter. Measurements with the same vane but with different supports gave nearly the same values for the meter factor.

One vane, No. 8, was tested in five different duct configurations. The meter factor is shown in figure 24 for these tests. The approximately 0.6 mm maximum differences in the meter bores are eliminated by plotting meter factor as a function of the average velocity. The meter factor of the vane in the five duct configurations varies by more than 4%. The lower three curves in figure 23 are in inverse relationship to the duct diameter. The likely

water treatment plant test site to determine whether the move affected the meter factor. The magnitude of the meter factor at the two locations agreed to about 1% in the flat part of the meter factor versus velocity curve. The velocity at which the meter factor increased on the high flow rate end was lowered because of the lower pressure at the treatment plant. In general, vanes with the same W and D gave the same meter factor with minor variations when the mountings were altered. Some of the variation in meter factor with both vane and suspension design in the early 1.5 in bore tests were probably caused by the gaskets used between the flanges and the wafer design meters. A 1 to 2 mm thick rubber gasket was used whose ID was around 1 cm larger than the pipe bore. Later, it was found that these gaskets could still extrude into the flow when the meter flange bolts were tightened. The extruded gaskets can slightly constrict the flow in the vicinity of the vane. This increases the flow velocity hence the measured frequency at that flow.

Three vanes with the same W and D, including vane 37 and 38, and one identical to 38 but not included in the table, were tested in the 4 diameter long 58.6 mm bore test section with the iron test section forming the inlet duct. The meter factors were the same within the data scatter. Measurements with the same vane but with different supports gave nearly the same values for the meter factor.

One vane, No. 8, was tested in five different duct configurations. The meter factor is shown in figure 24 for these tests. The approximately 0.6 mm maximum differences in the meter bores are eliminated by plotting meter factor as a function of the average velocity. The meter factor of the vane in the five duct configurations varies by more than 4%. The lower three curves in figure 23 are in inverse relationship to the duct diameter. The likely

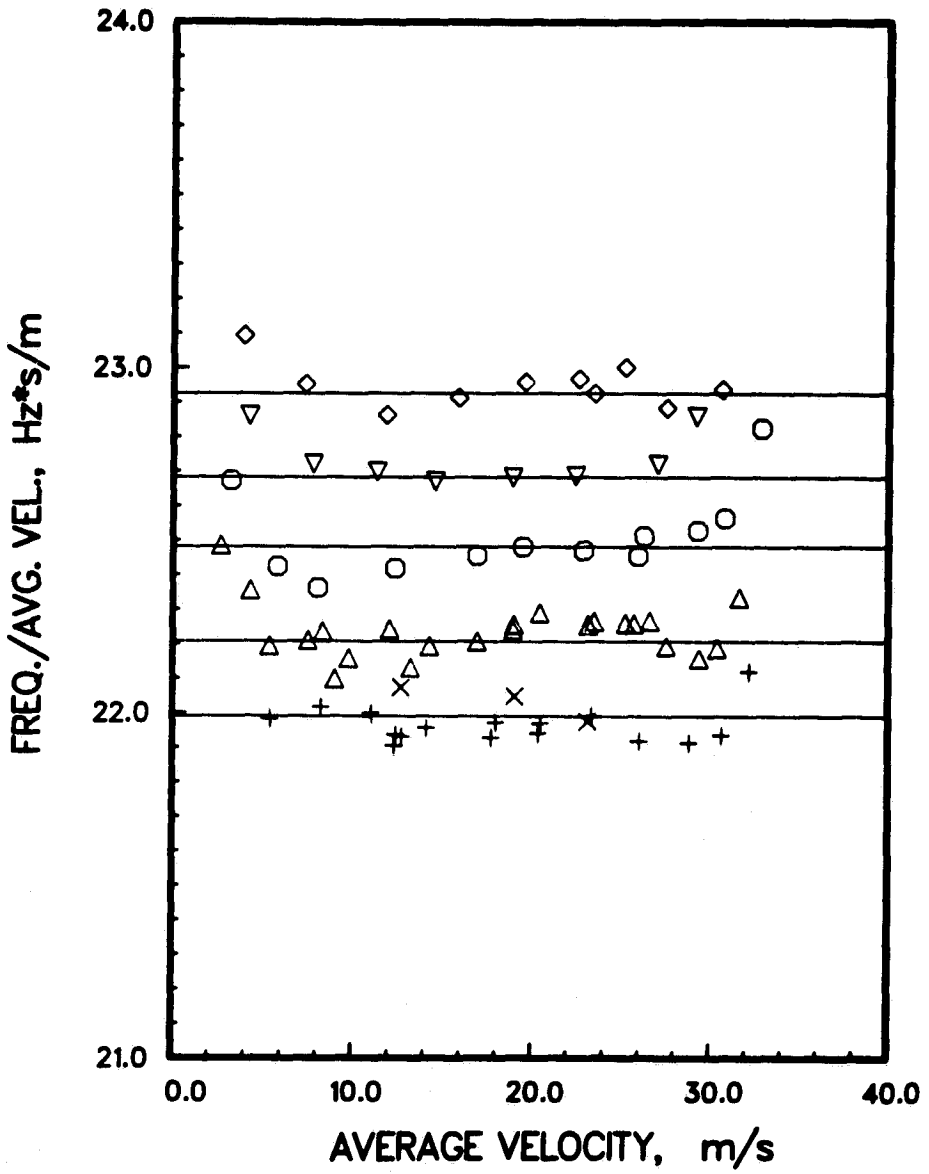

Figure 24. The effects of the duct on the meter factor of vane 8: Plus and X points, the 7035 duct ports; point up triangles, at the exit of the 7035 duct in a 4 diameter long meter body; circles; a straight single piece test section; diamonds, the 4 diameter meter body at the end of the straight test section; and the point down triangles, the same as the diamond points except that the flange on the end of the straight test section has been bushed.

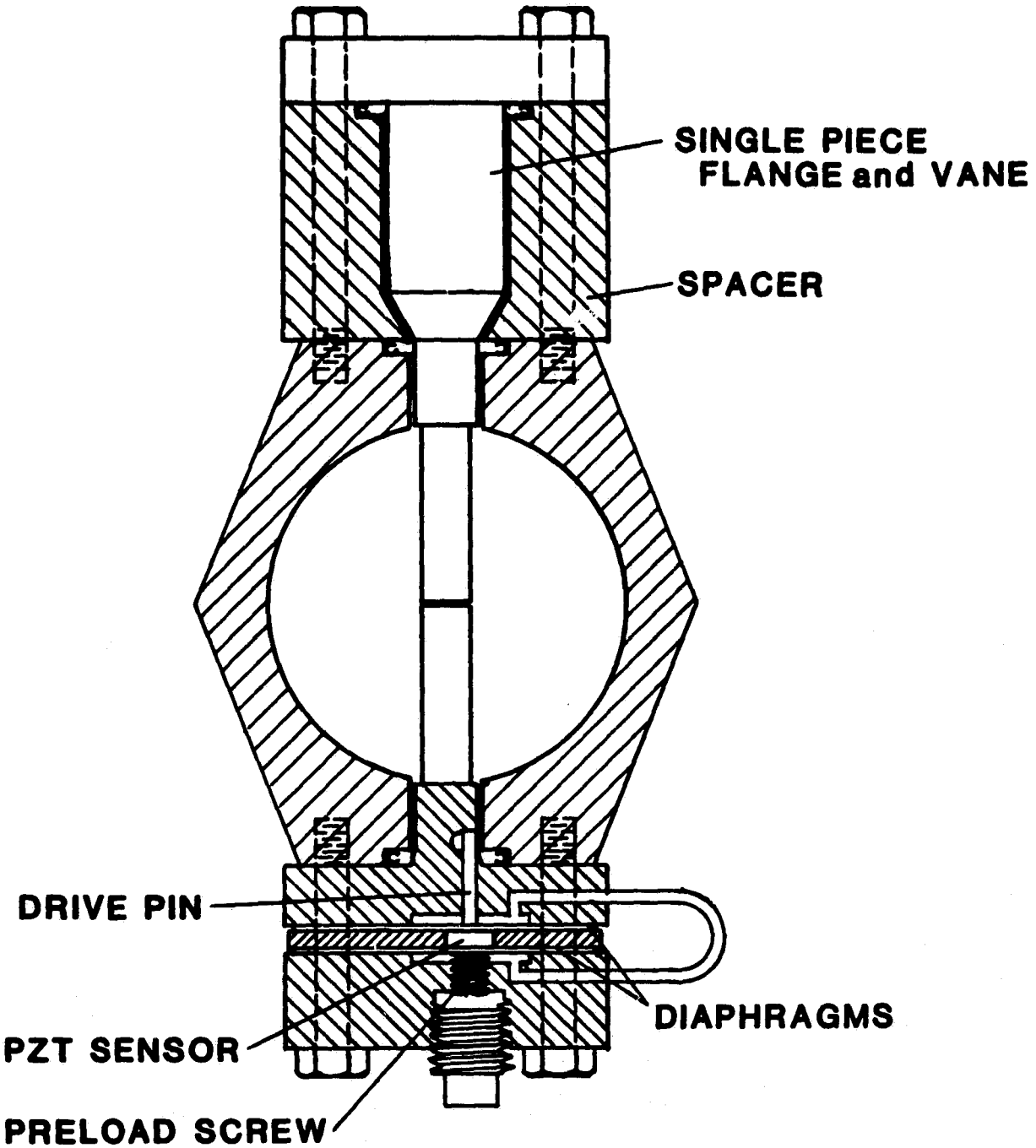

Figure 25. Double cantilevered vane. The same vortex sensor shown in figure 7 is used on the vane in this top port. This sensor is not illustrated for simplicity.

explanation for the hierarchy of the these curves is probably not the duct diameter but the wall roughness. The 7035 duct wall is probably the smoothest so the boundary layer is thinnest and the center line velocity is lowest. The 4 diameter long meter at the end of the 7035 duct may have a rougher interior. The interior roughness of the 7035 duct could not be measured for comparison. The transition joints from this duct to the meter certainly contribute a wall roughness. The iron test section has such a rough and uneven interior surface that an accurate measurement of diameter was not obtainable. The wall roughness would have to cause a 2% increase in the central flow velocity between the iron duct and the 7035 duct to account for the observed differences. For these three tests a figure 6 design sensing head was used.

The meter factors obtained for the upper two curves do not have a convenient explanation. The 4 diameter long meter containing the vane is downstream of the iron test section. This iron test section consisted of a section of 2½ in schedule 80 pipe to which schedule 40 flanges were welded. The ID of the flanges was about 5 mm greater than the bore of the test meter body. After the top curve in figure 24 was obtained, the flange was bushed to the meter ID, the flat gasket replaced by an O ring, and the vane was retested. The meter factor decreased about 1%. The meter factor of two other vanes showed only a small change or none at all when tested with and without the bushing in the flange. The only differences between the earlier vane 8 tests and these last two is the use of a head of the figure 7 design for sensing and the use of the FFT to measure frequency. The FFT and the counter generally gave the same frequencies when they were compared, leaving only the difference in sensing heads or some as yet unknown peculiarity in the meter run to explain the different meter factors.

The results shown in figure 24 demonstrate that the meter run contributes significantly to the overall meter performance. Thus, a meter must be calibrated in the duct in which it will be used for highest accuracy.

A few tests were done on a 28 mm (1.1 in) bore size meter. Though flow dependent spectrum lines were obtained, the lines were generally inferior to spectra obtained from 1½ in meters. The vanes that gave the best results were larger in cross section than a linear scale-down of the best 1½ in vane. Further work is needed to find the best meter design for the 28 mm duct size.

To briefly summarize this section, the meters tested produced a vortex generated output signal comparable to a commercial meter of similar size except that the signal is subject to more fade. Since the few counts lost at a given flowrate are small, no appreciable degradation of the meter performance results. The contour of the corners of the front face had a strong effect on the meter factor. Rectangular vanes with the pipe diameter to vane width ratio of about 8 and a W/D of 0.85 gave the best results in the 58.6 mm bore meter while W/D = 0.65 was better in the 59 mm duct. The vane calibration was dependent on the duct as well as the average velocity. The duct wall finish seems to be an important parameter. The meter factor is probably independent of the vane mounting as long as the mounting is tight.

5.4 Double Cantilevered Vanes

Though meters with either a link mounted vane or bayonet mounted on one end measured flow satisfactorily, the designs may prove unsafe for LOX duct applications. The main concern is rubbing surfaces caused by expansion of the duct under pressure and the distortion resulting from vibrations. A double cantilevered vane design is illustrated in figure 25. This vane spans the

pipe but is formed by two bars cantilevered in from each side of the pipe that almost touch in the middle. This design obviates the need for any mechanical attachment across the pipe. Double cantilevered designs were first tested in the 41 mm diameter test section.

The tests of vane shape and head designs were carried out using link type vanes to reduce the amount of machine work. A cantilevered vane and mounting flange is best made from a single piece of metal which requires much more machining.

The first test of the double cantilever design was vane 30. This vane was formed of two aluminum cantilevered vanes of the same cross section, one 17.8 mm long the other 22.4 mm long in a 41 mm bore meter body. The performance was similar to the vane 5 which it resembled but the meter factor was about 5% lower. The main difference between vane 5 and 30 was the slightly trapezoidal cross section of the latter.

The next test of the double cantilever, vane 31, was carried out using a pair of cantilevered vanes of the same cross section as vane 30 but with a greater asymmetry in length. The longer of the pair was 28.5 mm but the material was A-286 stainless steel. The short opposite vane was still aluminum. The meter factor was constant to within ±0.5%, and the S/N was larger than 30 dB though the line widths were between 5 and 7% of the frequency. The meter factor agreed well with a link vane of similar width. This may be fortuitous since the meter run was a single section of stainless steel pipe with ports rather than the wafer type used with the link vane though the bores were supposedly the same. The pipe ID is uneven, which precludes an accurate measurement. The only other 41 mm ID cantilevered pair tested, vane 32, consisted of two rigid stainless steel vanes of equal length.

A pressure sensing port was provided on each vane but on opposite sides. A hole up through the center of each vane communicated to opposite sides of a differential pressure transducer. The spectrum lines obtained were 20 dB or more above the noise but were dominated by the noise below about 250 Hz. This noise was independent of the pressure transducer employed for the sensor. The meter factor of this vane was about 30.3 Hz•s/m, about 3% lower than obtained for vane 5, a link vane of similar dimensions. The meter factor increased sharply below about 8 m/s and increased very slightly above. The scatter about an average curve was about ±0.6% above a flow of 8 m/s.

The first double cantilevered pair tested in the 58.6 mm size was vane 33 in the 4 diameter long test body. One vane was 33.5 mm long and made of A-286 stainless steel. A short aluminum vane completed the span of the vane across the pipe. The meter factor appeared to decrease linearly with increasing velocity giving an average value of about 21 Hz•s/m. The spectrum lines were under 5% wide and the S/N was 30 dB or more. At the highest flowrate tested, the meter frequency rather suddenly dropped as if something broke. No breakage was evident. The cause of the sudden decrease is unknown.

Vane 34 consisted of a pair of cantilevered vanes of equal length made of stainless steel. These vanes were designed for cryogenic sensors which required that the drive pin have an offset of about 4 mm so the sensor could be mounted with its axis on the port axis. This double cantilevered square cross section vane had a meter factor about 4.6% higher than vane 35, a link vane with nearly the same dimensions, rather than lower as was found with some of the 41 mm bore double cantilevered designs.

The meter factors of vanes 36 and 37 which were 34 and 35 reduced in depth to D/W = 0.85 still differed by 4.6%. The meter factors, of course,

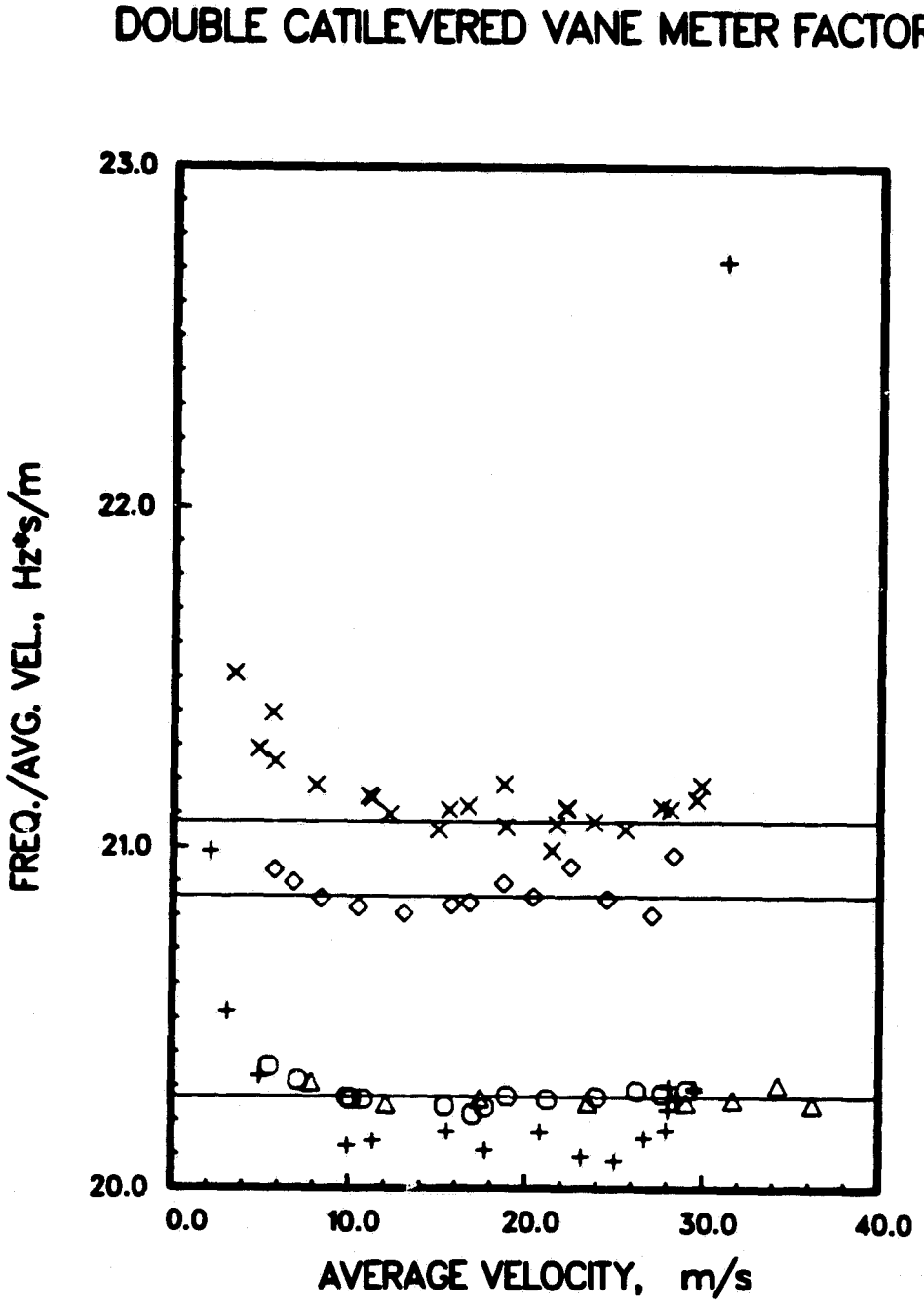

Figure 26. Comparison of meter factors of double cantilevered and link vanes of the same cross section. Circles show vane 37, the only link vane. The other curves are all for double cantilevered vanes. The plus points are vane 39, the X points are vane 40, the triangle points are vane 36.

increased when D was reduced. The meter factors of vanes 36 and 37 are compared in figure 26. The link vane, vane 37, was 0.1 mm wider, but link vane 38 which had the same width as No. 36, also gave the same meter factor as No. 37. The line widths were 3 to 4% for the three vanes and S/N was 30 to 40 dB.

The subsequent testing of double cantilevered vane 39 suggested a cause of the discrepancy between the meter factors of vane 36 and 37. Vane 39A consisted of the upper cantilevered vane of figure 25 but with a sensing head on it like that in figure 7. The other half of the vane, 39B, is the cantilevered vane shown in the lower port of figure 27 without the strain sensor. The meter factor obtained is shown in figure 26. The meter factor of this pair is almost the same as a link vane of the same dimensions. The meter factor of the cantilevered vane is more constant than that of the link vane. The No. 39 vane pair probably was mechanically stiffer than the No. 34 and 36 vane pair.

Vane 40 consisted of a fixed half, No. 39B, and a sensing half consisting of a modified half of vane 36. The modification is illustrated in figure 25 by the vane in the bottom port. The diaphragm seals of a meter of the figure 8 design have been eliminated by using a solder seal instead. A much more compact sensing head is possible because the sensor can be set off center within the port bolt pattern. Again, the meter factor was higher, figure 26, though not quite as large as obtained with vane 36.

Three other double cantilevered vanes, 41, 42, and 43, were tested using vane 39B as the vane opposite the sensing vane. The sensing half of the vane pair consisted of a piezoelectric pressure sensor in the side for vane 41. Vane 42 had a notched mount but with the notch depth no more than 4 mm rather

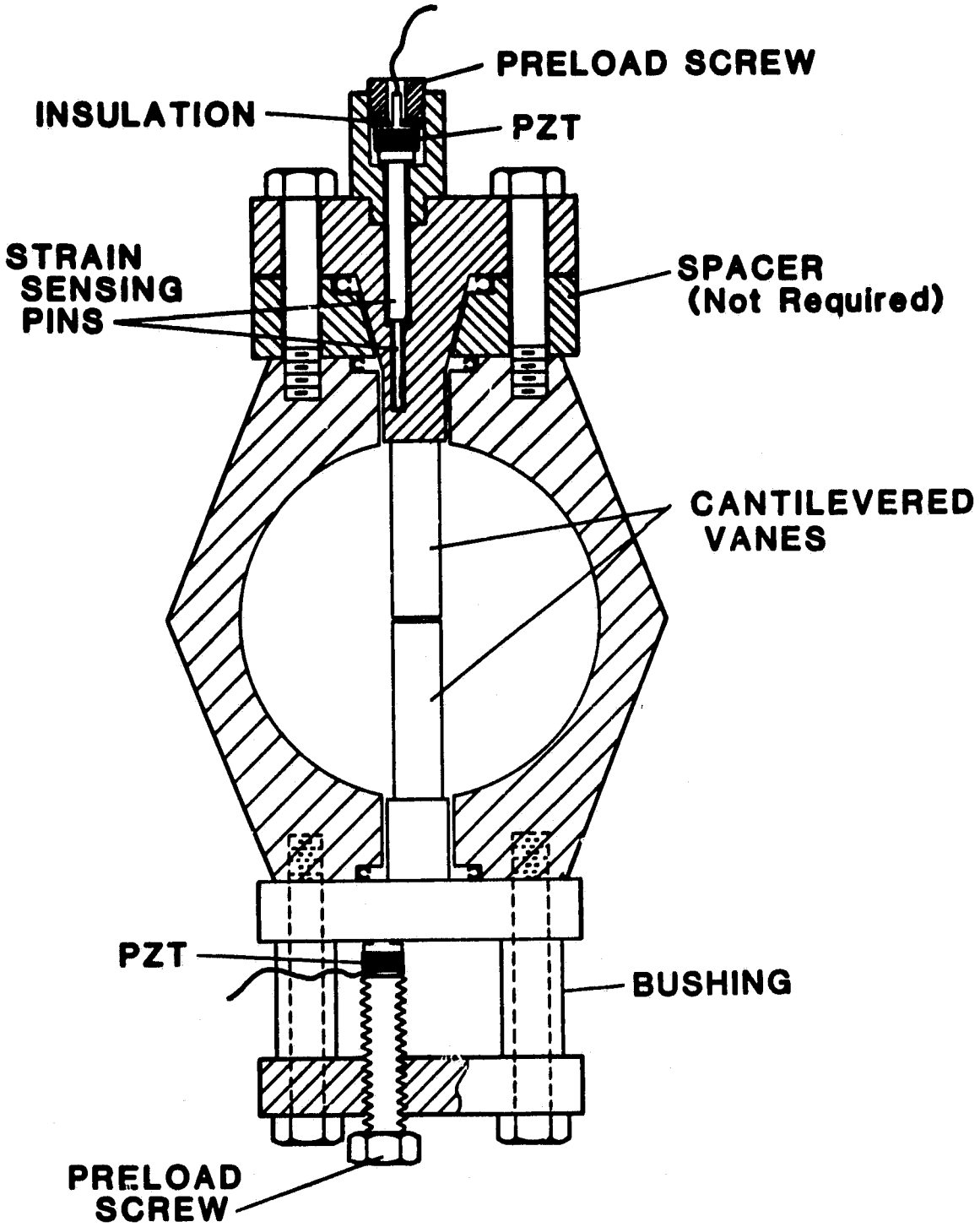

Figure 27. Cantilevered vane designs that eliminate the diaphragm seal. In the top port is vane 44. In the lower is vane 39B with a strain sensor on the mounting flange.

than the typical 5.5 mm. Vane 43 consisted of a vane made of A-286 steel whose front face width and depth were the same as 41 and 42 but the sides made 92° angles with the front face. These vanes all had nearly the same meter factor as vane 36, figure 26.

The much lower meter factor obtained for vane 39 suggested that the stiffness of the cantilevered vane support might contribute to the variability of the meter factor. However, when the top vane in figure 27, 44A, was tested opposite vane 39A, this pair, vane 44, produced a meter factor with the same value as vane 41, 42 and 43 rather than like vane 39 though the stiffness should have been similar. Vane 44A was about 0.1 mm narrower than vane 39A which could possibly account for the higher meter factor. Vane 45, consisting of vane 39B and vane 44A had a meter factor intermediate between vane 44 and vane 39. The spectrum line widths were only around 5% wide for vane 44 but were more than 7% wide for vane 45 for unknown reasons.

All the parameters controlling the performance of these cantilevered vanes cannot be discerned from this small number of samples. Apparently, the mechanical stiffness of the vane mounting has some bearing on the behavior. The performance of the double cantilevered vane seems much more sensitive to suspension than does the performance of the link vane. The meter factor as a function of flow velocity seems to be more constant for double cantilevered vanes than for the link vanes in the meter run used for these tests.

Some significant variations of the signal spectra with vane suspension occurred. Figure 28 compares spectra from vane 39 and vane 42 at three similar flowrates. At the highest flowrate a number of lines appear in the vane 42 spectrum. One of these lines is even larger than the vortex generated line. At higher flows the extra lines faded again. All the double

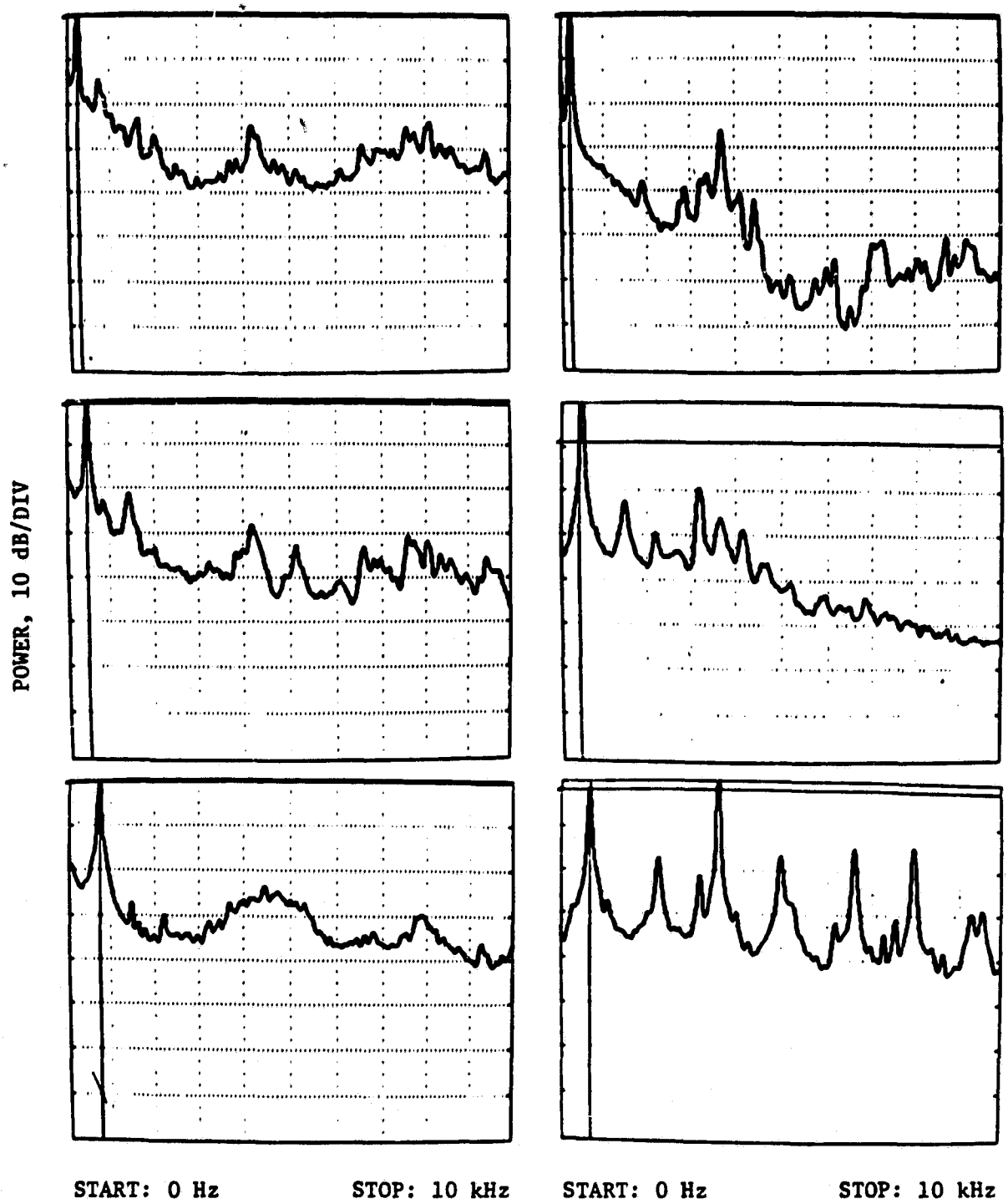

Figure 28. The three spectra on the left side are from vane 39 at average flow velocities of 12.1, 23.5 and 36.2 m/s from top to bottom. The three spectra on the right are for vane 42 at average flow velocities of 11.1, 24.0 and 32.5 m/s, top to bottom.

cantilevered vanes except 39 showed large spurious lines to some degree. The meter factor did not change value when the extra lines appeared. This suggests that the forces driving these modes may be something other than the vortex shedding process.

Though the diaphragm system of figure 7 and 8 should provide a satisfactory means of transmitting the vane strain to the detector, it is nevertheless more desirable to remove the strain sensing mechanism entirely from contact with the high pressure. The two sensing heads shown in figure 27 do this. The off-center PZT on the lower vane assembly senses the strain in the mounting flange resulting from the vortex shedding forces. The drive pins in the upper vane of the same figure are totally enclosed in the sensing head. The sensor is attached by an axial threaded hole so the detector senses the strain between the top flange and the end of the pin. Both these sensing methods produced narrow spectrum lines. The lines were inferior to the best obtained in that the signal amplitude was lower and the flow independent lines in the 2 to 5 kHz region of the spectra were higher in amplitude relative to the vortex generated line.

6. CANTILEVERED VANES

The cantilevered vane design has been discussed in section 5.5. The basic design originated with an attempt to measure flow with just one cantilevered vane inserted through one port and extending only partially across the pipe. Besides the advantage of requiring only one instrument port, the head loss due to the meter is reduced.

The concept was first tested by cutting off vanes 3 and 4. After obtaining a velocity dependent signal from these two vanes, some cantilevered

vanes were designed using PZT discs for sensors. The first dozen showed a poor to nonexistent vortex signal before a vane design was found that produced an even passable signal. Vane 50 produced the first passable vortex signal spectrum. The sensing mechanism consisted of a piston plunger in a hole down the axis of the vane sensing the time varying pressure at a side port on the vane. The piston acted against a PZT strain sensor.

Another 10 vane designs were tried before a successful design with a strain sensing vortex detector was developed. An additional eight vanes were tested before arriving at vane 51. The dimensions of the vane giving the best signal were, W = 5.1 mm, D = 4.3 mm and L = 17.8 mm. After yet another eight designs the figure 29 design evolved. This design fits through an SSME duct instrument port.

Figure 30 shows the meter factor as a function of flow velocity for vane 51 and 52. The sensing mechanism of vane 51 consisted of two PZT sensors measuring the strain introduced into the vane support and poled so the outputs resulting from a transverse force on the vane added. A 19 mm diameter port was necessary to install it. Vane 52 had the design shown in figure 29. The meter factor of vane 52 is lower than 51, probably because the vane mount is stiffer. The meter factors differ from those of vane 7 which had close to the same meter factor as vane 5, figure 11, even though the cross sections are identical and the sensing head is similar. The meter factor of the cantilevered vanes are flat to a much higher flowrate and is around 15% lower than the meter factor of vane 7. These differences stem from the same source; the flow is partially bypassing the cantilevered vane. The drag introduced by the vane causes the average flow velocity on the opposite side of the pipe to be higher than on the vane side. The vane sees a velocity lower than the

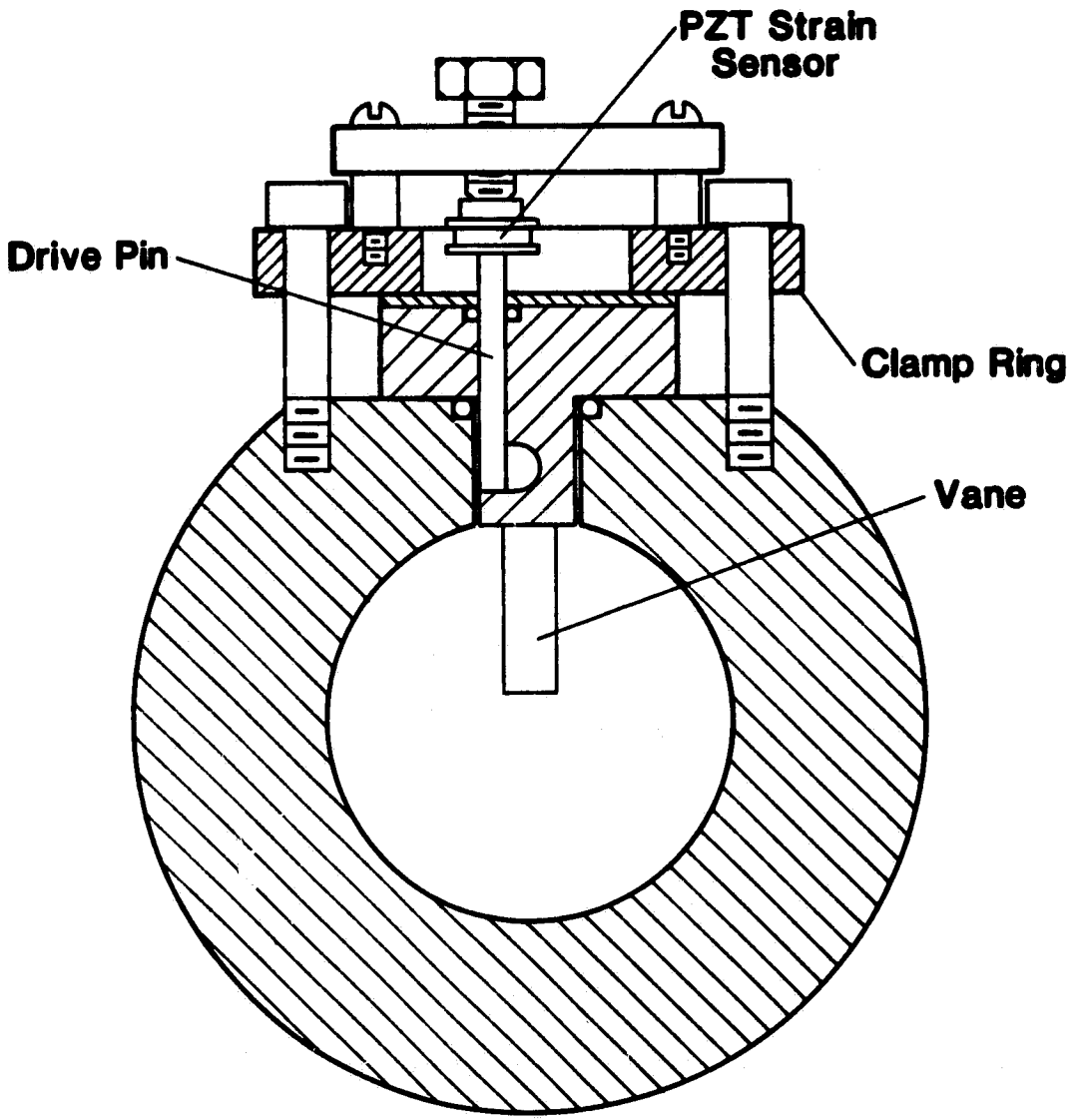

Figure 29. Illustration of a cantilevered vane that fits through an SSME port.

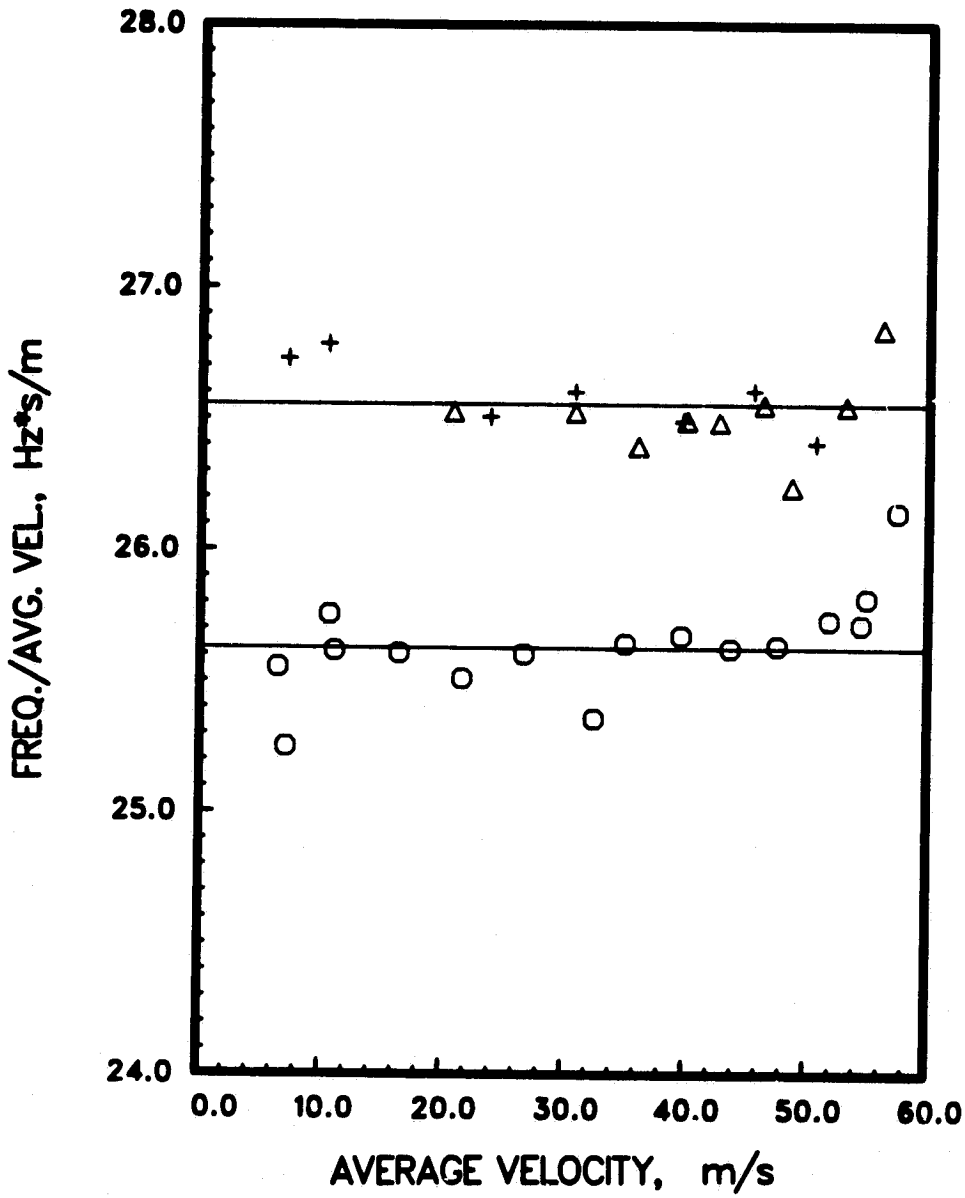

Figure 30. Meter factor for vane 51, triangles and pluses and vane 52, circles.

average velocity over the pipe at the same flowrate so the meter factor is smaller. The upper limit the flowmeter can measure is assumed determined by when cavitation occurs at the meter. Since the average flowrate is higher than the flow by the vane, a higher average flowrate can be measured before cavitation occurs.

Unfortunately, flow bypassing the end of the vane has negative aspects also. Some spectra from one of better performing cantilevered vanes, vane 53, are shown in figure 31. The line width is much wider and S/N much lower than for link vanes with the same dimensions. Vanes of various shapes, such as those of figure 3f and h, and various dimensions were tried to improve the vortex signal to no avail.

The poor performance of the cantilevered vane in terms of line width and S/N probably comes from a velocity gradient along the vane near the free end caused by the bypassing flow. The gradient means that the shedding frequency is varying from one part of the vane to the next. This is not conducive to having a single shedding frequency and results in a broadened line. That the single cantilevered vane works at all is more suprising than that it does not work as well as a full vane.

Modifications such as adding a thin disc onto the bottom of the vane or increasing D at the bottom were tried. The latter did not work at all. The disc made no detectable difference which is not surprising because it was small. A large one would not fit through the meter port. Any termination structure at the free end of the vane should really be independent of the vane and attached directly to the duct.

A pair of oppositely mounted 17.8 mm long cantilevered vanes were installed in one test in the 41 mm bore duct. This left a 5.4 mm wide gap

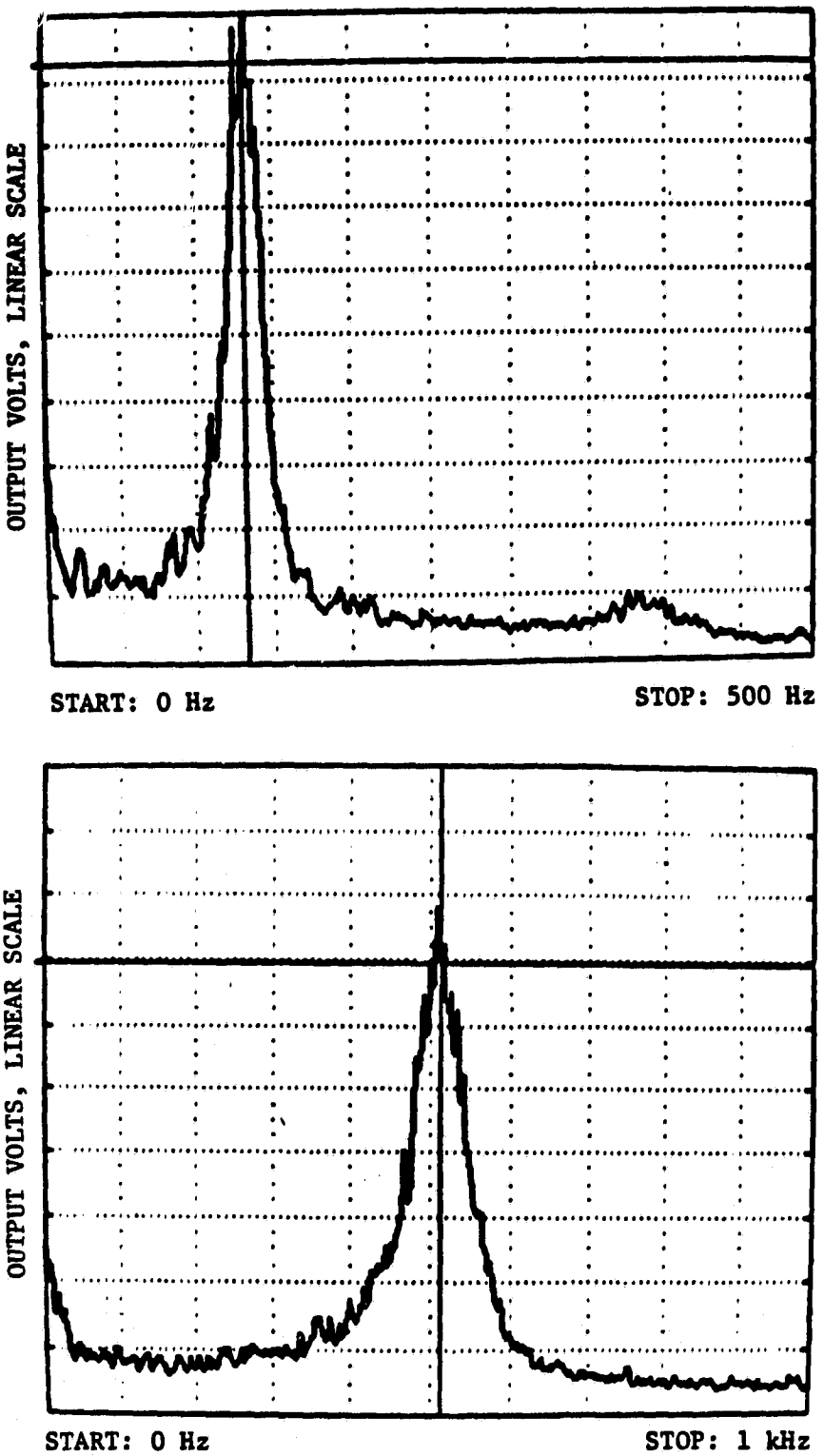

Figure 31. Two spectra from cantilevered vane 53, at 5.2 m/s, top, and 20.0 m/s, bottom.

between the ends. This increased the meter factor (28 instead of 26 Hz s/m, figure 30) as might be expected. The S/N ratio, however, was even poorer than that obtained for a single vane, probably because the flow velocity gradient at the end of the vanes was made even worse by the gap. This shows that the gap between the ends of double cantilevered vanes must be small if the vane is to perform like a link vane.

Vane 51 was tested under swirl conditions created by the swirl generator used to test vane 5. The signal was already degraded at a 5° generator setting and the meter factor reduced.

Even though the S/N ratio is markedly poorer and the line width is wider for the cantilevered vane than the link vane, a cantilevered design meter such as vane 52 or 53 could be usable in the 1½ in nominal size.

When the link vane designs were linearly scaled up from 41 mm to 59 mm diameter duct, the test results were as good or better than those obtained from the smaller diameter. Vanes 54 and 55 were scaled up versions of vane 52. Vane 54 was aluminum and scaled up linearly in cross section but was 3 mm short of the scaled up length. Vane 55 was stainless steel and scaled-up exactly. The vortex spectrum signal lines were wide and S/N was only about 15 dB. Vanes 56 and 57 retained the 5.1 mm width of the 41 mm ID meter but were longer. The test results were no better than those obtained from 54 and 55. Vane 56 was tested in the 41 mm meter and produced a S/N comparable to vane 52 even through it was longer. Vane 55 was subsequently tested in the meter at the exit end of the 7035 duct. The S/N was even poorer at that location, less than 10 dB and the signal line width was about 30% of the line frequency.

Because of the poor results obtained for the tests of the single cantilevered vane in the 59 mm bore ducts, further testing of this design was discontinued.

7. RING VANES

A ring shaped vane with the ring axis along the pipe axis sheds smoke ring like vortices alternately off the inner and outer surfaces. This design has been studied by more than one researcher, but the most extensive report in the literature is that by Takamoto and Koniya [9]. Ring shaped vanes were studied in this work briefly as a design that might be resistant to swirl. The velocity component producing the axial swirl is parallel to the edge of the vane and presumably would not affect the shedding from the ring. The ring vane has one obvious disadvantage. Since the ring has no contact with the wall, a support structure must be provided with its attendant flow disturbance. The support structure should minimally perturb the flow, especially at the front and sides of the ring. Adding a vortex detection mechanism compounds the design difficulty.

The ring vortex meters tested were all 1½ in nominal meters. First, the rings were mounted on the ends of three radial arms of 1/2 to 3/4 mm thick by about 10 mm wide stainless steel plates with the large surfaces parallel to the flow. The rings broke free from the arms in the first two tests. The detector consisted of a 3 mm diameter tube inserted along a diameter to sense transverse pressure. These tubes broke off as rapidly as the rings. On the third try the ring of vane 58 was brazed to three stainless steel support arms with about 40 mm length along the pipe axis. A thin metal reed with its length along the flow direction and its width perpendicular to both the flow and the pipe diameter was brazed to one of the support arms. A strain gage placed on this vane gave an observable vortex signal but the reed broke off the support as the flow was increased during the first test.

A second design, vane 59, was tried using 5 mm thick streamlined arms instead of thin blades for support of the vane. A ring supported by two arms with transverse pressure ports on the arms for sensing showed no vortex generated spectrum line.

Vane 60 consisted of a streamlined support bar spanning the pipe with the ring mounted ahead of it on two posts. The posts broke off on the first test. The joints holding the second set of heavier posts broke but the ring stayed in place and a good signal was obtained via a pressure port behind the center of the ring that opened into the flow. The ring was brazed again to the posts for a second test. This time the joints held, with the result that the meter factor changed. The meter design is illustrated in figure 32. The meter factors obtained with the support joints both loose and solid are shown in Figure 33. The meter factor for the first measurement during which the ring was loose from the supports was more constant with flow. A pressure port at the same location that sensed transverse pressure was tried but no spectrum line was seen.

The meter factor of this 11.8 mm ID by 16.4 mm OD ring is higher by a factor of 2 than the 5.1 mm wide link vane. Tests with the swirl generator, however, indicated a decrease of sensitivity with increasing swirl. No further testing was done for three reasons: no apparent improvement to swirl resistance was obtained, the vane would not insert through an 11.2 mm port, and the problem of introducing a vortex sensing mechanism at these high flow rates had not been satisfactorily solved.

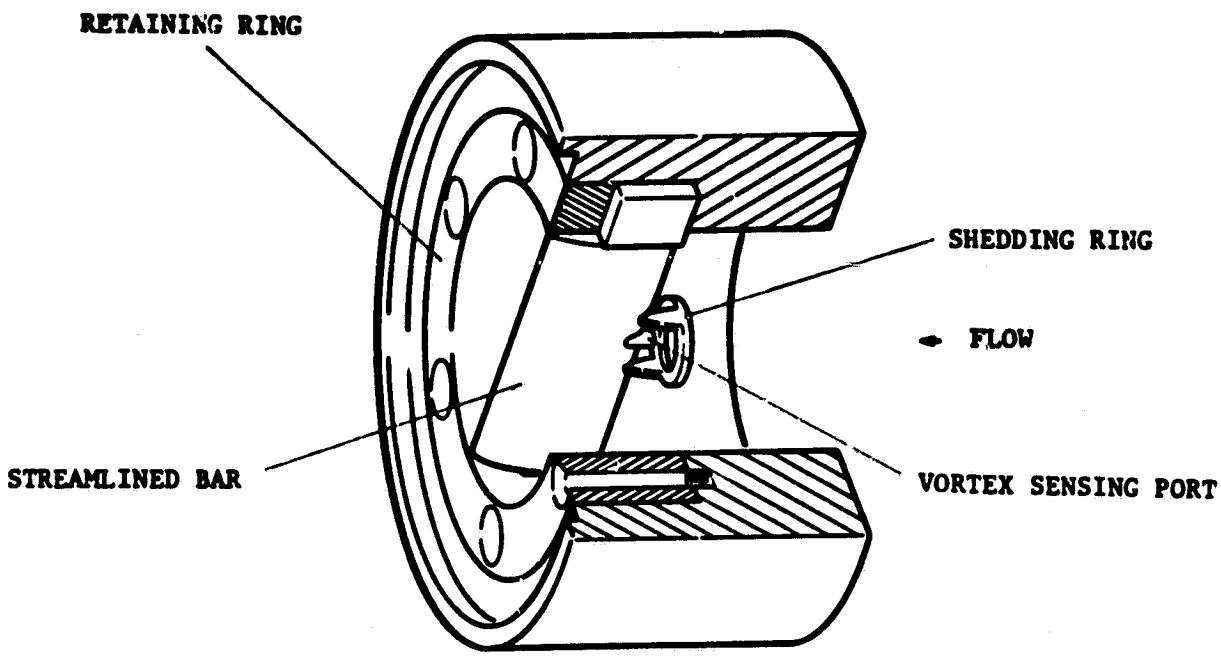

Figure 32. The drawing shows vane 60. The shedding element is a ring. The sensing port connected to a pressure tranducer exterior to the meter.

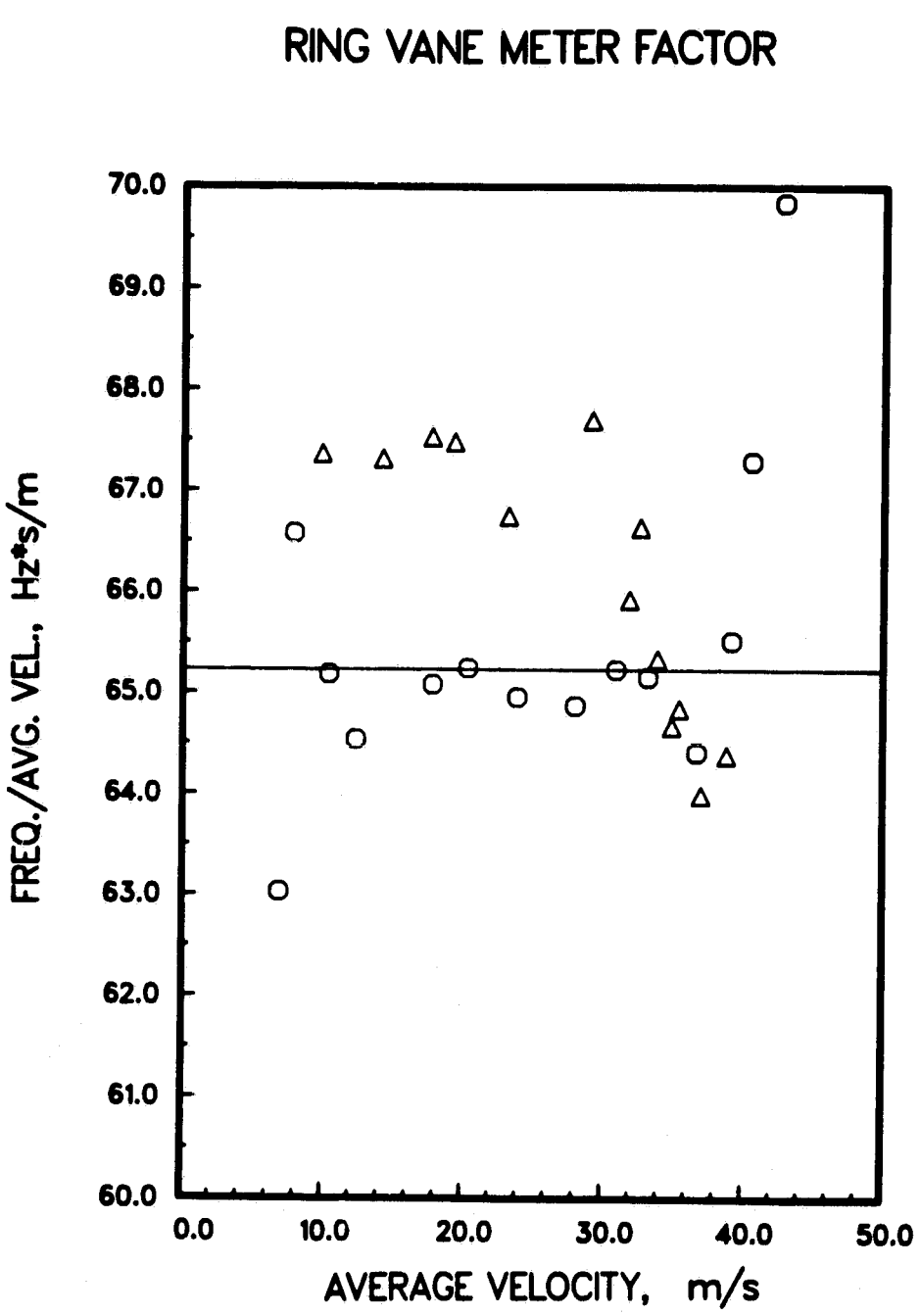

Figure 33. Meter factor as a function of velocity for vane 60. Circles, the first test with the ring loose. Triangles, the second test with ring solid.

8. AIR TEST RESULTS

High pressure hydrogen gas density can be simulated by compressed air. The compressibility and viscosity of compressed air differ from hydrogen, but the most significant difference is the velocity of sound. The sound velocity is 4 to 5 times higher in the hydrogen gas at the shuttle duct conditions than for ambient air. The air tests can show whether gas flow at the duct densities can be measured by the present meter designs. Air tests cannot be expected to demonstrate the flowmeter performance at 250 m/s, which is a Mach number of about 0.7 in air but only about 0.2 in hydrogen. Local velocities in the region of a slightly canted airfoil exceed Mach 1 in a free flow of Mach 0.5, so the flow around a rectangular shape must certainly exceed Mach 1 at Mach numbers well below 0.5 [17].

Only the first vane, No. 61, was tested in air flow at the three different hydrogen duct densities in which flow measurement is desired. These densities were represented by air pressures of 8.36 MPa (1213 psia), 3.87 MPa (562 psia), and 2.3 MPa (333 psia) respectively. The results of these tests are shown in figure 34 which shows the meter factor as a function of the Reynolds number for the three tests. The meter factors at the three pressures overlap up to velocities around 110 m/s, where the meter factors at the two lower pressures increase steeply with increasing flow velocity. This may be the onset of localized supersonic flow. The 8.36 MPa measurements were only carried to about 92 m/s, still below the transition velocity.

The x data points show the meter factor obtained for water flow measurements. The meter factor for water was more than 10% lower than for air. Though many manufacturers of commercial meters design to eliminate the sensitivity to fluid properties, the meter can be calibrated for the fluid to be used.

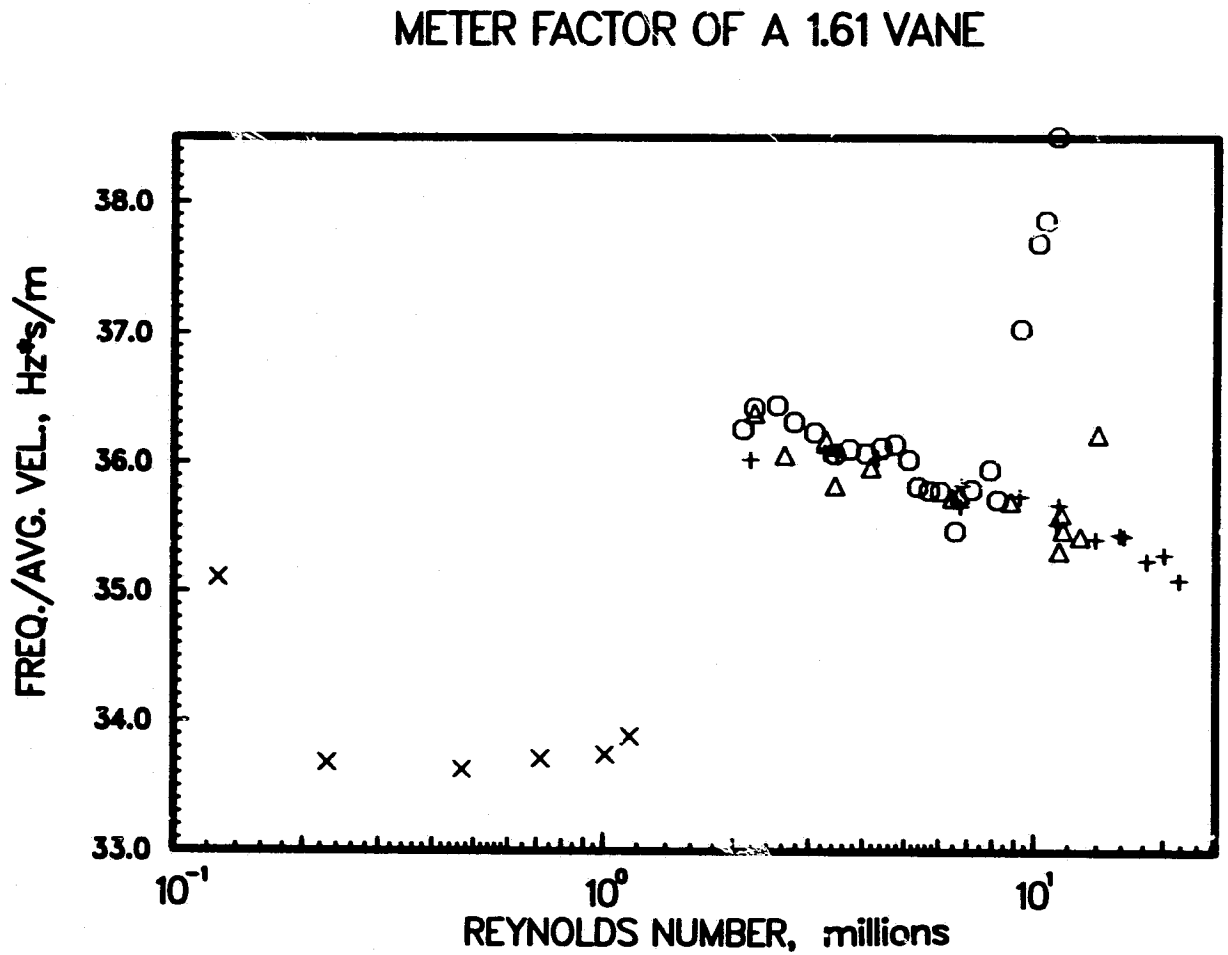

Figure 34. Meter factor as a function of Reynolds number for vane 61. X, water test. Circles, compressed air at 2.3 MPa (333 psi), traingles compressed air at 3.87 MPa (562 psi); and pluses, compressed air at 8.36 MPa (1213 psi).

The spectra were generally examined to 10 kHz since the vortex spectrum line frequency will approach 10 kHz at flow rates of 250 m/s. Noise lines occur mainly in the 5 to 8 kHz range, far enough above the vortex line that the highest density hydrogen flow can be measured with existing designs. The noise lines increase and decrease in magnitude as the flow varies. The increase in magnitude did not appear to shift the vortex line even when the line seems to be driven by a harmonic of the vortex frequency. Some of the extra lines may be driven by the flow noise rather than by the vortex shedding.

Vane 16, which has a triangular shape, gave the meter factor as a function of Reynolds number shown in figure 35. The slope is opposite that given by vane 61. The change of meter factor with velocity for water is opposite that for air. Spectrum lines for vane 16 are shown in figure 36 where they are compared to those of vane 61. The vortex generated lines of vane 16 appear somewhat narrower than for vane 61 and fewer noise lines appear below 5 kHz at the low flow rates. At higher flow rates, more noise lines occur in the vane 16 spectra than obtained from vane 61. Also, a sharp spectrum line is obtained to a higher flow rate for vane 16 than for vane 61.

Vane 5 was tested with air flow at 2.3 MPa. The spectra were noisy though the vortex generated lines were sharp. The meter factor was not a straight line and scattered above 75 m/s velocity.

One cantilevered vane was tested. The vortex spectrum line was small relative to the attendant noise lines. The meter factor between 50 and 1.0 m/s was constant.

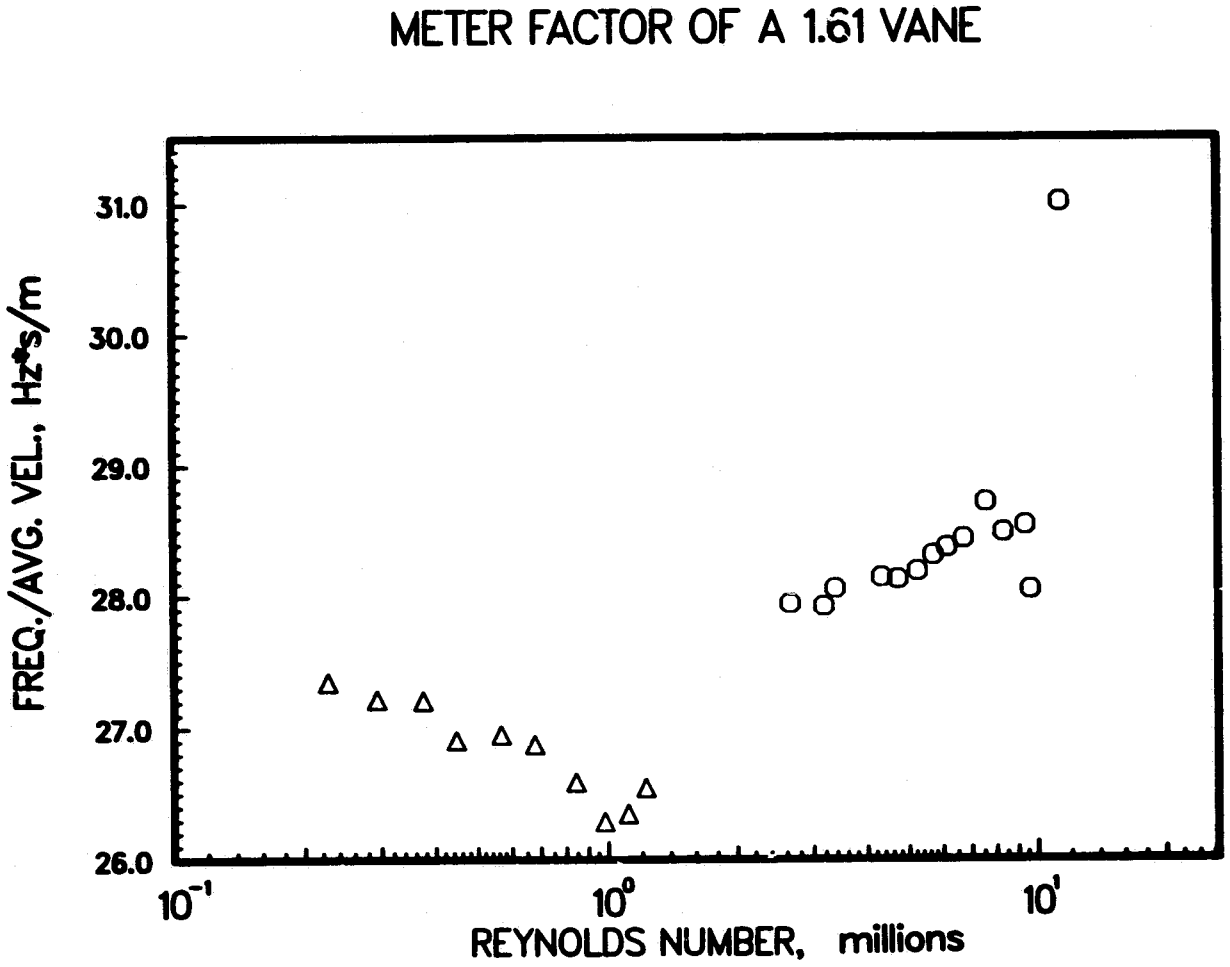

Figure 35. The circles show the meter factor as a function of Reynolds number for vane 16 at 2.3 MPa (333 psi). The triangles show the water flow test of vane 16.

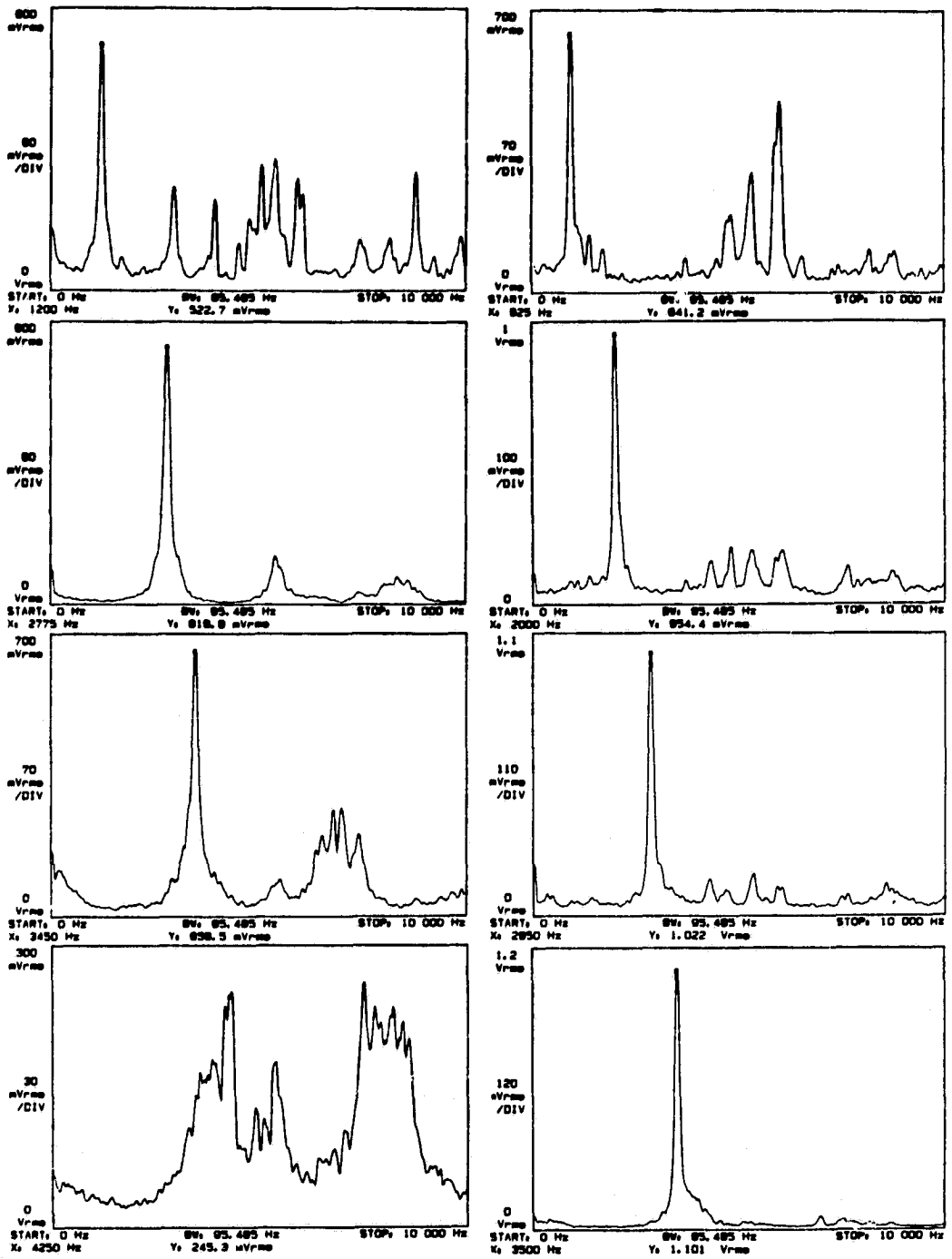

Figure 36. A comparison of spectra for vane 61 left column, to vane 16, right column, at a pressure of 2.3 MPa (333 psi). Top left, 33.2 m/s; top right, 33.7 m/s. Second left, 71.6 m/s; second right, 71.2 m/s. Third left, 97.5 m/s; third right 100.2 m/s. Bottom left, 121.1 m/s; bottom right, 123.3 m/s.

A second set of air flow tests were carried out on a 1.5 in meter. The test section for these tests was a single 25 diameters long stainless steel section with a brazed-on port block. Some vanes with a nominally triangular cross section were tried because vane 16 performed the best in the first air test. The depth of vane 62 was made less than vane 16 in an attempt to reduce the increase of the meter factor with increasing flow velocity.

Vane 62 gave the meter factor versus velocity curve shown in figure 37. The meter factor is not constant with flow and decreases more rapidly above about 135 m/s. It was the same for the test at 2.3 MPa (333 psi) and 1.46 MPa (212 psi). The lower pressure is below any shuttle duct density but is near the density capabilities of a NASA hydrogen flow facility. Because the same calibration nozzle was used for both tests the lower pressure tests permitted the higher velocities. The meter factor of the same vane for water is again lower than that for air. At least one strong flow independent line appears in most of the spectra of figure 38. The principal line remains in the 3.7 to 4 kHz range and is dominated by the vortex line especially above about 100 m/s flow. The presence of this line may cause the scatter at about 140 ms shown in figure 37. In any case, a flow dependent line persisted up to a velocity of about 180 m/s (590 ft/s), figure 38. The test results at the two gas pressures overlap better when plotted as a function of velocity. In contrast, the vane 61 meter factors at the three test pressures overlap better when plotted as a function of Reynolds number.

The meters designed for liquid flow gave sharp spectrum lines in gas flow even at densities less than 0.03 that of water. Noise lines approaching the magnitude of the vortex lines were generated at various flows. These should be reduced in magnitude if not eliminated completely for the meters to provide flow measurement to 250 m/s.

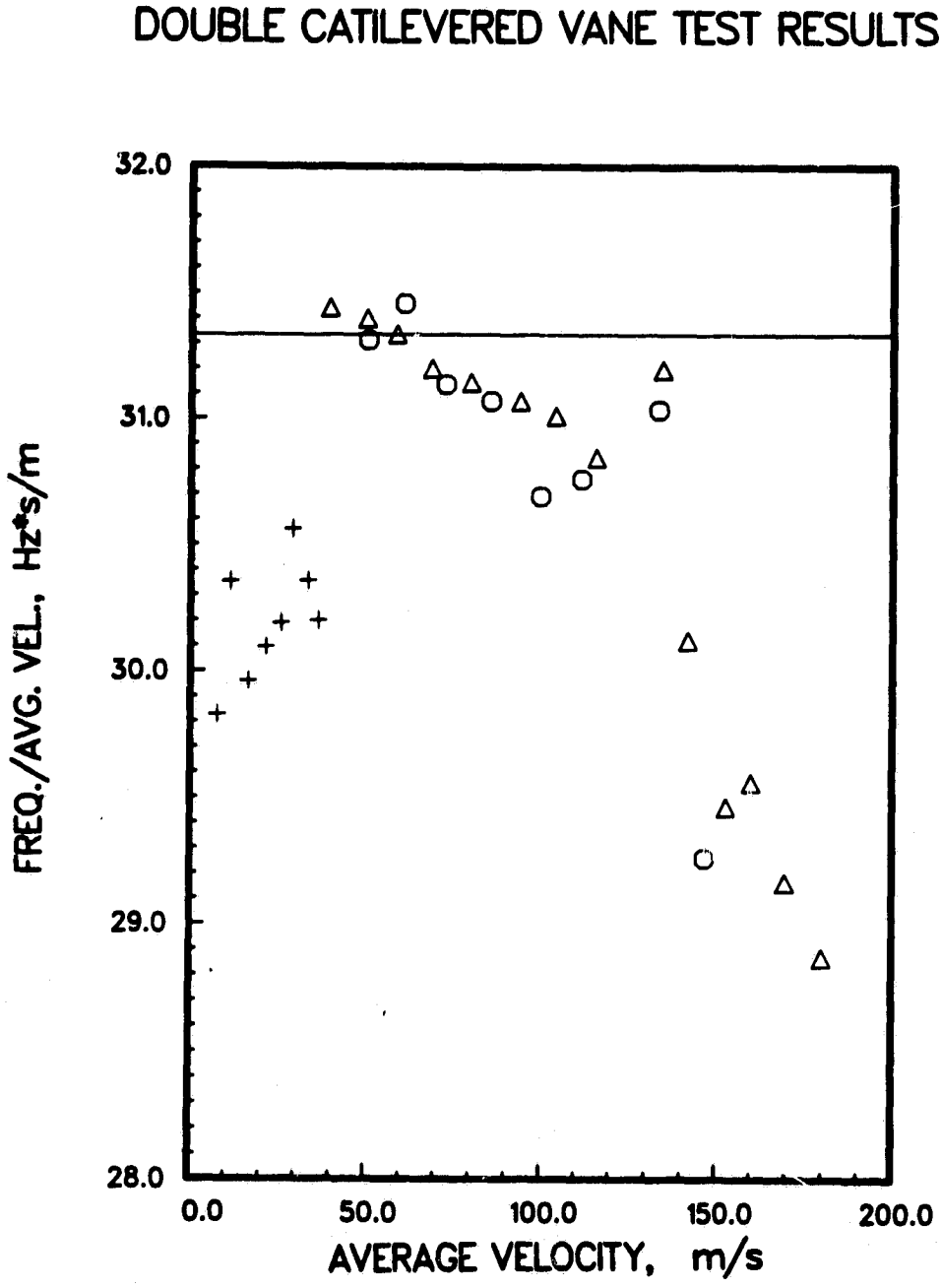

Figure 37. Meter factor of vane 62 as a function of velocity for: pluses, water test data; circles, 2.3 MPa (333 psi) air; and triangles 1.46 MPa (212 psi) air.

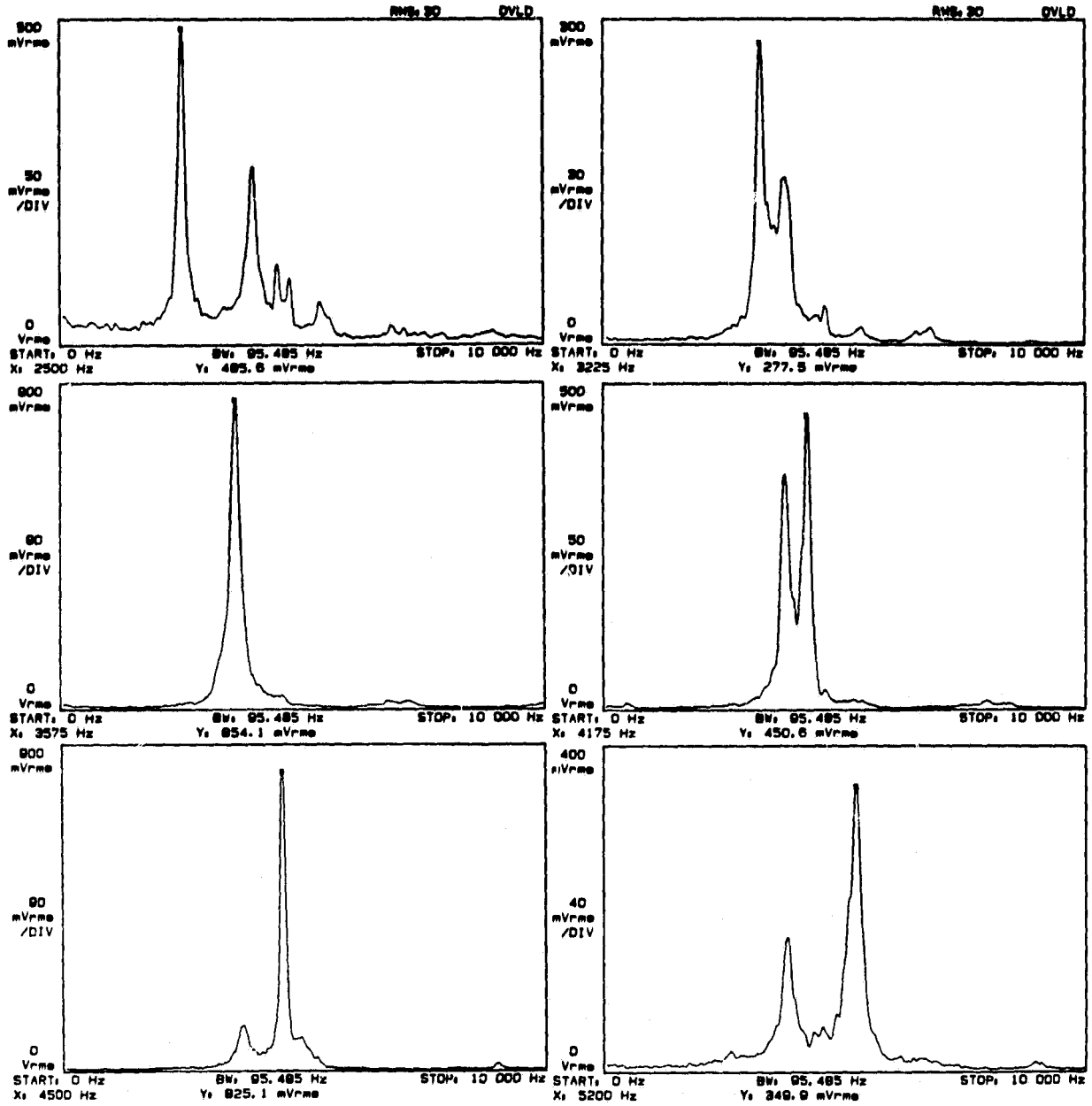

Figure 38. Some spectrum lines from vane 62 at air velocities, starting on the left side; top, 79.9 m/s and 104 m/s; middle, 115.8 m/s and 134.5 m/s; bottom, 152.7 m/s and 180 m/s.

9. CONCLUSIONS

A number of vortex shedding flowmeter designs were tested at high flow velocities in a water flow test facility. The following conclusions can be drawn from the results obtained for vanes consisting of a uniform cylinder spanning the pipe:

1) A vane with a width 1/8 the pipe diameter can measure flow at velocities up to 55 m/s with a maximum pressure loss less than 0.7 kPa (100 psi). This loss is proportional to the flow velocity squared.

2) Up to a duct bore of 59 mm (2.3 in) some of the successful vane designs tested can be installed in a diametrically opposite pair of the standard 11.2 mm diameter SSME instrument ports.

3) The vanes mounted in the SSME ducts in straight sections as short as six diameters in length can give sharp signal spectrum lines and a linear response without any upstream flow conditioning. The vane should be mounted with its axis perpendicular to the plane of the preceding bend.

4) A vane with a rectangular cross section and a ratio of depth to width (D/W) between 0.67 to 0.85 seemed to give the best results in terms of linearity,signal fade, and signal-to-noise power ratio (S/N).

5) The sensitivity of one vane varied by 4% depending on the meter body and the pipe preceding the meter. This was probably caused in part by the differences in the duct wall finishes.

6) The sensitivity could be varied over a range of at least 12% just by the shape of the corners of the front face of a vane with a rectangular cross section.

Air at the density of the hydrogen gas in the SSME ducts was used to test a few of the meters designed for and tested in water. The following general results were obtained:

1) The meters designed for water sensed gas flow to densities of 0.026 that of water.

2) A vortex line was obtained to a velocity of 180 m/s (590 ft/s) for one vane. The much lower velocity of sound for air probably limited the velocity.

3) A triangular cross section appears to produce superior spectrum lines when measuring gas flow.

4) The meter factor in Hz·s/m for air was found to be slightly larger than for water for the vanes tested.

5) The highest Reynolds number attained was 22×10^6. This is about twice that of the LOX flow in any of the SSME ducts so no Reynolds number limit should be encountered for LOX flow.

6) Some other lines, probably some mechanical resonances, approach the magnitude of the vortex signal in the air test spectra and should be eliminated.

Vanes partially spanning the pipe and cantilevered from one side possibly performed well enough to be used as meters in the 1½ in nominal size only. A vane consisting of a ring placed with its axis parallel to and centered in the pipe also produced a flow dependent spectrum line up to velocities of 40 m/s. The problems of mounting the ring and detecting the vortices generated in the severe flow environment do not make the ring design particularly attractive.

As long as the link vanes tightly fit the support on the ends, the design of the support seemed to have little effect on the meter factor for a single piece vane spanning the pipe and mechanically attached to both supports.

Link vanes of the same dimension gave the same meter factor. This was not true for double cantilevered vanes. The meter factor seemed to increase

as the stiffness of the mount decreased. Only one pair of cantilevered vanes gave nearly the same meter factor as a single piece vane of the same dimensions. It was not clear that these were stiffer than the others. Because of the small cross section of the vane and mounting port, vane movement probably affects all these vanes regardless of design.

Most of the testing was done using a sensing mechanism that transmits mechanical motion through a seal. This seal has been eliminated by a design that measures the strain in the vane structure without penetrating into the high pressure interior of the duct. So far, the S/N was poorer for this detector than the detectors that penetrate into the duct, but some additional development could eliminate this difference.

In general, the vortex flowmeter designs tested would measure water flows to velocities greater than 50 m/s. No limitation in measuring gas flow to the required 250 m/s was encountered beyond what was assumed to be Mach number effects.

10. ACKNOWLEDGMENTS

This work was supported by National Aeronautics and Space Administration, Marshall Space Flight Center through Government Order #H-63458B. The author is indebted to the Public Service Company of Colorado and to the City of Boulder Water Utility for providing the high pressure water so necessary for these tests. The author would also like to thank Douglas M. Ginley who assisted with parts of this work.

11. REFERENCES

[1] Bean, H.S. Editor, Fluid Meters, Their Theory and Application, 6th Edition, The American Society of Mechanical Engineers, New York, (1971).

[2] White, D.F., Rodely, A.E., and McMurtrie, C.L., "The Vortex Shedding Flowmeter", Flow, Its Measurement and Control in Science and Industry, Instrument Society of America, 1 (2) 967-974, (1974).

[3] Lynworth, L.C., Physical Acoustics, Vol. XIV, Mason, W.P., and Thurston, R.M., editors; Academic Press, New York (1979).

[4] Inkley, F.A., Walden, D.C., and Scott, D.J., "Flow Characteristics of Vortex Shedding Flowmeters," Meas. and Control (GB) 13, 166 (1980).

[5] Wiktorowicz, W.E., "Flow Measurement by Vortex Shedding Meters," Proceedings, 57th School of Hydrocarbon Measurement, Norman, OK, 1982, 618. Available from K.E. Starling, 202 West Boyd, Norman, OK 73019.

[6] Prandtl, L., Essentials of Fluid Dynamics, Hafner, New York 1952; page 183 ff.

[7] Cousins, T., Foster, S.A., and Johnson, P.A., "A Linear and Accurate Flowmeter using Vortex Shedding," Symposium of Power Fluidics for Process Control, 45-56. Guildford, England: University of Surrey, 1973.

[8] Corpron, G.P., Mattar, W.M., Richardson, D.A., and Sgourakes, G.E., "Fluctuating Pressure Profile and Sensor design for a Vortex Flowmeter," ASME Annual Winter Meeting (San Francisco, CA Dec 15-18, 1978). American Society of Mechanical Engineers, New York, 1979.

[9] Takamoto, M., and Komiya, K., "A Vortex Ring Shedding Flowmeter," Acta Imeko, Akadémiai Kiadó, Budapest, Hungry 1982.

[10] Kalkhof, H-G., "Influence of the bluff body shape on the measurement characteristics of vortex flowmeters," International Conference on the metering of Petroleum and its Products, London Press Centre, London ED4, 1985.

[11] Roshko, A., "Experiments on flow past a circular cylinder at very high reynolds number," Journal of Fluid Mechanics 10, 345-356 (1961).

[12] Ericsson, L.E., "Karman Vortex Shedding and the Effect of Body Motion," AIAA Journal 18, 935-944 (1980).

[13] Flora, C. and Matsuura, T.K., "Vortex Flowmetering," Meas. and Control (GB) 15, 165-170 (1982).

[14] Colorado Engineering Experiment Station Inc, 54043 County Road 37, Nunn, Colorado 80648. Their choked nozzle flow standards were used for the flow velocity calibration.*

[15] Padmanabhan, M. and Janik, C.R., "Swirling Flow and Its Effect on Wall Pressure Drop Within Pipes", Vortex Flows, ASME Winter Annual Meeting (Chicago, IL, Nov. 16-20, 1980). American Society of Mechanical Engineers, New York (1981).

[16] Miller, R.W., Flow Measurement Engineering Handbook, McGraw-Hill, New York (1983).

[17] Mair, W.A., and Beavan, J.A., Modern Developments in Fluid Mechanics, High Speed Flow, Vol. II, L. Howarth, Editor, Oxford University Press, London (1953).

*This is not intended to be a product endorsement.

NBS Technical Publications

Periodical

Journal of Research—The Journal of Research of the National Bureau of Standards reports NBS research and development in those disciplines of the physical and engineering sciences in which the Bureau is active. These include physics, chemistry, engineering, mathematics, and computer sciences. Papers cover a broad range of subjects, with major emphasis on measurement methodology and the basic technology underlying standardization. Also included from time to time are survey articles on topics closely related to the Bureau's technical and scientific programs. Issued six times a year.

Nonperiodicals

Monographs—Major contributions to the technical literature on various subjects related to the Bureau's scientific and technical activities.

Handbooks—Recommended codes of engineering and industrial practice (including safety codes) developed in cooperation with interested industries, professional organizations, and regulatory bodies.

Special Publications—Include proceedings of conferences sponsored by NBS, NBS annual reports, and other special publications appropriate to this grouping such as wall charts, pocket cards, and bibliographies.

Applied Mathematics Series—Mathematical tables, manuals, and studies of special interest to physicists, engineers, chemists, biologists, mathematicians, computer programmers, and others engaged in scientific and technical work.

National Standard Reference Data Series—Provides quantitative data on the physical and chemical properties of materials, compiled from the world's literature and critically evaluated. Developed under a worldwide program coordinated by NBS under the authority of the National Standard Data Act (Public Law 90-396). NOTE: The Journal of Physical and Chemical Reference Data (JPCRD) is published quarterly for NBS by the American Chemical Society (ACS) and the American Institute of Physics (AIP). Subscriptions, reprints, and supplements are available from ACS, 1155 Sixteenth St., NW, Washington, DC 20056.

Building Science Series—Disseminates technical information developed at the Bureau on building materials, components, systems, and whole structures. The series presents research results, test methods, and performance criteria related to the structural and environmental functions and the durability and safety characteristics of building elements and systems.

Technical Notes—Studies or reports which are complete in themselves but restrictive in their treatment of a subject. Analogous to monographs but not so comprehensive in scope or definitive in treatment of the subject area. Often serve as a vehicle for final reports of work performed at NBS under the sponsorship of other government agencies.

Voluntary Product Standards—Developed under procedures published by the Department of Commerce in Part 10, Title 15, of the Code of Federal Regulations. The standards establish nationally recognized requirements for products, and provide all concerned interests with a basis for common understanding of the characteristics of the products. NBS administers this program as a supplement to the activities of the private sector standardizing organizations.

Consumer Information Series—Practical information, based on NBS research and experience, covering areas of interest to the consumer. Easily understandable language and illustrations provide useful background knowledge for shopping in today's technological marketplace.

Order the **above** *NBS publications from: Superintendent of Documents, Government Printing Office, Washington, DC 20402.*

Order the **following** *NBS publications—FIPS and NBSIR's—from the National Technical Information Service, Springfield, VA 22161.*

Federal Information Processing Standards Publications (FIPS PUB)—Publications in this series collectively constitute the Federal Information Processing Standards Register. The Register serves as the official source of information in the Federal Government regarding standards issued by NBS pursuant to the Federal Property and Administrative Services Act of 1949 as amended, Public Law 89-306 (79 Stat. 1127), and as implemented by Executive Order 11717 (38 FR 12315, dated May 11, 1973) and Part 6 of Title 15 CFR (Code of Federal Regulations).

NBS Interagency Reports (NBSIR)—A special series of interim or final reports on work performed by NBS for outside sponsors (both government and non-government). In general, initial distribution is handled by the sponsor; public distribution is by the National Technical Information Service, Springfield, VA 22161, in paper copy or microfiche form.